SYSTEMS TECHNOLOGY, INC.
Inglewood, California

TECHNICAL REPORT NO. 124-1

A SYSTEMS ANALYSIS OF LONGITUDINAL PILOTED CONTROL IN CARRIER APPROACH

BY
C. H. CROMWELL
I. L. ASHKENAS

JUNE 1962

PERFORMED UNDER
CONTRACT NO. NOw 61-0519-c
FOR
BUREAU OF NAVAL WEAPONS
DEPARTMENT OF THE NAVY
WASHINGTON, D. C.

TECHNICAL REPORT NO. 124-1

A SYSTEMS ANALYSIS OF LONGITUDINAL PILOTED CONTROL IN CARRIER APPROACH

(Final Report)

C. H. Cromwell
I. L. Ashkenas

June 1962

Performed under
Contract No. NOw 61-0519-c
for
Bureau of Naval Weapons
Department of the Navy
Washington, D. C.

FOREWORD

This report covers the first, and analytical, phase of a program to investigate piloting problems of carrier approach using systems analysis methods to attack the problem. The research was sponsored by the Airframe Design Division of the Bureau of Naval Weapons under Contract NOw 61-0519-c. Mr. C. H. Cromwell served as project engineer, and Mr. Harold Andrews served as technical monitor for the Bureau of Naval Weapons.

Special mention is due to Mr. Tulvio Durand for his contributions to the technical appendices of the final report, and to R. N. Nye and D. Lewis for their careful work in preparing the manuscript.

ABSTRACT

The pilot's longitudinal control of an aircraft making a carrier approach is studied using systems analysis techniques. The pilot, airframe, and mirror optical landing aid are considered as elements in a closed-loop system. Mathematical expressions to approximate each element are derived or described. Various possible piloting techniques are examined by appropriately varying the pilot's transfer function, and by closing multiple control loops around the system. The question of whether the pilot should use stick or throttle for altitude control is examined. It is shown that the minimum approach speeds of five out of seven jet aircraft, all limited by the "ability to control altitude and arrest rate of sink," can be predicted if it is assumed that the pilot uses throttle for altitude control.

CONTENTS

FIGURES

TABLES

SYMBOLS

a, b, c, etc. A, B, C, etc.	Polynomial coefficients
a_{ij}	Coefficients of the independent motion quantities (Eq A-16) in equations of motion
C_D	Drag coefficient
C_M	Pitching moment coefficient
D	Drag
g	Acceleration due to gravity
G(s)	Open-loop transfer function
h	Altitude, positive upward
h_d	Altitude displayed by mirror, i.e., the distance the meatball is below (above) the datum bar (Fig. 1)
I_y	Moment of inertia about the Y axis
K	Open-loop gain; the frequency-invariant portion of a transfer function as $s \rightarrow 0$, particularized by subscript
m	Mass (Eq B-3)
M	Pitching acceleration due to externally applied torques
$N_{q_i\delta_e}$, $N_{q_i\delta_T}$	Numerator of q_i/δ_e or q_i/δ_T transfer function, particularized by substituting motion quantity involved for q_i (see Eq A-8 and A-9)
$N_{\delta_e\delta_T}^{q_iq_j}$	Coupling numerator, particularized by substituting motion quantities involved for q_i, q_j (see Eq A-23)
q	Pitching velocity; general symbol for motion quantity
R	Range, distance from aircraft to mirror (Fig. 1)
s	Laplace operator, $\sigma + j\omega$
T	Time constant, particularized by subscript
T_I	Pilot-adopted lag time constant

T_L	Pilot-adopted lead time constant
T_N	Pilot-adopted neuromuscular lag time constant
u	Linear perturbed velocity along the X axis
U_o	Linear steady state velocity along the X axis
w	Linear perturbed velocity along the Z axis
x_m	Distance from source light to mirror (Fig. 1)
X	Forward acceleration along the X axis
Y_p	Pilot describing function (Eq 1), particularized for the control loop involved by suitable subscripts (see, e.g., Eq 12)
z_T	Vertical distance between c.g. and thrust line, positive downward
Z	Vertical acceleration along the Z axis
α	Instantaneous angle of attack (deg)
α_{TL}	Angle of attack of the thrust line
γ	Flight path angle
δ	Control deflection, particularized by subscript
Δ	Increment change
Δ	Denominator of airframe transfer functions; characteristic equation when set equal to zero
ϵ	Instantaneous glide path angular error (Fig. 1)
ζ	Damping ratio of linear second-order transfer function quantity, particularized by subscript
θ	Pitch angle
σ	The real portion of the complex variable, $s = \sigma \pm j\omega$
τ	Pilot reaction time
ω	Frequency; $j\omega$ is the imaginary portion of the complex variable, $s = \sigma \pm j\omega$
ω	Undamped natural frequency of a second-order mode, particularized by subscript

Subscripts

c	Command; controlled element (vehicle)
CL	Closed loop
e	Elevator, as in δ_e
ϵ	Incremental error
m	Mirror
min	Minimum
p	Pilot, as in δ_p for pilot's controlled deflection
p	Phugoid
sp	Short period
T	Throttle, as in δ_T
α, h, θ, u	Pertaining to control of the variable indicated, as in A_θ, K_{p_h}, etc.
α, δ_e, δ_T, q, u, w	Indicates partial derivative, e.g., $M_w = \frac{\partial M}{\partial w}$, $Z_{\delta_T} = \frac{\partial Z}{\partial \delta_T}$

Note: Primes on a transfer function or time constant indicate that it has been modified by inner-loop closures, the number of primes corresponding to the number of closures.

SECTION I

INTRODUCTION

A. BACKGROUND OF THE REPORT

As new generations of high performance carrier-based aircraft are designed and introduced into fleet operation, the carrier-landing approach speed increases. These speeds are reaching the point of arresting gear limits, are posing aircraft structure design problems, and are causing piloting problems attributed to fast closure rates between aircraft and carrier. The remedy to all of these problems is simply to reduce approach speeds, yet the effect of modern design trends has been to increase them.

As speeds increase it also becomes more important to predict at the design stage what the eventual pilot-selected approach condition will be, and this requires an appreciation of the factors that cause the pilot to set his minimum allowable value. Early attempts at predicting approach speeds simply chose a fixed margin above the power-on stall speed, usually about 15 percent. With the advent of sweptwing jet aircraft it was soon found that this simple criterion was no longer adequate and more elaborate methods were devised. Pilots were complaining of problems in controlling the aircraft, both longitudinally and laterally, so the second generation of approach speed criteria considered the ability of the aircraft to maneuver, usually in response to discrete step-type control inputs (e.g., Ref. 1). Criteria based on this concept have enjoyed only limited success in predicting approach speeds and have not led to a real understanding of the piloting problems because they do not realistically consider the pilot's role in control of the aircraft.

A fundamentally different approach to the problem is used in this report. The pilot, his aircraft, and the mirror display are regarded as elements of a closed-loop feedback control system. The pilot is assumed to perform the same role as an autopilot in an automatic landing system; that is, he compares what the aircraft is doing with what he wants it to do and he actuates the controls in response to the errors that he observes in altitude, airspeed, etc. Thus he performs the sensor-actuator function of the autopilot. The

analytical method, using this concept, employs the well-developed mathematical techniques of servo system analysis which are used to study any automatic flight control system. The evaluation process at any given approach speed (and therefore fixed vehicle dynamics) consists of making a series of loop closures while varying the pilot's mathematical "autopilot" characteristics. When a near-optimum closed-loop system has been obtained the results are judged by two criteria: First, is the closed-loop performance, as a tracking system, adequate for the assigned task (in this case to successfully complete the approach to a carrier landing)? Second, does attainment of that system performance require too much dynamic equalization from the pilot? (This latter point refers to the adaptive capability of the pilot and whether this capability is being exceeded or not.)

As approach speed is lowered and the aircraft's dynamic characteristics change, some speed is found below which these criteria can no longer be satisfied. This is predicted to be the minimum acceptable approach speed. The cause of the limitation is connected with airframe dynamics, defined in the terms used in control systems analysis (i.e., frequencies, damping ratios, etc.). However a knowledge of the relationship between these airframe transfer function parameters and their associated aerodynamic stability derivatives (i.e., approximate factors of the transfer functions in terms of stability derivatives, as given in Ref. 2) allows the approach speed limit to be related to the aircraft's basic aerodynamics. The net result of the investigation is therefore the same as with other prediction methods: aerodynamic characteristics are correlated with the minimum approach speed. It is only the analytical concept of treating the problem as a closed-loop system problem which differs from previous methods.

The treatment of handling qualities problems by servo analysis techniques has been a slowly evolving process. Early programs were aimed at measuring and analyzing the dynamic characteristics of the human pilot (i.e., his "transfer function"); much of this work up to 1956 is summarized in Ref. 3. Lateral and longitudinal attitude control, using the mathematical model of the pilot determined in Ref. 3, are examined analytically in Ref. 4 and 5, and the basic theory thereby developed is confirmed by the handling qualities flight and simulator tests reported in Ref. 6 through 9. A general summary

of this systems viewpoint of handling qualities is given in Ref. 9, which also contains a preliminary exposure of some results of the present study. The interested reader is referred to these reports for further documentation and an extensive bibliography on the subject. Section II of this report contains a description of the pilot's servo characteristics in adequate detail for this report.

B. SCOPE OF THE REPORT

The factors that pilots report as defining the minimum approach speed can arbitrarily be divided into two categories, static and dynamic. As used here, static factors are those which can be predicted from geometry or aerodynamic performance considerations, such as cockpit visibility limits, maximum attitude for tail-to-deck clearance, proximity to stall, prestall buffet; dynamic factors are those indicating controllability problems. Typical pilot descriptions of the latter are control sensitivity, lateral-directional control, ability to control pitch attitude, and ability to control altitude or arrest rate of sink. This type of factor is dynamic in that it involves the aircraft's dynamic stability and control characteristics, or, in the context used in this report, it involves the aircraft's characteristics as a control system element.

Since the analysis method used herein treats the pilot-aircraft-mirror combination as a system, the type of problem studied is necessarily limited to the "dynamic" factors mentioned above. Further restricting the scope, only longitudinal control problems characterized by "the ability to control altitude or arrest rate of sink" are considered. Such problems are the most mysterious of those currently encountered and appear to require more than the present repertory of analysis procedures (including Ref. 4 and 5) to explain. Finally, even in this case, any possible effects due to low static margin, or aft c.g., are eliminated to reduce the initial complexity of the problem. This allows examination of only the basic longitudinal control factors involved in the ability to control altitude or arrest rate of sink.

C. OUTLINE OF THE REPORT

The next section describes the system aspects of the approach problem and includes a brief mathematical description of the elements of the system: the airframe, pilot, and mirror display. Appropriate transfer functions are derived or described with reference to derivations contained in Appendix A.

Section III summarizes the closed-loop system characteristics of the three potential control techniques available to the pilot and discusses their implications with respect to approach handling qualities. Generic properties of these control systems are shown in Appendix B, and a specific airplane example is given in Appendix C.

One of the control techniques from Section III is used in Section IV, in conjunction with simplified equations of motion, to derive a criterion for predicting the minimum acceptable approach speed. This criterion is shown to predict successfully the flight test minimum speed for five of seven aircraft specifically limited by the factor "ability to control altitude or arrest rate of sink."

The final section summarizes the results of the previous two sections, considers certain paradoxical questions raised therein, and recommends research directed to answering these (and other) questions.

SECTION II

SYSTEM ASPECTS OF CARRIER APPROACH

A. THE SYSTEM

In this section the analogy of the pilot-aircraft-mirror complex to a closed-loop feedback control system is developed, and the mathematical description of each of the elements is discussed.

Figure 1 is a sketch of the aircraft-mirror-carrier geometry. A source light aft of the mirror is reflected by the mirror to the pilot. He sees an orange disc in the mirror, termed the "meatball." A glide slope is set by a row of horizontal green datum lights (adjacent to the mirror) which appear at the same height as the meatball when the aircraft is on the correct approach path. When the aircraft goes below the preset glide slope (usually set at 4°) the meatball drops below the datum bar, and when the aircraft climbs the meatball climbs. Thus altitude errors as seen by the pilot correspond to vertical displacements (on the mirror) between the meatball and the datum bar. These display errors are limited only by the depth of the light cone, which allows a maximum angular error of $3/4^{\circ}$. (The kinematics of the display are defined more explicitly in a later part of this section.)

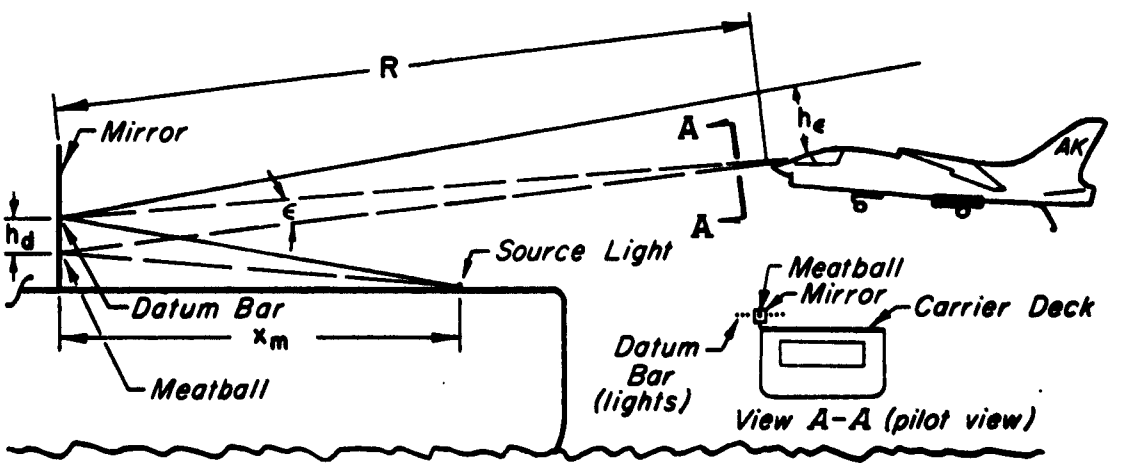

Figure 1. Geometry of the Aircraft-Mirror-Carrier System

The other variables which the pilot can monitor are pitch attitude, by reference to his outside-of-cockpit visual field, and airspeed and angle of attack. The latter two require some form of indicator since the pilot has no direct way of determining their value.

Since the pilot performs the same feedback operation as an autopilot (at least as regards control of altitude error), an autopilot type of system block diagram with the human pilot performing the sensor-actuator functions of the autopilot is appropriate. Such a block diagram is shown in Fig. 2, where all probable feedback quantities and the two control output possibilities, stick and throttle, are indicated. The exact pilot role is completely unspecified in Fig. 2, and the determination of the possible feedbacks that can be effectively used and the details of such usage are the object of the systems analysis activities reported in Sections III and IV. Such activities require transfer functions specifying the dynamics of each element in the block diagram. With each element so described (or at least approximated), the transfer functions can be lumped together into a system transfer function, and the over-all system's suitability for a carrier landing approach examined.

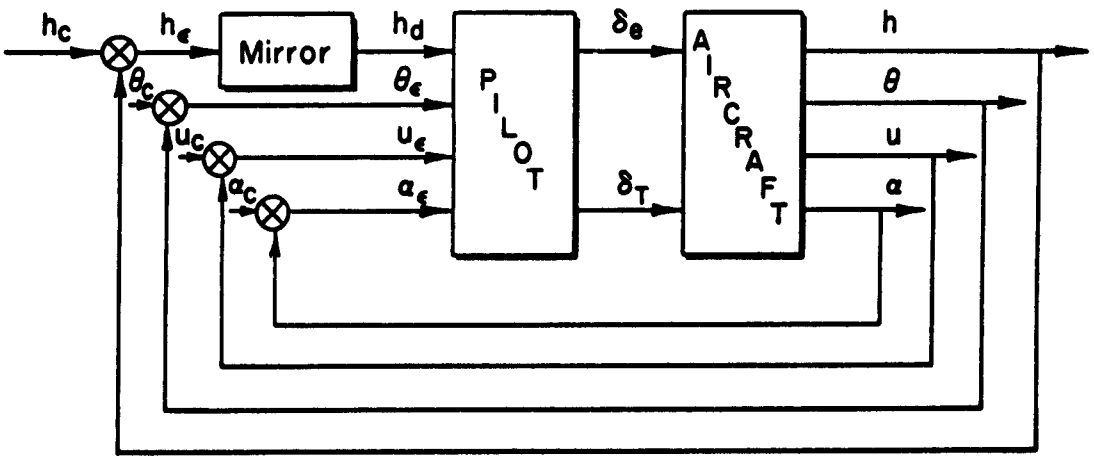

Figure 2. Multiple Loop Feedback Control System Block Diagram

B. TRANSFER FUNCTIONS OF THE SYSTEM ELEMENTS

1. The Aircraft

Reference 10 derives longitudinal transfer functions from the equations of motion. The process is standard in stability and control analysis and will not be repeated here. Note only that the same assumptions are used (small perturbations, linearized equations, etc.). Also, the effect of a 4^{o} glide angle on the transfer functions is negligible, so level flight equations can be used.

Because most of the possible pilot roles involve simultaneous manipulation of stick and throttle, "coupling" transfer functions (Ref. 11) appropriate to each multiple loop situation are also required. These are not as common as the conventional transfer functions, so their detailed derivations are given in Appendix A. The notation used therein is maintained throughout the rest of this report and is consistent with that of Ref. 11.

Seven aircraft were used for specific case studies because their minimum approach speed is reported (Ref. 1) to be dictated by the "ability to control altitude or arrest rate of sink." These aircraft are the F8U-1, F7U-3, F4D-1, F11F-1, F9F-6, F-100A, and F-84F. The aerodynamic and physical data on each are compiled in Ref. 1 and were used to compute trim conditions and the corresponding nondimensional derivatives. These derivatives were converted to dimensional form and used in the transfer function computations. The trim speeds selected for investigation were the average flight test minimum approach speed plus and minus about seven knots. This spread was picked because the mean approach speed used in fleet squadrons is usually about seven knots higher than the flight test reported minimum acceptable value, and the selected interval allows examination of the effect of this nominal speed change.

2. The Pilot

The form of the pilot describing function* is

$$Y_p = K_p e^{-\tau s} \frac{(T_L s + 1)}{(T_I s + 1)(T_N s + 1)} \qquad (1)$$

where

τ = pilot reaction time

T_N = pilot neuromuscular lag (his actuator lag) time constant

K_p = pilot gain

T_L = pilot-adopted lead time constant

T_I = pilot-adopted lag time constant

} Pilot sets these as required by the system

The neuromuscular lag time constant is of the order of 0.10 sec for center-stick control and contributes only slightly in the pilot's effective bandwidth region (less than 1 cps). Accordingly, this lag is usually approximated by $e^{-0.1s}$ and combined with the reaction time to give an "effective τ," typically about 0.20 sec in tracking situations. This eliminates the $(T_N s + 1)$ term from the transfer function, so that the simplest form characterizing the pilot is a gain plus a time delay,

$$Y_p = K_p e^{-\tau s} \qquad (2)$$

In this simple form, the pilot's gain is just the amount he moves the control (τ sec later) in response to a given magnitude of observed error.

The criteria which the pilot uses to set his gain have been deduced by examining measured pilot describing functions from many single-loop control

---

*It is important to note that only the quasi-linear portion of the pilot's output is described by this form and that it does not imply linearity in the point-by-point sense, but rather on the average. Thus, e.g., threshold in perception and consequent discrete manipulations of control are still representable by Eq 1.

experiments. These are criteria specifying the kind of closed-loop tracking system performance that the pilot desires. Briefly stated, the requirements are:

(a) A stable system

(b) Good low frequency performance (This may be interpreted as the ability to control the low frequency but relatively high power disturbances, such as those associated with atmospheric turbulence, which tend to make the tracking task more difficult. To the servo analyst this criterion requires a flat closed-loop frequency response with a gain of 1.0 over the disturbance input range.)

(c) Adequate closed-loop damping for oscillatory closed-loop systems (This requirement is considered met by the pilot when the closed-loop damping ratio is 0.35 or greater.)

If the pilot cannot meet these criteria with a simple gain response, he adopts a servo type of equalization, $(T_L s + 1)/(T_I s + 1)$. This can be lead, lag, lag-lead, or lead-lag, within his dynamic capabilities. When he is forced to do so to meet the system performance requirements, his opinion rating of the aircraft deteriorates. The more extreme the equalization required, the worse is the opinion rating. Generating lead, which requires sensing error rate (as opposed to error position, or magnitude) causes the most degradation in opinion. Generating lag requires integration, or time averaging, of the errors. Lag time constants can apparently be as high as 10 sec with only minor effects on opinion (Ref. 6), whereas lead time constants greater than about 1 sec are apparently quite difficult (Ref. 5).

A basic assumption regarding the pilot's equalizing efforts is that he always makes the minimum (or easiest) adjustments that he can get away with. If extreme adjusting on his part only slightly improves the system, then he will not make the effort. This carries over to multiple loop control situations in the assumption that he always closes the minimum number of loops that gives satisfactory control. In other words, he will only control as many variables as he has to in order to complete the approach.

To summarize qualitatively the mathematical description of the pilot's servo characteristics, he prefers to operate as a simple gain controller, the major limitation to this ability being his reaction-time-limited controllable frequency range. If necessary for system stability or for good low frequency control, he will adopt equalization using minimum adjustments, similar to

those that a good servo or autopilot designer would specify. However, a system requiring large amounts of equalization will not get a good handling qualities rating from the pilot.

3. The Mirror System

Referring to Fig. 1, define

x_m = distance from source light to mirror

R = distance from aircraft to mirror

h_ϵ = distance aircraft is below (above) the correct glide path

h_d = distance the meatball is below (above) the datum bar

ϵ = visual angle subtended by h_d

Assuming that the angles involved are small,

$$\frac{h_d}{x_m} \doteq \frac{h_\epsilon}{x_m + R}$$

so that

$$\epsilon \doteq \frac{h_d}{R} \doteq \frac{x_m h_\epsilon}{R(x_m + R)} \tag{3}$$

and taking the time derivative

$$\dot{\epsilon} \doteq \frac{x_m}{R(x_m + R)} \dot{h}_\epsilon + \frac{x_m(x_m + 2R)}{R^2(x_m + R)^2} \left(-\frac{dR}{dt}\right) h_\epsilon$$

$$\doteq \frac{x_m}{R(x_m + R)} \left[\dot{h}_\epsilon + \frac{U_o(x_m + 2R)}{R(x_m + R)} h_\epsilon\right] \tag{4}$$

To obtain altitude rate information from the mirror display, the pilot must sense the quantity $\dot{\epsilon}$. However, experimental flight test data from Ref. 13, as analyzed in Ref. 12, indicate that a pilot has an effective visual threshold for sensing vertical rates of about 0.004 rad/sec. Since the pilot cannot detect meatball velocities which produce a lower angular rate, Eq 4 can be solved (albeit heuristically) for the range at which the pilot can begin to obtain altitude lead (rate) information:

Source light to mirror distance, x_m, is typically 170 ft. Also, Ref. 16 shows that the standard deviation of sink speed at touchdown is about 3 ft/sec at a 170-ft/sec engaging speed. Assuming this represents a typical approach error, Eq 4 can be solved for the range at which $\dot{\epsilon} = 0.004$, assuming $h_\epsilon = 0$. This yields a value of R = 285 ft. Equation 4 indicates that the meatball rate is also a function of height error, h_ϵ. Assuming $\dot{h}_\epsilon = 0$, and limiting the error to the mirror's 3/4° cone angle,

$$\frac{h_\epsilon}{x_m + R} = 3/4^\circ = 0.0131 \text{ rad}$$

$$\dot{\epsilon} = 0.004 = \frac{U_o x_m (x_m + 2R)}{R^2 (x_m + R)} \left(\frac{h_\epsilon}{x_m + R} \right) = \frac{170^2 (170 + 2R)}{R^2 (170 + R)} (0.0131)$$

which yields R = 400 ft.

These two numbers indicate that lead information is ordinarily available only in the last 2 to 3 sec of the approach. For analytical purposes it is safe to assume that the pilot must make most of his 30-sec approach without using lead equalization. What this means to the control problem is discussed in the next section and illustrated specifically in Appendixes B and C, where altitude control is examined with and without lead equalization.

Consider now the pilot's ability to detect and discriminate altitude position errors. Equation 3 shows that for the accepted threshold value of ϵ, one minute of arc,

$$(h_\epsilon)_{\text{threshold}} \doteq 1.71 \left(\frac{R}{1000} \right)^2 \text{ ft}$$

That is, at 5000 ft range, detectable altitude errors must be greater than about 45 ft, whereas at 2000 ft range they must be greater than about 7 ft. Outside such thresholds the pilot can get a better indication of his altitude error by referencing the observed ϵ to the visual angle subtended by either the meatball diameter or the length of the datum bar. For example, the angle subtended by the datum bar, ϵ_d, is given by

$$\epsilon_d = \frac{l_d}{R}$$

and the ratio, ϵ/ϵ_d, by

$$\frac{\epsilon}{\epsilon_d} \doteq \frac{h_d}{l_d} \doteq \frac{x_m}{l_d} \frac{h_\epsilon}{(x_m + R)} \qquad (5)$$

In other words the gain, between the observed meatball height measured as a fraction of the datum bar length, and the altitude error, is inversely proportional to range rather than range squared as in Eq 3. Therefore, in the analytical work described later it is assumed that the mirror display gives only a gain change, and its dynamic and time-varying characteristics are ignored, especially since they do not vary significantly with aircraft approach speed.

In either case, the predominant effect of the mirror dynamics is to introduce a time-varying (range-varying) gain in the altitude loop. This time variation is not sensitive to small (10 percent) changes in approach speed and can be eliminated as a speed-sensitive factor in setting the minimum approach speed (however, it may be an important contributor to the over-all difficulty of the approach task). The possibility of obtaining altitude rate information from the mirror aid is practically nil and is not a factor in setting any one aircraft's minimum speed (lack of such information may also be an important part of the carrier approach problem).

SECTION III

CLOSED-LOOP CHARACTERISTICS OF POSSIBLE PILOTING TECHNIQUES

The previous section described the mathematical characteristics of the individual elements of the system shown in Fig. 2; this section will consider the effects of the alternative ways of closing the loops shown in that figure. There is a continuing debate among pilots as to how the carrier approach should be flown. That is, should altitude be controlled with stick and airspeed with throttle or should altitude be controlled with throttle and airspeed with the stick? Current fleet squadron publications recommend the latter method ($h \rightarrow \delta_T$, $u \rightarrow \delta_e$), although they often say to control airspeed with attitude (i.e., pitch attitude). Many test pilots, on the other hand, recommend the first method ($h \rightarrow \delta_e$, $u \rightarrow \delta_T$). The subject of this debate, "what is the optimum control technique for carrier approach?," may be paraphrased herein to "what are the optimum feedback loops for the pilot to close?" This section will compare the characteristics of three potential methods for controlling the approach by comparing their closed-loop frequency response characteristics.

There are four output variables that the pilot can use for control purposes, as indicated in Fig. 2. These are altitude (relative to the desired glide path), airspeed, angle of attack, and pitch attitude. Of these, both altitude and pitch attitude are discernible to the pilot by reference to the mirror display and horizon. In order to determine airspeed or angle of attack, however, the pilot must shift his focus to scan some instrument within the cockpit area. In addition to the usual instrument panel airspeed indicator, current Navy jet aircraft have an angle of attack "indexer" mounted on the glare shield over the instrument panel. This instrument gives the pilot an "on speed" signal for about 2-1/2 knots either side of the desired approach speed, then indicates "slightly slow (fast)" for the next 2-1/2 knots, and finally indicates slow (fast) for all speeds beyond that range.

The reason airspeed and angle of attack can be referred to synonymously during the approach is that altitude and pitch attitude loops are always

assumed closed by the pilot. If these loops are reasonably tight, then two degrees of freedom are removed from the system and airspeed and angle of attack are closely dependent. The angle of attack indexer is always heavily damped (i.e., lagged) to filter out short-period oscillations, so the resulting low frequency variations give a direct indication of airspeed changes. This assertion is borne out analytically in Appendix C.

Since there are four control variables (h, θ, u, α) and two controls (δ_e, δ_T), a large number of potential control techniques could be studied. Practically, however, the list can be narrowed to three possibilities. These three are discussed in the remainder of this section.

A. PILOT CLOSURE OF THE $\theta \rightarrow \delta_e$ LOOP

It has been assumed in all of the analytical work discussed in following subsections that the pilot always closes a pitch attitude loop, $\theta \rightarrow \delta_e$. In other words, he uses the elevator to hold to his selected approach attitude. There are several justifications for this assumption:

1. It is the only loop useful in controlling short-period motions (remembering that the α indexer is highly damped).

2. It is a powerful way to increase phugoid damping because it effectively provides altitude rate damping (for phugoid motions, where $\alpha \doteq$ constant, $\dot{h} = U_o\gamma \doteq U_o\theta$).

3. There is ample evidence from time histories of carrier approach that the pilot in fact does this (these show a high frequency elevator motion at what would be the closed-loop short-period frequency).

4. The pilot gets benefits 1 and 2, regardless of how he chooses to control altitude or airspeed, merely by controlling his pitch attitude relative to the horizon.

To give a more quantitative example of the benefits of attitude control, a typical carrier-based jet aircraft has a short-period frequency of about 1.5 rad/sec and a lightly damped phugoid ($\zeta_p \doteq 0.10$) with a frequency of about 0.20 rad/sec (see Appendix C). Closing the $\theta \rightarrow \delta_e$ loop with enough "gain" (a measure of the pilot's corrective control movements) to double the short-period frequency will increase phugoid damping to $\zeta_p \geq 0.80$ and

decrease phugoid frequency slightly. The pilot now has an "equivalent airframe" with double the initial static stability and at least an eight-fold increase in phugoid damping, just from closing the $\theta \rightarrow \delta_e$ loop.

With this basic "inner loop" assumed closed, and the resulting well-damped "equivalent airframe," it is instructive to compare the effects of various possible methods of altitude control. This is assumed to be the primary task in a carrier approach, with airspeed control secondary. The following subsections discuss altitude control with elevator, with throttle, and with combined elevator and throttle. The discussions are primarily in terms of the closed-loop frequency response characteristics that the pilot obtains, using the specified control technique. An effort has been made to keep the presentation as nonmathematical as possible, however, so the arguments presented below attempt also to appeal to physical reasoning. Should these arguments not be convincing, recourse may be had to the appendixes for more detailed and technical expositions.

B. ALTITUDE CONTROL WITH ELEVATOR ($h \rightarrow \delta_e$, $\theta \rightarrow \delta_e$, u or $\alpha \rightarrow \delta_T$)

Changes in altitude and airspeed are phugoid phenomena; in other words, they are associated with the low frequency phugoid mode. Closure of one or more control loops does not change this basic situation, but it may change the phugoid frequency and damping significantly. Therefore the effect of a loop closure on altitude control may be described primarily by its influence on the phugoid mode. The types of loop closures to be considered are associated with (1) a simple gain (with reaction time) pilot transfer function (i.e., proportional control), (2) pilot lead adaptation (i.e., proportional plus rate control), and (3) the effect of flight at speeds above and below minimum drag. As was shown in Section II, the pilot must operate through most of the approach as a pure gain in altitude control. Root locus plots in Appendix B show that this loop closure ($h \rightarrow \delta_e$) will increase the phugoid frequency and, initially at least, will cause almost no change in damping (total damping, $\zeta\omega$, as opposed to damping ratio, ζ). As gain is further increased the frequency will continue to increase but damping will begin to deteriorate until the phugoid oscillation finally becomes unstable. Starting from the well-damped condition resulting from the $\theta \rightarrow \delta_e$ inner

loop, the phugoid frequency can typically be increased by a factor of four, e.g., from 0.20 rad/sec to 0.80 rad/sec, before instability results and can almost be doubled at constant damping. This very desirable "stiffening" of the altitude control mode occurs regardless of speed relative to that for minimum drag. The only drawback in the phugoid frequency range is the decrease in damping when the pilot's gain gets too high.

This drawback can be overcome by the addition of altitude rate damping. But, as shown in Section II, pilot-generated lead (i.e., rate damping) comes from his sensing "meatball" vertical velocities and is available only in the last few seconds of the approach. Assuming that a 1-sec lead time constant is the best the pilot can do (see Section II), then the benefit to phugoid damping will only be a slight improvement over the no-lead case, as illustrated in Appendix B (Fig. B-11). Larger lead time constants can greatly improve height control with elevator, but are well beyond human pilot capability using the existing optical landing system for height control. Since the assumed pilot maximum lead of about 1-sec does not give a significant improvement in height control, it is concluded that the system's phugoid characteristics with a straight gain assumed for the pilot transfer function will best represent the altitude-control-with-elevator case. To repeat, these phugoid characteristics are (1) a "stiffening" of frequency for low pilot gains, but (2) a decrease in damping leading to system instability as pilot gain is increased too much.

The final consideration, and a most important one, is the effect of reducing the approach speed below minimum drag. When an $h \rightarrow \delta_e$ loop is closed, a very low frequency time constant is introduced into the system which is associated primarily with the airspeed response of the system. As the aircraft goes from the front to the back side of the drag curve, this time constant shifts from being stable to being unstable. Thus, when trimmed on the back side of the drag curve,* the increased drag, as the

*Comments pertaining to the back or front side of the drag curve, or to speeds below or above that for minimum drag, hereafter imply operation with respect to the speed at which the time constant changes sign. As shown in Ref. 2, this speed, while primarily a function of drag characteristics, is also influenced by thrust variations with speed (for constant throttle setting) and by thrust eccentricities about the c.g. which make the partial derivative of pitching moment with respect to speed, C_{M_u}, nonzero.

aircraft slows down in response to up-elevator motions intended to increase altitude, will actually cause altitude to decrease (after the initial transients die out). Further up-elevator deflections to increase the now steadily decreasing altitude will result in a divergent altitude motion (increasing rate of descent) characterized by the negative time constant alluded to above. Hence comes the pilot's complaint of "ability to control altitude or arrest rate of sink."

The pilot can stabilize this divergent mode by overpowering drag changes with thrust changes. Closure of either an airspeed ($u \rightarrow \delta_T$) or angle of attack ($\alpha \rightarrow \delta_T$) loop with the throttle will perform this function and, in essence, convert the back side condition to an effective front side condition. But the pilot is then required to close a third loop and to use more than some minimum gain in that loop in order to stabilize the system. Requiring such throttle activity on the pilot's part in order to achieve system stability (the highest priority closed-loop system performance criterion postulated in Section II) dictates that he have a "good" display of airspeed or angle of attack error information in order to proportion his throttle corrections. A "good" indicator should (intuitively) be located so the pilot does not have to shift his focus from the meatball, and it should provide a linear and smoothly responding error signal. The cockpit airspeed indicator is essentially inaccessible to the pilot because it requires shifting his gaze completely away from the mirror. The α indexer, mounted on the top of the instrument panel's glare shield, is almost within the pilot's view, but it suffers from the nonlinear nature of its indication (which gives essentially only five speed indications—on speed, slightly slow or fast, and too slow or fast). Since the α indexer does not satisfy the criteria for a "good" display, the pilot's task is made more difficult than necessary for closing this control loop. In support of this assertion it should be noted that when an automatic throttle is installed in an aircraft to perform this function for the pilot, he is willing to reduce his minimum approach speed (see, e.g., Ref. 14).

To summarize the characteristics of altitude control with elevator, the basic phugoid oscillation is stiffened by pilot pure gain, or proportional, control. Damping deteriorates as gain gets high, and the lead equalization

that the system needs is beyond human pilot capability with the present mirror display. These phugoid characteristics occur on both front and back side of the drag curve, but on the back side a drag instability exists that requires pilot closure of an auxiliary throttle loop. Closure of this loop is predicated on a usable display of airspeed or angle of attack error information.

C. ALTITUDE CONTROL WITH THROTTLE ($h \rightarrow \delta_T$, $\theta \rightarrow \delta_e$, u or $\alpha \rightarrow \delta_e$)

Control of altitude with throttle has distinctly different characteristics than control with elevator. In the first place, this method of control does not have the basic instability on the back side of the drag curve that is inherent with the $h \rightarrow \delta_e$ loop closure. The reason for this is that pilot operation of the throttle to hold altitude eliminates the thrust deficiencies that occur with elevator control. So the basic difference in response dynamics between front and back side of the drag curve operation is no longer present.

A second important difference is in the closed-loop phugoid characteristics. Pilot gain in an $h \rightarrow \delta_T$ loop has the effect of decreasing (total) damping of the phugoid while altering frequency only slightly (decreases for low gain, then increases). The low frequency and damping results in large phugoid oscillations and sluggish response. The aircraft becomes more susceptible to the high power but low frequency atmospheric turbulence disturbances which make control difficult.

A final point is that a much larger amount of lead equalization (rate damping), using throttle as the control, is required to make the phugoid characteristics "good" in the sense that elevator control in conjunction with a reasonable lead time constant is good (high frequency and high damping). The cause of these poor closed-loop dynamics is the long time lag between thrust changes and lift changes, too long to be overcome by a reasonable lead. Navy jet aircraft have a low thrust-line angle of attack in the approach configuration, 5° to 20° being typical. Since the pilot is trying to control altitude, or height, he should be using a vertical force. Instead, he is applying a nearly horizontal force and then converting the resulting airspeed change into lift by holding θ, and possibly u or α,

constant with the elevator. This control method has such a long lag between thrust change and height change that even very large load time constants cannot overcome the lift lag and produce a well-damped high frequency system.

In conclusion, then, this method of control is characterized by a deterioration in phugoid response as pilot throttle gain increases. Its only virtue is its basic stability on the back side of the drag curve.

D. ALTITUDE CONTROL WITH ELEVATOR AND THROTTLE ($h \rightarrow \delta_e, \delta_T$; $\theta \rightarrow \delta_e$; u or $\alpha \rightarrow \delta_e, \delta_T$)

The final possibility open to the pilot is to use both stick and throttle to correct the observed errors in altitude (and airspeed or angle of attack). The net effect of this control technique will be to combine the features of the two previous methods, the degree of combination depending on the relative vigor with which stick and throttle are used. In other words, the two preceding methods represent the limiting cases for this more general method.

Considering operation on the back side of the drag curve, the effect of the throttle will be to stabilize the altitude divergence caused by the elevator loop closure. There will be a minimum ratio of throttle to elevator motion required to achieve system stability (eliminate the thrust deficiences), and this minimum value will increase as the (back side) slope of the drag curve increases. On the other hand, as the throttle movements become larger relative to elevator control, the undesirable effect of degrading the phugoid frequency and damping will increase. Obviously there must be some compromise made by the pilot between stabilizing the altitude-divergence mode and destabilizing the phugoid mode. This compromise requires that he very carefully ratio (or coordinate) his stick and throttle movements.

The main advantage of this control technique, then, is the potential combination of the beneficial characteristics of the two other methods, system stability and good phugoid response, without relying on closing an auxiliary u or α loop. The main drawback is the very precise coordination of stick and throttle required of the pilot in order that the optimum balance between these two characteristics be maintained.

E. PILOT OPINION CONSIDERATIONS

Table I, which summarizes the foregoing, shows that the pilot is faced with three choices as regards his basic control of altitude; he can use elevator alone, he can use throttle alone, or he can use a combination of both.

TABLE I

SUMMARY OF PREDOMINANT LOOP-CLOSURE EFFECTS

LOOP	EFFECT ON		
	Phugoid	Short Period	Altitude Control
$\theta \rightarrow \delta_e$	Increases damping considerably, decreases frequency slightly	Decreases damping slightly, increases frequency	No effect
$h \rightarrow \delta_e$	Decreases damping, increases frequency markedly	No major effect	Destabilizes
$h \rightarrow \delta_T$	Decreases damping slightly, decreases then increases frequency	No major effect	Stabilizes
$h \rightarrow \delta_e, \delta_T$	Combines above		

The advantage of elevator alone is the high closed-loop phugoid frequency attainable, which implies a good, fast-responding, altitude tracking system able to suppress atmospheric turbulence inputs and follow carrier motions. However, this system has the disadvantage of requiring a minimum level of auxiliary throttle activity to avoid instability when flying on the back side of the drag curve. The second method is to control altitude with throttle. This sytem is characterized by a low frequency, poorly damped phugoid which implies a sluggish, oscillatory response; but the system is inherently stable. The third system, coordinated stick and throttle control, combines the good features of the other two—high phugoid frequencies with system stability provided by the $h \rightarrow \delta_T$ closure. The drawback is that the pilot must ratio his stick and throttle movements carefully to achieve this good control.

Which method will the pilot use? The argument for his using the first method ($h \rightarrow \delta_e$) is that it gives a fast-responding altitude control. It does, however, require that angle of attack or airspeed information be presented to the pilot in such a way that he can use it. The argument for his using the second method ($h \rightarrow \delta_T$) is that it is initially stable so there is no minimum requirement for system stability. The penalty is that this method has the poorest control characteristics. And finally, coordinating stick and throttle to control altitude ($h \rightarrow \delta_e, \delta_T$) can have the good features of both, but requires a very precise coordination between the two controls.

The answer to what the pilot can or will do depends to a large extent on the pilot's dynamic capabilities in multiple loop tasks (his ability to perform the required sensor-actuator functions utilizing the available information) as well as on the previously described closed-loop system performance characteristics. In the article quoted below (Ref. 15), a Navy test pilot describes the pilot's viewpoint of the system characteristics just discussed.

> "The pilot instinctively attempts to make glide path corrections initially with longitudinal control only. It is therefore extremely desirable that the airplane have maneuvering capability at a constant thrust setting for small changes in angle of attack (approximately 1-2 degrees). If, as in the F8U, these small changes in angle of attack produce correspondingly large excursions in airspeed, the alternative technique must be evaluated, that of varying rate of descent with power. In this type of approach, the airplane is maintained at a desired angle of attack and thrust corrections are used exclusively to make glide path corrections. . . When the desired vertical accelerations cannot be obtained with this technique, as in the case with the F8U, a combination of two techniques is required in which both thrust and longitudinal control are initiated simultaneously. This technique produces the necessary rapid corrections in glide path although it requires precise coordination throughout the control process."

The pilot is saying, then, that his priority ranking of the systems is the same as the order in which they were discussed, except that he seems to rule out elevator-alone control of altitude below minimum drag speed. From the systems analysis point of view this is clearly the wrong thing for him to do, yet the next section presents an analytical development which gives convincing evidence that the pilot in fact does choose the throttle-control-of-altitude method. The last section presents some possible arguments as to why this should be so.

SECTION IV

A MINIMUM APPROACH SPEED CRITERION DERIVED FROM SIMPLIFIED MULTIPLE LOOP CONSIDERATIONS

A. DERIVATION OF THE CRITERION

The previous section has shown the advantages and disadvantages of the various control techniques that are available to the pilot for making the approach. In this section one particular control method will be used as the basis for deriving a criterion for predicting the minimum acceptable approach speed.* For the analysis, it is assumed that the pilot uses the elevator to control pitch attitude and the throttle to control altitude. The analytical expression for the closed-loop phugoid frequency, in terms of aircraft stability parameters and pilot gain terms, is derived from a simplified set of equations. Then it is shown that at a certain speed below minimum drag this closed-loop frequency begins to decrease as pilot gain in the elevator loop increases. Reasons are explained why this should represent the minimum acceptable approach speed in terms of altitude control.

A review of the conclusions drawn in Section III indicates that altitude control problems in the approach are low frequency in nature; that is, they are associated with the (closed-loop) phugoid motions of the aircraft. This qualitative assertion is borne out quantitatively in Appendix B, where it is shown that the phugoid branch of the altitude control root locus is the one presenting control problems. This occurs regardless of the control technique chosen by the pilot, but most pronouncedly so when the pilot attempts to control flight path with throttle. Since short-period attitude control is generally not a problem, it is safe to neglect the short-period terms in the equations of motion and look only at the phugoid equations. This has the advantage of reducing the order of the equations to the point where they provide easily factored solutions. Since the phugoid frequencies are of the order of 0.2 rad/sec, pilot reaction time, τ, will contribute only slightly

*Reference 9 contains a preliminary exposure of these results.

in this region and need not be included in the pilot model. Also, since lag equalization is generally not helpful here (Appendix B) and lead time constants, T_L, corresponding to the pilot's desired maximum of about 1 sec have no benefit, the influences of pilot equalization in the frequency region of interest will also be negligibly small. Both τ and T_L effects will contribute phase angle changes of only a few degrees at these low frequencies and therefore cannot affect the results. Thus the pilot transfer functions can be approximated as pure gains (simple proportional control):

$$Y_{\delta_e\theta} = \frac{\partial\delta_e}{\partial\theta_\epsilon} = K_{p_\theta}$$

$$Y_{\delta_T h} = \frac{\partial\delta_T}{\partial h_\epsilon} = K_{p_h} \qquad (6)$$

The phugoid equations of motion (Ref. 2), assuming $X_{\delta_e} = 0$, are

$$\begin{array}{lllll} (s - X_u)u & -X_w w & +g\theta & +0 & = X_{\delta_T}\delta_T \\ -Z_u u & +(s - Z_w)w & -U_o s\theta & +0 & = Z_{\delta_T}\delta_T + Z_{\delta_e}\delta_e \\ -M_u u & -M_w w & +0 & +0 & = M_{\delta_T}\delta_T + M_{\delta_e}\delta_e \\ 0 & w & -U_o\theta & +sh & = 0 \end{array} \qquad (7)$$

where the last equation expresses the kinematic relationship between altitude, h, and the independent degrees of freedom, u, w, θ. Recognizing that Eq 6 may be rewritten as

$$\delta_e = K_{p_\theta}\theta_\epsilon = -K_{p_\theta}\theta \qquad (8)$$

$$\delta_T = K_{p_h}h_\epsilon = -K_{p_h}h \qquad (9)$$

(because the "error signal" to the pilot is the reverse of the aircraft's motion), substitution of Eq 8 and 9 into the right side of Eq 7 eliminates

the control deflection variables and yields a new set of equations with "equivalent stability derivatives." This set of equations gives a new characteristic determinant, which is the system's closed-loop characteristic equation. It can be expressed in the form

$$as^3 + bs^2 + cs + d = 0 \tag{10}$$

where the coefficients a through d contain aircraft stability derivatives and pilot gain terms. This closed-loop equation can then be factored into the form

$$K\left(s + \frac{1}{T_{h_T}''}\right)\left(s^2 + 2\zeta_p''\omega_p''s + \omega_p''^2\right) \quad 0 \tag{11}$$

(the double prime notation indicates two loops have been closed), and the closed-loop system tested to see if it meets the pilot's system requirements (performance criteria). This procedure is the one followed in Ref. 9 and completely avoids the use of servoanalytic methods. However, a more instructive procedure, to follow, uses the conventional servoanalysis method of successive loop closures, rather than the "augmented derivative" approach, to arrive at the same result. More insight into the effect of each closure can be gained by this latter method, as will be demonstrated. Transfer function equations for the multiple feedback loops involved are derived in Appendix A for three degrees of freedom, and since the basic process is the same, no justification of the specialized phugoid transfer function form used here will be presented.

The open outer-loop transfer function for throttle control of altitude, with a $\theta \rightarrow \delta_e$ inner loop closed, may be written

$$\left(\frac{h}{\delta_T}\right)_{\theta \rightarrow \delta_e} = \frac{N_{h_{\delta_T}} + Y_{\delta_e\theta} N^{h\ \theta}_{\delta_T \delta_e}}{\Delta + Y_{\delta_e\theta} N_{\theta_{\delta_e}}} \tag{12}$$

where the various terms of interest in this case are:

$$N_{h\delta_T} = \left(Z_{\delta_T}M_\alpha - M_{\delta_T}Z_\alpha\right)\left(s + \frac{1}{T_{h_T}}\right), \quad \text{the } h \rightarrow \delta_T \text{ transfer function numerator (phugoid only)}$$

$$N^{h\ \theta}_{\delta_T\delta_e} = \left(M_{\delta_T}Z_\alpha - Z_{\delta_T}M_{\delta_e}\right)\left(s + \frac{1}{T_{h,\theta}}\right), \quad \text{the } h \rightarrow \delta_T,\ \theta \rightarrow \delta_e \text{ coupling numerator}$$

$$\Delta = -M_\alpha s\left(s^2 + 2\zeta_p\omega_p s + \omega_p^2\right), \quad \text{the open-loop characteristic (phugoid only)}$$

$$N_{\theta\delta_e} = M_{\delta_e} s\left(s + \frac{1}{T_{\theta_1}}\right)\left(s + \frac{1}{T_{\theta_2}}\right), \quad \text{the } \theta \rightarrow \delta_e \text{ transfer function numerator (phugoid only)}$$

$$Y_{\delta_e\theta} = K_{p_\theta}\ ;\ Y_{\delta_T h} = K_{p_h} \quad \text{see Eq o}$$

The closed-loop will be determined in two steps, by first closing the $\theta \rightarrow \delta_e$ loop and then the $h \rightarrow \delta_T$ loop. Adding the two denominator terms in Eq 12 gives the new characteristic equation with the $\theta \rightarrow \delta_e$ inner loop closed:

$$-M_\alpha\left(1 - K_{p_\theta}\frac{M_{\delta_e}}{M_\alpha}\right)s\left(s^2 + 2\zeta_p'\omega_p' s + \omega_p'^2\right)$$

$$= -M_\alpha s\left\{\left(1 + K_\theta\right)s^2 + \left(2\zeta_p\omega_p + K_\theta\left[\frac{1}{T_{\theta_1}} + \frac{1}{T_{\theta_2}}\right]\right)s + \left(\omega_p^2 + K_\theta\frac{1}{T_{\theta_1}T_{\theta_2}}\right)\right\} \quad (13)$$

where the single prime notation denotes one loop has been closed. Equating coefficients identifies

$$K_\theta = -K_{p_\theta}\frac{M_{\delta_e}}{M_\alpha} \quad (14)$$

$$2\zeta_p'\omega_p' = \frac{2\zeta_p\omega_p + K_\theta\left(\frac{1}{T_{\theta_1}} + \frac{1}{T_{\theta_2}}\right)}{1 + K_\theta} \quad (15)$$

$$\omega_p'^2 = \frac{\omega_p^2 + K_\theta\frac{1}{T_{\theta_1}T_{\theta_2}}}{1 + K_\theta} \quad (16)$$

In finding the $\theta \rightarrow \delta_e$ loop effect on the altitude control numerator, it is now assumed for simplicity that the thrust line passes through the c.g. of the aircraft. For this special case, $M_{\delta_T} = M_u = 0$, and the two time constants associated with the numerator of Eq 12 can be shown to be identical, i.e.,

$$\frac{1}{T_{h,\theta}} = \frac{1}{T_{h_T}} = -X_u + \frac{X_{\delta_T}}{Z_{\delta_T}} Z_u \tag{17}$$

The altitude control zero, $1/T'_{h_T}$, thus is not a function of K_θ and is in fact also given by Eq 17.

Equation 12, the altitude control open-loop transfer function, with the $\theta \rightarrow \delta_e$ inner loop closed, has been factored in steps 13 through 17 and is now:

$$\left(\frac{h}{\delta_T}\right)_{\theta \rightarrow \delta_e} = \frac{-Z_{\delta_T}\left(s + \frac{1}{T'_{h_T}}\right)}{s\left(s^2 + 2\zeta'_p\omega'_p s + \omega'^2_p\right)} \tag{18}$$

The altitude loop must now be closed to obtain the characteristic equation of the system: the sum of the numerator and denominator of the open-loop transfer function (where the open-loop transfer function is $K_{p_h}(h/\delta_T)_{\theta \rightarrow \delta_e}$). Equating this sum to the general form for a factored cubic equation gives

$$\left(s + \frac{1}{T''_{h_T}}\right)\left(s^2 + 2\zeta''_p\omega''_p s + \omega''^2_p\right) = s^3 + 2\zeta'_p\omega'_p s^2 + (\omega'^2_p + K_h)s + K_h \frac{1}{T'_{h_T}} \tag{19}$$

where $K_h = K_{p_h}(-Z_{\delta_T})$.

By way of illustrating the mathematical process which has been carried out, typical root locus plots which correspond to the two loop closures indicated by Eq 12 and 18 are shown in Fig. 3. In this figure, the inner-loop ($\theta \rightarrow \delta_e$) closure results in the single-primed quantities corresponding to those in Eq 13 and 18 for a given gain, K_θ (indicated by the symbol ■). These quantities are the open-loop poles of the altitude control outer loop and are accordingly transferred (as symbol ✕) to the outer-loop plot. The

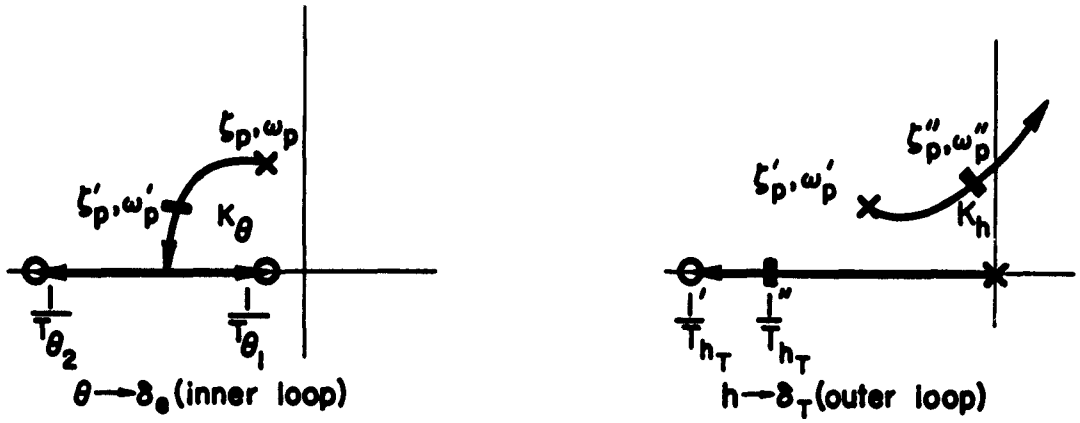

Figure 3. Root Locus Illustration of Successive Loop Closures

second closure, corresponding to a given value of K_h, yields the double-primed quantities of Eq 19 (again indicated by the symbol ■). A coupling closure required in the general case to determine the value of $1/T'_{h_T}$ (compare Eq 12 and 18) is not required because of Eq 17 which holds for $M_{\delta_T} = M_u = 0$, the case of interest here.

Anticipating, now, the final result, it is desired to find the effect of the inner-loop gain, K_θ, on ω''_p, the final closed-loop phugoid frequency at which altitude oscillations will occur. If some arbitrary value of phugoid damping ratio is assumed to be the pilot's altitude loop closure criterion, then specifying this damping ratio will uniquely specify the altitude control gain, K_h, for the <u>given</u> attitude gain, K_θ, already chosen in closing the attitude control inner loop. If the pilot sets his throttle gain to achieve this damping ratio,(damping ratio is a response factor most evident to him), then the closed-loop system performance is specified. Assuming, purely for mathematical convenience, a closed-loop damping ratio of zero ($\zeta''_p = 0$), the closed-loop frequency, ω''_p, may be determined as follows:

Expanding the left side and then equating coefficients in Eq 19,

$$s^2 \text{ terms: } \frac{1}{T''_{h_T}} + 2\zeta''_p\omega''_p = 2\zeta'_p\omega'_p$$

$$s \text{ terms: } \frac{1}{T''_{h_T}} 2\zeta''_p\omega''_p + \omega''^2_p = \omega'^2_p + K_h \tag{20}$$

$$\text{Constant terms: } \frac{1}{T''_{h_T}} \omega''^2_p = K_h \frac{1}{T'_{h_T}}$$

Setting $\zeta''_p = 0$ in the above equations and eliminating K_h and T''_{h_T} yields

$$(\omega''_p)^2_{\zeta''_p = 0} = \frac{\frac{1}{T'_{h_T}} \omega'^2_p}{\frac{1}{T'_{h_T}} - 2\zeta'_p\omega'_p} \tag{21}$$

Noting that $1/T'_{h_T}$ is independent of K_θ for this special case, the single-primed quantities are defined in Eq 15, 16, and 17, and Eq 21 can be written in the more basic form

$$(\omega''_p)^2_{\zeta''_p = 0} = \frac{\frac{1}{T_{h_T}} \left(\omega_p^2 + K_\theta \frac{1}{T_{\theta_1} T_{\theta_2}} \right)}{\left[(1 + K_\theta) \frac{1}{T_{h_T}} - 2\zeta_p\omega_p - K_\theta \left(\frac{1}{T_{\theta_1}} + \frac{1}{T_{\theta_2}} \right) \right]} \tag{22}$$

Equation 22 indicates that for $\zeta''_p = 0$ (and the general trends of Fig. 3 indicate that the results are not appreciably altered by small, finite values of ζ''_p) the closed-loop phugoid frequency is a function only of the pilot's θ-loop gain and of basic aircraft stability parameters. In order to find the effect of that θ-loop gain on the phugoid frequency, the partial derivative is taken, giving

$$\frac{\partial (\omega''_p)^2_{\zeta''_p = 0}}{\partial K_\theta} = \frac{\frac{1}{T_{\theta_1} T_{\theta_2}} \left(\frac{1}{T_{h_T}} - 2\zeta_p\omega_p \right) + \omega_p^2 \left(\frac{1}{T_{\theta_1}} + \frac{1}{T_{\theta_2}} - \frac{1}{T_{h_T}} \right)}{T_{h_T} \left[(1 + K_\theta) \frac{1}{T_{h_T}} - 2\zeta_p\omega_p - K_\theta \left(\frac{1}{T_{\theta_1}} + \frac{1}{T_{\theta_2}} \right) \right]^2} \tag{23}$$

The form of Eq 23 indicates the possibility of a change in sign for some combination of the numerator parameters, which are all functions of airspeed. It can (and will) be shown that this partial derivative is always positive for flight on the front side of the drag curve but that at an airspeed somewhere on the back side of the drag curve it becomes zero, and, as speed is further decreased, it becomes increasingly negative.

What is the significance of this sign reversal in terms of flying qualities? The answer to this question may be determined by considering, in frequency response terms, what the pilot wants for a closed-loop control system. Since the phugoid frequencies are low, implying "sluggish response" to altitude control efforts, the pilot's primary desire is to "tighten up" this system by increasing the frequency (or, in servo parlance, the bandwidth) of response. Furthermore, if he is making the approach through turbulent air, it may be <u>imperative</u> that he increase the frequency in order to overcome the gust spectrum inputs disturbing his aircraft. His normal reaction will be to increase the gain in the attitude control loop; in other words, to tighten up his elevator control. This increases inner-loop phugoid damping, and, for flight on the front side of the drag curve, it also increases ω_p''. But at some speed on the back side of the drag curve, tighter elevator control suddenly begins to degrade the aircraft's altitude response by decreasing its bandwidth characteristic. The pilot senses that his normal elevator control reactions are making altitude errors larger, yet he cannot remedy the situation because increasing throttle gain only decreases the phugoid damping. Decreasing his elevator gain allows larger pitch attitude oscillations although helping altitude control. Presumably this "control reversal" effect, if it may be so termed, will be disconcerting enough to make the pilot limit his approach to speeds at or above the reversal point.

A possible criterion for the minimum acceptable approach speed, based on the previous argument, is therefore the reversal point given by setting the partial derivative of Eq 23 to zero,

$$\frac{1}{T_{\theta_1} T_{\theta_2}} \left(\frac{1}{T_{h_T}} - 2\zeta_p \omega_p \right) + \omega_p^2 \left(\frac{1}{T_{\theta_1}} + \frac{1}{T_{\theta_2}} - \frac{1}{T_{h_T}} \right) = 0 \qquad (24)$$

Eq 24 being valid for cases where the thrust line of the aircraft passes through the c.g.

A review of all the assumptions made in the foregoing derivation may be useful in clarifying the development. These were as follows:

1. Phugoid equations adequately represent the frequency region of interest
2. The pilot controls pitch attitude with elevator and altitude with throttle, and may be approximated by a simple gain in each loop
3. The final closed-loop phugoid damping ratio is zero
4. The thrust line offset from the aircraft c.g. is zero

Assumptions 1 and 2 are not restrictive; that is, they are basic to the handling qualities theory. Assumption 3 was made to predetermine the magnitude of the pilot's altitude control gain; and the specific value of $\zeta_p'' = 0$ was chosen merely to simplify the form of the criterion. In justification of Assumption 3, it should be noted that for second-order systems in single-loop tasks, at least, the pilot seems to set his gains to get a constant damping ratio (or phase margin). The altitude control root locus in Fig. 3 indicates that phugoid frequency increases as the damping ratio decreases in the region near neutral stability. Therefore the pilot can trade off ζ_p'' and ω_p'' or vice versa, in order to minimize his altitude errors. It is difficult to predict what specific value of damping he would probably choose, but <u>any</u> constant value will serve to show the <u>trend</u> of ω_p'' as K_θ changes.

The final assumption was made so that $1/T_{h_T'}$ would equal $1/T_{h_T}$. When there is a finite thrust offset, $1/T_{h_T'}$ becomes a function of the attitude gain, K_θ, and the criterion in the form of Eq 24 is not valid. Then, to find the speed at which the derivative is zero, it is simplest to revert to the basic formula for $\omega_p''^2$ given in Eq 21, use two representative values of K_θ to compute values of $1/T_{h_T'}$, $\omega_p'^2$, $2\zeta_p'\omega_p'$, and finally $\omega_p''^2$; and take the derivative as the ratio, $\Delta\omega_p''^2/\Delta K_\theta$. Values of K_θ of 1.0 and 2.0 are typical for pilot attitude control and have been used in specific cases to compute this derivative; furthermore, the point of zero slope has been found to be more sensitive to airspeed than to different (but reasonable) values of K_θ. Thus the original assumption that the thrust line offset is zero can be bypassed when necessary and does not restrict the general applicability of the suggested criterion.

B. TESTING THE CRITERION: AGREEMENT BETWEEN PREDICTIONS AND FLIGHT TEST MINIMUM APPROACH SPEEDS

Seven of the 21 aircraft for which aerodynamic data are tabulated in Ref. 1 are specifically limited in carrier approach speed by "the ability to control altitude or arrest rate of sink." For all seven, the minimum speed was on the back side of the thrust-required curve. These seven are the F8U-1, F7U-3, F4D-1, F-100A, F-84F, F11F-1, and F9F-6. Transfer functions were computed for each aircraft for at least three flight conditions corresponding to the flight-test-determined minimum approach speed plus and minus about seven knots. The partial derivative $(\partial\omega_p''^2/\partial K_\theta)_{\zeta_p''=0}$ was evaluated for each aircraft at each speed using the general procedure outlined above. Values of $K_\theta = 1.0$ and 2.0 were used to compute $\omega_p''^2$ from Eq 22, and the derivative was assumed to be given by the difference, i.e.,

$$\frac{\partial\omega_p''^2}{\partial K_\theta} = (\omega_p''^2)_{K_\theta = 2} - (\omega_p''^2)_{K_\theta = 1} \tag{25}$$

Two aircraft with no thrust line offset from the c.g., the F4D-1 and the F9F-6, were computed in the same way rather than using Eq 23, primarily for consistency.

The results of the calculations are plotted in Fig. 4 in the form of criterion derivative versus airspeed. The individual points for each aircraft are jointed by straight lines because no other particular form of curve-fairing seemed appropriate for so few points. The airspeed at which the line crosses $\partial\omega_p''^2/\partial K_\theta = 0$ is then the criterion minimum approach speed. These predicted speeds are compared with actual flight test results, taken from Ref. 1, in Table I.

For the F-100A and F9F-6 the value of the criterion derivative is still positive in the speed range considered limiting by the pilots. In other words some factor other than "reversal" appears to be limiting for these two cases. For the five aircraft for which the criterion predicts a minimum speed, that speed is close enough to the flight test speed(s) to be considered a valid prediction. This fact must be considered impressive evidence that the pilot is using throttle to control altitude. Yet this was shown in

TABLE II

COMPARISON OF CRITERION-PREDICTED
MINIMUM APPROACH SPEED AND FLIGHT TEST SPEED(S)

AIRCRAFT	FLIGHT TEST SPEED (Knots)	CRITERION SPEED (Knots)
F8U-1	133, 134, 135	132
F7U-3	108,* 115, 117	109
F4D-1	114,* 117, 119, 120	121
F-84F	132*	131
F11F-1	128, 131	125
F-100A	157*	None predicted for $U_o > 140$
F9F-6	115, 118	None predicted for $U_o > 108$

*FCLP (field carrier landing practice) result

Section III to be the poorest method (in terms of servo performance) of altitude control. This raises the fundamental question of why the pilot has chosen the nonoptimum system; possible explanations for his choice are postulated in the following section.

One further item requires comment. When the F4D-1 values of $\omega_p''^2$ were first computed, the reversal derivative came out negative at all speeds around the flight test V_{min}; in other words, the F4D-1 was below its theoretical minimum. While rechecking the aerodynamic data it was noted that the F4D-1 has a large elevator drag term, X_{δ_e} being on the order of $0.30\ Z_{\delta_e}$. This factor had been neglected in the machine program computing the $\theta \rightarrow \delta_e$ transfer functions since it is normally small, and when it was included in those computations the criterion was successful in predicting the approach speed. This fact has important design implications because it indicates that a large positive $C_{D_{\delta_e}}$ significantly reduced the F4D-1 approach speed (or at least the criterion-predicted approach speed).

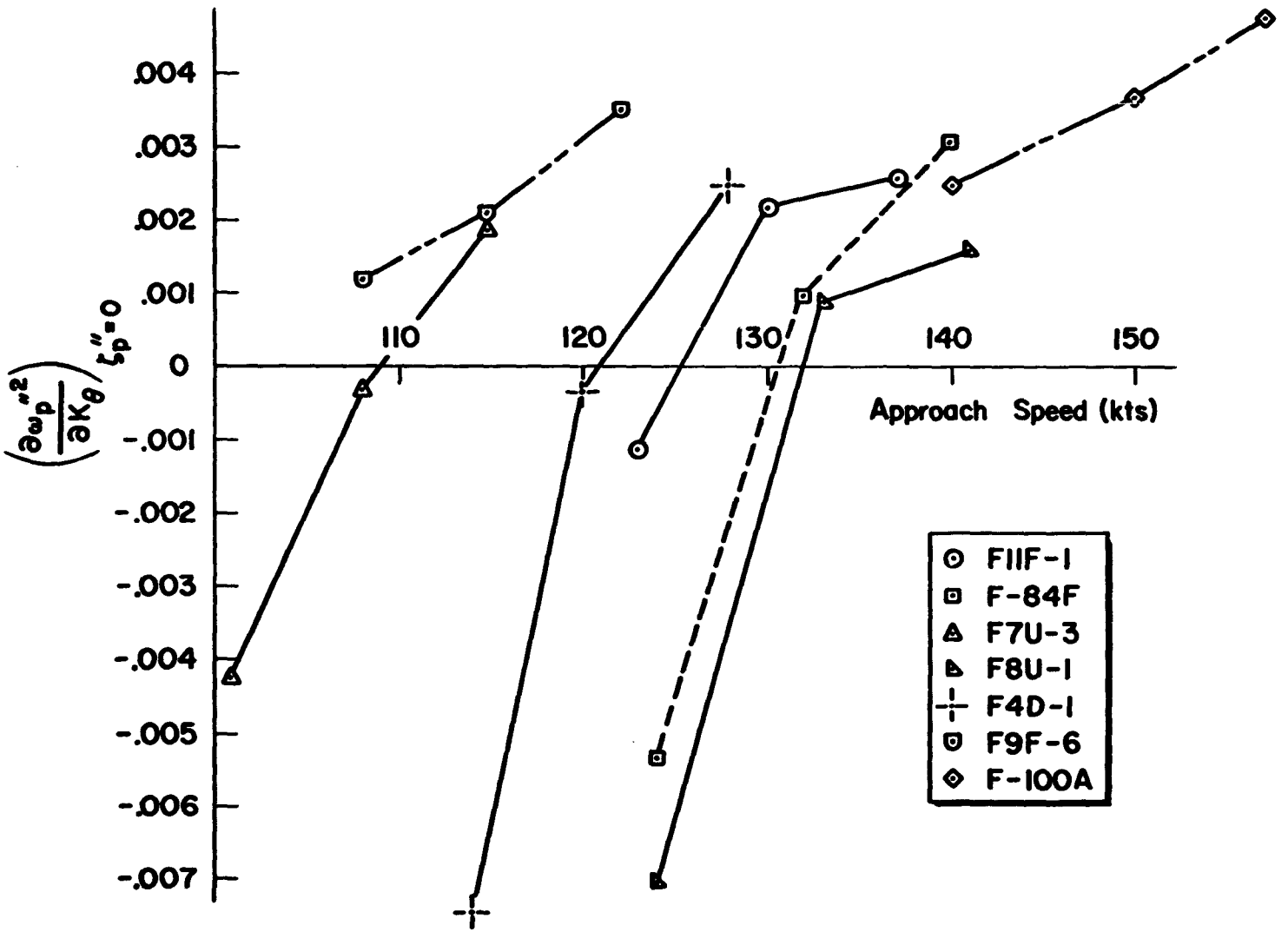

Figure 4. Criterion Versus Approach Speed

SECTION V

SUMMARY AND CONCLUSIONS

Multiple-loop analyses have disclosed that required piloting techniques differ considerably between approaches made on the "back" and on the "front" side of the drag curve. In the latter instance, the pilot can theoretically make flight path corrections with the elevator alone, and does not need throttle inputs except for "initial" trim power adjustments. Reference 15 points out that this is the natural way to fly the approach. However, when the speed is decreased below minimum drag speed, the closed-loop system becomes unstable if the pilot uses the stick as his altitude controller.

Several courses of action are then possible, depending on the type and quality of information available to the pilot. Assuming only that available by reference to the mirror-approach display (altitude-error and attitude), he can theoretically stabilize and control the system, for speeds less than minimum drag, by controlling attitude with elevator and altitude with throttle. The resulting closed-loop performance would appear marginal in terms of bandwidth, especially for rough air and/or sea-state conditions. But as speed is progressively reduced, the achievement of even this marginal performance eventually becomes "negatively dependent" on elevator control. Thus, while increasing "tightness" of attitude control with elevator improves performance at speeds well above the approach speed, a similar increase in attitude control "tightness" eventually begins to degrade performance as speed is reduced. Such degradation is sure to be considered undesirable because it means that the pilot, by trying harder to control the system, is actually making it worse.

Calculated minimum approach speeds based on incipient degradation (i.e., zero effect of "tightening" elevator control), match well with flight test minimum speeds for five of seven aircraft suspected to be speed-limited specifically by the "ability to control altitude." Although such corroborating evidence is not completely conclusive, it lends considerable support to the argument that, for aircraft operating on the back side of the drag curve,

1. Pilots choose to control altitude with throttle (in addition to controlling attitude with elevator). Other methods with theoretically superior dynamic performance are bypassed.

2. The "control reversal" effect, associated with this pilot-selected method of control is sufficiently disconcerting to limit the minimum approach speed. The speed for incipient reversal therefore provides an easily calculated criterion for minimum approach speed.

But what of the other control methods that are available to the pilot? Assuming the additional information provided by suitable angle of attack or airspeed displays, the pilot can theoretically use the elevator for height and attitude control, and throttle to hold angle of attack or airspeed constant. Essentially, the throttle manipulations involved in this mode of operation reverse the "backside" effect of an increase in drag as speed decreases to an "effective frontside" net decrease in drag as speed decreases. Thus the pilot gets good longitudinal response as long as he is able to maintain thrust required with the throttle.

Another alternative is to coordinate stick and throttle to control altitude. This theoretically eliminates the need for a good airspeed or angle of attack indicator and also permits the pilot to fly the approach using only two feedback loops. The benefits of fast-responding elevator control and stable throttle control are obtained at the expense of a requirement for very carefully coordinated stick and throttle action.

In the course of arriving at these conclusions, other more complicated (up to five feedbacks) modes of control have also been investigated analytically. Although some of these were found to result in suitable systems, they are, in the final analysis, considered inappropriate because the gains in performance (if any) are not commensurate with the increase pilot effort required.

Both of the alternative piloting techniques discussed above are theoretically superior to the throttle-alone method of controlling altitude in the approach. They both should eliminate the "ability to control altitude or

arrest rate of sink" as a dynamic control problem in carrier approach. The question then arises as to why this type of limitation apparently exists, since α information is displayed in all current carrier aircraft. Also, why is a criterion based on only altitude and pitch attitude information so successful in predicting the speed at which this limitation occurs? If it is assumed that the criterion's success indicates that the pilot does in fact use throttle to control altitude, it must then be explained why he has chosen the nonoptimum system. The following are possible explanations:

1. The nonlinear type of α indexer installed in fleet aircraft prevents effective pilot use of this device, thus requiring that the pilot revert to the other ($h \rightarrow \delta_T$) technique.

2. It is beyond the pilot's dynamic capabilities to effectively close three loops and use the α indexer in multiple-loop tasks.

3. The closed-loop performance benefits which the pilot is dynamically capable of achieving by the best method are not required due to the low frequency content of the forcing function (carrier wake, atmospheric turbulence, carrier motions).

4. The pilot is unaware of the benefits to be gained by close control of α with throttle, and is performing the simpler task (two loops versus three) which still yields acceptable results.

These explanations have one common factor: they depend on assumptions as to the pilot's actual performance in the loop. The analyses used as the basis for this report's conclusions are all predicated on extrapolating actual human transfer function measurements in single-loop tracking tasks to predicted behavior in multiple-loop flight control situations. To investigate these predictions and to answer other questions which may arise, it is necessary to perform a series of well-designed flight simulator experiments. Results of such experiments which are inconsistent with the present mathematical pilot model will give rise to refinements in the analysis process which may in turn lead to auxiliary experiments. This type of experimental program, and the attendant analysis-refinement activities, is a logical extension of the purely analytical work reported herein. It is worth noting

that, as in the classical scientific process, a theory has been derived, and a series of experiments can be evolved to test the theory. To complete the process requires that results of an experimental program be fed back into refinement of the original postulates.

A final theoretical prediction is in order. The discussions in Section III stated that elevator-alone control of altitude, with either u or α controlled by throttle, produced the best response characteristics of the three possibilities studied. When automatic throttles are installed in an aircraft, the pilot is of necessity forced to control altitude with elevator since he no longer manipulates the throttle. Experimental flight test programs have verified this system because lower minimum approach speeds have resulted (Ref. 14). Section III also stated that the optimum system resulted when a large lead time constant was added to the altitude loop to damp the phugoid, but that such leads were beyond human pilot capability with the mirror type of optical height display. In order to produce significant lead, the pilot would have to be given aircraft vertical sink rate information. Therefore the optimum system for carrier approach will consist of an automatic throttle control and some form of projected or "heads-up" display of aircraft sink speed. Exactly how this display would be presented would have to be determined experimentally. But there would seem to be no question that this information will greatly help the pilot in the carrier approach.

REFERENCES

1. Eberle, R. B., D. B. Schoelerman, and N. A. Smykacz, Criteria for Predicting Landing Approach Speed Based on an Analog Computer Analysis of 21 Jet-Propelled Aircraft, Chance Vought Report AER-EOR-13202, 25 October 1960.

2. Ashkenas, Irving L., and Duane T. McRuer, Approximate Airframe Transfer Functions and Application to Single Sensor Control Systems, WADC TR 58-82, June 1958.

3. McRuer, Duane T., and Ezra S. Krendel, Dynamic Response of Human Operators, WADC TR 56-524, October 1957. (ASTIA AD 110 693)

4. Ashkenas, I. L., and D. T. McRuer, The Determination of Lateral Handling Quality Requirements from Airframe-Human Pilot System Studies, WADC TR 59-135, June 1959.

5. McRuer, Duane T., Irving L. Ashkenas, and C. L. Guerre, A Systems Analysis View of Longitudinal Flying Qualities, WADD TR 60-43, January 1960. (ASTIA AD 249 386)

6. Jex, Henry R., and Charles H. Cromwell, III, Theoretical and Experimental Investigation of Some New Longitudinal Handling Qualities Parameters, ASD TR 61-26, March 1961.

7. Harper, Robert P., Jr., In-Flight Simulation of Re-Entry Vehicle Handling Qualities, IAS Paper No. 60-93, June 1960.

8. Durand, T. S., and H. R. Jex, Handling Qualities in Single-Loop Roll Tracking Tasks: Theory and Simulator Experiments, ASD-TDR-62-507, May 1962.

9. Ashkenas, I. L., and D. T. McRuer, A Theory of Handling Qualities Derived from Pilot-Vehicle System Considerations, IAS Paper No. 62-39, January 1962.

10. Dynamics of the Airframe, Northrop Aircraft, Inc., BuAer Report AE-61-4II, September 1952.

11. D. T. McRuer, I. L. Ashkenas, and H. R. Pass, Analysis of Multiloop Vehicular Control Systems, ASD-TDR-62-1014, December 1962.

12. Cromwell, C. H., Review of "In-Flight Measurement of the Time Required for a Pilot to Respond to an Aircraft Disturbance," Helmut A. Kuehnel, NASA TN D-221, March 1960, Systems Technology, Inc., TM-58-III, 29 July 1960.

13. Kuehnel, Helmut A., In-Flight Measurement of the Time Required for a Pilot to Respond to an Aircraft Disturbance, NASA TN D-221, March 1960.

14. Lina, L. J., R. A. Champine, and G. J. Morris, Flight Investigation of an Automatic Throttle Control in Landing Approaches, NASA Memo 2-19-59L, March 1959.

15. Rapp, Fred L., Lt. Cmdr., Determination of Optimum Approach Speeds for Carrier Landings, Naval Weapons Bulletin No. 3-61, September 1961.

16. Lindquist, Dean C., A Statistical Evaluation of Airplane Structural Landing Parameters in Mirror-Aid Landing Operations Aboard Aircraft Carriers, Bureau of Aeronautics Report No. AD-224-1, April 1959.

17. McRuer, Duane T., Unified Analysis of Linear Feedback Systems, ASD-TR-61-118, July 1961. (ASTIA AD 270 593)

APPENDIX A

DERIVATION AND SUMMARY OF TRANSFER FUNCTIONS FOR BOTH SINGLE-LOOP AND MULTIPLE-LOOP CONTROL

The linearized longitudinal equations of motion for an aircraft in a general flight condition are developed in Ref. 10. If those very general equations are further specialized by dropping terms negligible in carrier approach,* the equations can be written, in Laplace transform style, with stability axes, and assuming inputs only from control deflections, as follows:

$$(s - X_u)u \quad -X_w w \quad +g\theta = X_\delta \delta \qquad \text{(A-1)}$$

$$-Z_u u \quad +(s - Z_w)w \quad -U_o s\theta = Z_\delta \delta \qquad \text{(A-2)}$$

$$-M_u u \quad -(\dot{M}_w s + M_w)w \quad +(s^2 - M_q s)\theta = M_\delta \delta \qquad \text{(A-3)}$$

These are the usual basic longitudinal equations, in dimensional stability derivative form, that are used for stability and control analysis. Since altitude control has a major role in carrier approach, an additional kinematic equation relating aircraft variables to change in altitude may be written, again using Laplace transform notation,

$$\begin{aligned} \sin\gamma = \gamma &= \dot{h}/U_o \\ \gamma &= \theta - \alpha \\ sh &= U_o\theta - U_o\alpha \end{aligned} \qquad \text{(A-4)}$$

If this equation is added to the previous three, a general set of four equations is formed which can be solved simultaneously to yield solutions for u, w, θ, or h. Making the usual change in variable of

$$\alpha = w/U_o \qquad \text{(A-5)}$$

gives the basic set of equations used in this report.

$$\begin{array}{lllll} (s - X_u)u & -X_\alpha\alpha & +g\theta & +0 & = X_\delta\delta \\ -Z_u u & +U_o(s - Z_{\dot{w}})\alpha & -U_o s\theta & +0 & = Z_\delta\delta \\ -M_u u & -(M_{\dot{\alpha}}s + M_\alpha)\alpha & +(s^2 - M_q s)\theta & +0 & = M_\delta\delta \\ 0 & +U_o\alpha & -U_o\theta & +sh & = 0 \end{array} \qquad \text{(A-6)}$$

---

*For example, the difference between level flight and a glide path of -4 deg was checked and found to be insignificant.

If the control inputs are assumed to be zero, the classical "characteristic equation" is the solution of the set of Eq A-6. This will be denoted $U_o s\Delta$ in this report, which makes Δ represent the standard fourth order solution shown in factored generalized form:

$$U_o s\Delta = U_o s(s^2 + 2\zeta_p\omega_p s + \omega_p^2)(s^2 + 2\zeta_{sp}\omega_{sp} s + \omega_{sp}^2) \qquad \text{(A-7)}$$

where the approximate factors (Ref. 2) are:

$$\begin{aligned}
\omega_{sp}^2 &\doteq Z_w M_q - M_\alpha \\
2\zeta_{sp}\omega_{sp} &\doteq -(Z_w + M_q + M_{\dot{\alpha}}) \\
\omega_p^2 &\doteq \frac{g(M_w Z_u - M_u Z_w)}{Z_w M_q - M_\alpha} \\
2\zeta_p\omega_p &\doteq -X_u - \frac{M_u(X_\alpha - g)}{Z_w M_q - M_\alpha}
\end{aligned}$$

(As a quick check that Eq A-7 is the solution of Eq A-6 with $\delta = 0$, the equations may be solved by determinants. Breaking down the 4 x 4 determinant by going down the right hand, or h, column, it may be seen that the only term remaining is s times the usual 3 x 3 determinant, yielding $U_o s\Delta$.)

To obtain numerator transfer functions from Eq A-6, the usual method of determinants (see Ref. 10) may be employed. As an example, the θ/δ transfer function is denoted

$$\frac{\theta}{\delta} = \frac{U_o s N_{\theta_\delta}}{U_o s\Delta} = \frac{N_{\theta_\delta}}{\Delta} \qquad \text{(A-8)}$$

and $U_o s N_{\theta_\delta}$ is found by substitution of the control derivatives column for the θ stability derivatives column. For this example X_δ replaces g, Z_δ replaces $-U_o s$, M_δ replaces $s^2 - M_q s$, and 0 (zero) replaces $-U_o$. Then the determinant is solved, yielding (again in factored generalized form):

$$N_{\theta_\delta} = A_\theta\left(s + \frac{1}{T_{\theta_1}}\right)\left(s + \frac{1}{T_{\theta_2}}\right) \qquad \text{(A-9)}$$

where the approximate factors are:

$$\begin{aligned}
A_\theta &\doteq M_\delta \\
\frac{1}{T_{\theta_1}} &\doteq -X_w\left(\frac{M_u - \frac{M_\delta}{Z_\delta} Z_u}{M_w - \frac{M_\delta}{Z_\delta} Z_w}\right) \\
\frac{1}{T_{\theta_2}} &\doteq \frac{Z_\delta}{M_\delta}\left(M_w - \frac{M_\delta}{Z_\delta} Z_w\right) - X_u
\end{aligned}$$

Similar transfer functions may be derived for the response of the aircraft in u, α, and h to a control input δ. Employing the same notation used in Ref. 2, but making each numerator consistent with the use of Δ alone, the transfer functions are written in unfactored form as follows:

$$\Delta = As^4 + Bs^3 + Cs^2 + Ds + E$$

$$\frac{\theta}{\delta} = \frac{N_\theta}{\Delta} = \frac{As^2 + Bs + C}{\Delta}$$

$$\frac{u}{\delta} = \frac{N_u}{\Delta} = \frac{As^3 + Bs^2 + Cs + D}{\Delta} \qquad \text{(A-10)}$$

$$\frac{\alpha}{\delta} = \frac{N_\alpha}{\Delta} = \frac{As^3 + Bs^2 + Cs + D}{U_o\Delta}$$

$$\frac{h}{\delta} = \frac{N_h}{\Delta} = \frac{As^3 + Bs^2 + Cs + D}{s\Delta}$$

The values of coefficients A, B, etc., for the transfer functions indicated above are given in Table A-1, as are the appropriate factored forms. To avoid confusion as to the proper denominator, all numerators are made consistent with the use of Δ alone, e.g., $sN_h = As^3 + Bs^2 + Cs + D$. Note that to specify either elevator or throttle control, the appropriate subscript can be added to the control derivative, e.g., X_{δ_e} or X_{δ_T}.

The results, which so far are straightforward and probably well known to the reader, will now be extended to include human pilot closed-loop control of multiple loops. The reader should consult Ref. 11 for a more generalized and thorough treatment of multiple-loop control; the interest here is the derivation and tabulation of those multiple-loop transfer functions relating specifically to the carrier-approach problem.

The human pilot's controller transfer function can be denoted in general form by

$$Y_{\delta_i q} = \frac{\partial \delta_i}{\partial q_\epsilon} \qquad \text{(A-11)}$$

where δ_i is the control used and q_ϵ is the error in the variable controlled. A more specific example is

$$Y_{\delta_e \theta} = \frac{\partial \delta_e}{\partial \theta_\epsilon} \qquad \text{(A-12)}$$

and θ_ϵ represents the error in θ that the pilot is attempting to correct. To use this notation it has been assumed that the pilot closes a unity feedback

TABLE A-1

TRANSFER FUNCTION COEFFICIENTS AND FACTORED FORMS

	A	B	C	D	E
Δ	1	$-M_q - M_{\dot{\alpha}} - Z_w - X_u$	$Z_wM_q - M_\alpha - X_wZ_u + X_u(M_q + M_{\dot{\alpha}} + Z_w)$	$-X_u(Z_wM_q - M_\alpha) + X_wZ_uM_q - M_u(X_\alpha - g) + gZ_uM_{\dot{w}}$	$g(Z_uM_w - M_uZ_w)$
	$(s^2 + 2\zeta_p\omega_p s + \omega_p^2)(s^2 + 2\zeta_{sp}\omega_{sp}s + \omega_{sp}^2)$				
N_θ	$M_\delta + Z_\delta M_{\dot{w}}$	$X_\delta(Z_uM_{\dot{w}} + M_u) + Z_\delta(M_w - X_uM_{\dot{w}}) - M_\delta(X_u + Z_w)$	$X_\delta(Z_uM_w - Z_wM_u) + Z_\delta(M_uX_w - M_wX_u) + M_\delta(Z_wX_u - X_wZ_u)$		
	$A_\theta\left(s + \frac{1}{T_{\theta_1}}\right)\left(s + \frac{1}{T_{\theta_2}}\right)$				
N_u	X_δ	$-X_\delta(Z_w + M_q + M_{\dot{\alpha}}) + Z_\delta X_w$	$X_\delta(Z_wM_q - M_\alpha) - Z_\delta(X_wM_q + gM_{\dot{w}}) + M_\delta(X_\alpha - g)$	$g(M_\delta Z_w - Z_\delta M_w)$	
	$A_u\left(s + \frac{1}{T_{u_1}}\right)\left(s + \frac{1}{T_{u_2}}\right)\left(s + \frac{1}{T_{u_3}}\right)$ or $A_u\left(s + \frac{1}{T_{u_1}}\right)(s^2 + 2\zeta_u\omega_u s + \omega_u^2)$				
U_oN_α	Z_δ	$X_\delta Z_u - Z_\delta(X_u + M_q) + M_\delta U_o$	$X_\delta(M_uU_o - Z_uM_q) + Z_\delta X_uM_q - M_\delta U_oX_u$	$g(Z_\delta M_u - M_\delta Z_u)$	
	$A_w\left(s + \frac{1}{T_{w_1}}\right)(s^2 + 2\zeta_w\omega_w s + \omega_w^2)$				
sN_h	$-Z_\delta$	$-X_\delta Z_u + Z_\delta(M_q + M_{\dot{\alpha}} + X_u)$	$X_\delta Z_u(M_q + M_{\dot{\alpha}}) - Z_\delta[X_u(M_q + M_{\dot{\alpha}}) - M_\alpha] - M_\delta Z_\alpha$	$-X_\delta(Z_\alpha M_u - Z_u M_\alpha) + Z_\delta[M_u(X_\alpha - g) - M_\alpha X_u] + M_\delta[Z_\alpha X_u - Z_u(X_\alpha - g)]$	
	$A_h\left(s + \frac{1}{T_{h_1}}\right)\left(s + \frac{1}{T_{h_2}}\right)\left(s + \frac{1}{T_{h_3}}\right)$ or $A_h\left(s + \frac{1}{T_{h_1}}\right)(s^2 + 2\zeta_h\omega_h s + \omega_h^2)$				

loop and his transfer function is called Y_p, but note that this Y_p is still general in form. It can consist of any of the possible forms described in Section II.

Deriving the pilot-controlled $\theta \rightarrow \delta_e$ system transfer function, Eq A-12 may be written

$$\begin{aligned} \delta_e &= Y_{\delta_e\theta}\theta_\epsilon \\ \theta_\epsilon &= \theta_c - \theta \end{aligned} \tag{A-13}$$

and letting θ_c be defined as zero,

$$\delta_e = -Y_{\delta_e\theta}\theta \tag{A-14}$$

Substituting the right side of Eq A-14 into Eq A-6 and collecting terms in θ gives

$$\begin{array}{lllll} (s - X_u)u & -X_\alpha\alpha & +(g + Y_{\delta_e\theta}X_{\delta_e})\theta & +C & = 0 \\ -Z_u u & +U_o(s - Z_w)\alpha & +(-U_o s + Y_{\delta_e\theta}Z_{\delta_e})\theta & +0 & = 0 \\ -M_u u & -(M_{\dot\alpha}s + M_\alpha)\alpha & +(s^2 - M_q s + Y_{\delta_e\theta}M_{\delta_e})\theta & +0 & = 0 \\ 0 & +U_o\alpha & -U_o\theta & +sh & = 0 \end{array} \tag{A-15}$$

Rewriting Eq A-15 in matrix form and for convenience introducing the notation a_{ij} for the coefficients of the motion quantities u, α, θ results in

$$\begin{bmatrix} a_{11} & a_{12} & a_{13} + Y_{\delta_e\theta}X_{\delta_e} & 0 \\ a_{21} & U_o a_{22} & a_{23} + Y_{\delta_e\theta}Z_{\delta_e} & 0 \\ a_{31} & a_{32} & a_{33} + Y_{\delta_e\theta}M_{\delta_e} & 0 \\ 0 & U_o & -U_o & s \end{bmatrix} \begin{bmatrix} u \\ \alpha \\ \theta \\ h \end{bmatrix} = 0 \tag{A-16}$$

This can be broken down, using the laws for determinants, into

$$s \begin{vmatrix} a_{11} & a_{12} & a_{13} \\ a_{21} & U_o a_{22} & a_{23} \\ a_{31} & a_{32} & a_{33} \end{vmatrix} + Y_{\delta_e\theta}s \begin{vmatrix} a_{11} & a_{12} & X_{\delta_e} \\ a_{21} & U_o a_{22} & Z_{\delta_e} \\ a_{31} & a_{32} & M_{\delta_e} \end{vmatrix} = 0 \tag{A-17}$$

and this may be recognized as

$$U_o s\left[\Delta + Y_{\delta_e\theta} N_{\theta_{\delta_e}}\right] = 0 \qquad \text{(A-18)}$$

which is the closed-loop characteristic equation (i.e., closed-loop denominator) of the open-loop transfer function

$$\frac{Y_{\delta_e\theta} N_{\theta_{\delta_e}}}{s\Delta} \qquad \text{(A-19)}$$

(Note that the open-loop transfer function $N(s)/\Delta(s)$ has the closed-loop transfer function $N(s)/[\Delta(s) + N(s)]$.) This may seem like a lot of effort to prove what block diagram algebra would have shown immediately, namely that the pilot transfer function multiplied by the airframe transfer function is the system (open-loop) transfer function. However, the technique becomes useful in deriving multiple-loop transfer functions by avoiding very complicated block diagram breakdowns.

As an example, consider pilot control of airspeed with throttle and pitch attitude with elevator. Making the appropriate pilot transfer function substitutions, Eq A-6 in determinant form becomes

$$\begin{vmatrix} a_{11} + Y_{\delta_T u} X_{\delta_T} & a_{12} & a_{13} + Y_{\delta_e\theta} X_{\delta_e} & 0 \\ a_{21} + Y_{\delta_T u} Z_{\delta_T} & U_o a_{22} & a_{23} + Y_{\delta_e\theta} Z_{\delta_e} & 0 \\ a_{31} + Y_{\delta_T u} M_{\delta_T} & a_{32} & a_{33} + Y_{\delta_e\theta} M_{\delta_e} & 0 \\ 0 & U_o & -U_o & s \end{vmatrix} \begin{vmatrix} u \\ \alpha \\ \theta \\ h \end{vmatrix} = 0 \qquad \text{(A-20)}$$

Breaking this determinant down, it becomes

(A-21)

$$s \begin{vmatrix} a_{11} & a_{12} & a_{13} + Y_{\delta_e\theta} X_{\delta_e} \\ a_{21} & U_o a_{22} & a_{23} + Y_{\delta_e\theta} Z_{\delta_e} \\ a_{31} & a_{32} & a_{33} + Y_{\delta_e\theta} M_{\delta_e} \end{vmatrix} + sY_{\delta_T u} \begin{vmatrix} X_{\delta_T} & a_{12} & a_{13} + Y_{\delta_e\theta} X_{\delta_e} \\ Z_{\delta_T} & U_o a_{22} & a_{23} + Y_{\delta_e\theta} Z_{\delta_e} \\ M_{\delta_T} & a_{32} & a_{33} + Y_{\delta_e\theta} M_{\delta_e} \end{vmatrix}$$

The first determinant may be recognized as the one in Eq A-16, while the second one may be further reduced to

$$U_o s Y_{\delta_T u} N_{u_{\delta_T}} + s Y_{\delta_T u} Y_{\delta_e \theta} \begin{vmatrix} X_{\delta_T} & a_{12} & X_{\delta_e} \\ Z_{\delta_T} & U_o a_{22} & Z_{\delta_e} \\ M_{\delta_T} & a_{32} & M_{\delta_e} \end{vmatrix} \tag{A-22}$$

Introducing the notation

$$U_o N^{u\ \theta}_{\delta_T \delta_e} \equiv \begin{vmatrix} X_{\delta_T} & a_{12} & X_{\delta_e} \\ Z_{\delta_T} & U_o a_{22} & Z_{\delta_e} \\ M_{\delta_T} & a_{32} & M_{\delta_e} \end{vmatrix} \tag{A-23}$$

what this new determinant represents is the effect of control in one loop on the zeros of the other loop—in other words, the control coupling between the two loops. Notice that the notation employed suggests the replacement of the u and θ columns in the matrix equations of motion by the appropriate control parameters in accordance with Eq A-23. Such replacement gives the appropriate coupling transfer function whether the basic 3 x 3 or the augmented 4 x 4 matrix of Eq A-6 is utilized. Notice further that there is no coupling between two variables being controlled with the same control (e.g., $N^{\theta\ h}_{\delta_e \delta_e} = 0$). To explain, if altitude and attitude are both being controlled with elevator, the pilot in correcting altitude simply changes his commanded pitch attitude so there is no coupling effect. This is borne out mathematically by noting that if the elevator control derivatives were substituted in both the h and θ columns in Eq A-6, the solution of the determinant would be zero since any determinant with two identical rows or columns is identically equal to zero.

The final closed-loop characteristic equation for the multiple-loop control of $u \rightarrow \delta_T$ and $\theta \rightarrow \delta_e$, or of Eq A-20, has now become

$$U_o s \left[\Delta + Y_{\delta_e \theta} N_{\theta_{\delta_e}} + Y_{\delta_T u} N_{u_{\delta_T}} + Y_{\delta_e \theta} Y_{\delta_T u} N^{u\ \theta}_{\delta_T \delta_e} \right] = 0 \tag{A-24}$$

There are two open-loop system transfer functions which can give this closed-loop system, and these are

$$Y_{\delta_T u}\left(\frac{u}{\delta_T}\right)_{\theta \rightarrow \delta_e} = \frac{Y_{\delta_T u}\left(N_{u\delta_T} + Y_{\delta_e\theta} N^{u\ \theta}_{\delta_T \delta_e}\right)}{\Delta + Y_{\delta_e\theta} N_{\theta\delta_e}} \qquad \text{(A-25)}$$

$$Y_{\delta_e\theta}\left(\frac{\theta}{\delta_e}\right)_{u \rightarrow \delta_T} = \frac{Y_{\delta_e\theta}\left(N_{\theta\delta_e} + Y_{\delta_T u} N^{u\ \theta}_{\delta_T \delta_e}\right)}{\Delta + Y_{\delta_T u} N_{u\delta_T}} \qquad \text{(A-26)}$$

The notation on the left side of the equation denotes which loop is being considered as the outer loop and which as the inner loop (e.g., in Eq A-25, $\theta \rightarrow \delta_e$ is the inner loop).

The longitudinal coupling numerators have been derived and their coefficients and factored forms are tabulated in Table A-2, taken from Ref. 11. (Note that the same convention is employed as in Table A-1, i.e., the term "A" is the coefficient of the highest power in s and the last term is the coefficient of s^0, i.e., a constant.)

Now the previous two-loop pilot control result can be generalized by considering potential control with five loops: $\theta \rightarrow \delta_e$; $u \rightarrow \delta_e, \delta_T$; $h \rightarrow \delta_e, \delta_T$; or $\theta \rightarrow \delta_e$; $\alpha \rightarrow \delta_e, \delta_T$; $h \rightarrow \delta_e, \delta_T$. The closed-loop characteristic equation can be written out by inspection, just by summing the terms of the following equations:

1. The aircraft characteristic equation Δ
2. All of the single-loop numerators
3. All of the coupling numerators between control loops

Once the closed-loop equation is known, the open-loop equations for appropriate controlled variables can be written by separating the numerator and denominator terms for the open loop from the closed loop. As an example, consider $\theta \rightarrow \delta_e$; $u \rightarrow \delta_e, \delta_T$; $h \rightarrow \delta_e, \delta_T$. The closed-loop characteristic equation is

TABLE A-2

LONGITUDINAL COUPLING NUMERATOR COEFFICIENTS AND FACTORED FORMS

	A	B	C
$N^{\theta\ u}_{\delta_e \delta_T}$ or $-N^{u\ \theta}_{\delta_e \delta_T}$	$M_{\delta_e} X_{\delta_T} - M_{\delta_T} X_{\delta_e} + M_{\dot{w}}(Z_{\delta_e} X_{\delta_T} - Z_{\delta_T} X_{\delta_e})$	$M_w(Z_{\delta_e} X_{\delta_T} - Z_{\delta_T} X_{\delta_e}) + Z_w(X_{\delta_e} M_{\delta_T} - X_{\delta_T} M_{\delta_e}) + X_w(M_{\delta_e} Z_{\delta_T} - M_{\delta_T} Z_{\delta_e})$	
	$A_{\theta u}\left(s + \frac{1}{T_{\theta u}}\right)$		
	$A_{\theta u} \doteq X_{\delta_T} M_{\delta_e}$; $\frac{1}{T_{\theta u}} \doteq -Z_w + M_w \frac{Z_{\delta_e}}{M_{\delta_e}}$		
$sN^{\theta\ h}_{\delta_e \delta_T}$ or $-sN^{h\ \theta}_{\delta_e \delta_T}$ or $U_o N^{a\ \theta}_{\delta_e \delta_T}$ or $-U_o N^{\theta\ a}_{\delta_e \delta_T}$ or $sN^{a\ h}_{\delta_e \delta_T}$ or $-sN^{h\ a}_{\delta_e \delta_T}$	$Z_{\delta_e} M_{\delta_T} - Z_{\delta_T} M_{\delta_e}$	$X_u(M_{\delta_e} Z_{\delta_T} - M_{\delta_T} Z_{\delta_e}) + Z_u(X_{\delta_e} M_{\delta_T} - X_{\delta_T} M_{\delta_e}) + M_u(Z_{\delta_e} X_{\delta_T} - Z_{\delta_T} X_{\delta_e})$	
	$A_{\theta h}\left(s + \frac{1}{T_{\theta h}}\right)$		
	$A_{\theta h} \doteq -Z_{\delta_T} M_{\delta_e}$; $\frac{1}{T_{\theta h}} \doteq -X_u + \frac{X_{\delta_T}}{Z_{\delta_T}}\left(Z_u - M_u \frac{Z_{\delta_e}}{M_{\delta_e}}\right)$		
$sN^{h\ u}_{\delta_e \delta_T}$ or $-sN^{u\ h}_{\delta_e \delta_T}$	$X_{\delta_e} Z_{\delta_T} - X_{\delta_T} Z_{\delta_e}$	$(X_{\delta_T} Z_{\delta_e} - Z_{\delta_T} X_{\delta_e})(M_q + M_{\dot{w}})$	$Z_\alpha(X_{\delta_e} M_{\delta_T} - X_{\delta_T} M_{\delta_e}) + (X_\alpha - g)(Z_{\delta_T} M_{\delta_e} - M_{\delta_T} Z_{\delta_e}) + M_\alpha(X_{\delta_T} Z_{\delta_e} - X_{\delta_e} Z_{\delta_T})$
	$A_{hu}\left[s^2 + 2(\zeta\omega)_{hu} + \omega^2_{hu}\right]$		
	$A_{hu} \doteq -X_{\delta_T} Z_{\delta_e}$; $2(\zeta\omega)_{hu} \doteq -(M_q + M_{\dot{w}})$; $\omega^2_{hu} \doteq -\left(M_\alpha - \frac{\dot{X}_{\delta_e}}{Z_{\delta_e}} Z_\alpha\right)$		
$U_o N^{\alpha\ u}_{\delta_e \delta_T}$ or $-U_o N^{u\ \alpha}_{\delta_e \delta_T}$	$X_{\delta_T} Z_{\delta_e} - Z_{\delta_T} X_{\delta_e}$	$U_o(X_{\delta_T} M_{\delta_e} - M_{\delta_T} X_{\delta_e}) - M_q(X_{\delta_T} Z_{\delta_e} - Z_{\delta_T} X_{\delta_e})$	$g(M_{\delta_e} Z_{\delta_T} - Z_{\delta_e} M_{\delta_T})$
	$A_{\alpha u}\left(s + \frac{1}{T_{\alpha u_1}}\right)\left(s + \frac{1}{T_{\alpha u_2}}\right)$		
	$A_{\alpha u} \doteq X_{\delta_T} Z_{\delta_e}$; $\frac{1}{T_{\alpha u_1}} \doteq \frac{g}{U_o}\left(\frac{Z_{\delta_T}}{X_{\delta_T}} - \frac{Z_{\delta_e}}{M_{\delta_e}} \frac{M_{\delta_T}}{X_{\delta_T}}\right)$; $\frac{1}{T_{\alpha u_2}} \doteq \frac{U_o M_{\delta_e}}{Z_{\delta_e}}$		

$$\Delta + Y_{\delta_e\theta}N_{\theta_{\delta_e}} + Y_{\delta_e u}N_{u_{\delta_e}} + Y_{\delta_T u}N_{u_{\delta_T}}$$
$$+ Y_{\delta_e h}N_{h_{\delta_e}} + Y_{\delta_T h}N_{h_{\delta_T}} + Y_{\delta_e\theta}Y_{\delta_T u}N^{\theta\ u}_{\delta_e\delta_T}$$
$$+ Y_{\delta_e\theta}Y_{\delta_T h}N^{\theta\ h}_{\delta_e\delta_T} + Y_{\delta_e u}Y_{\delta_T h}N^{u\ h}_{\delta_e\delta_T}$$
$$+ Y_{\delta_T u}Y_{\delta_e h}N^{u\ h}_{\delta_T\delta_e} = 0 \qquad \text{(A-27)}$$

Three outer open-loop transfer functions can be written from this equation as a function of various inner loop closures:

$$\left(\frac{\theta}{\theta_\epsilon}\right)_{\substack{u \to \delta_e,\delta_T \\ h \to \delta_e,\delta_T}} = \frac{Y_{\delta_e\theta}\left(N_{\theta_{\delta_e}} + Y_{\delta_T u}N^{u\ \theta}_{\delta_T\delta_e} + Y_{\delta_T h}N^{\theta\ h}_{\delta_e\delta_T}\right)}{\Delta \quad Y_{\delta_e u}N_{u_{\delta_e}} + Y_{\delta_T u}N_{u_{\delta_T}} + Y_{\delta_e h}N_{h_{\delta_e}} + Y_{\delta_T h}N_{h_{\delta_T}} + Y_{\delta_e u}Y_{\delta_T h}N^{u\ h}_{\delta_e\delta_T} + Y_{\delta_T u}Y_{\delta_e h}N^{u\ h}_{\delta_T\delta_e}} \qquad \text{(A-28)}$$

$$\left(\frac{u}{u_\epsilon}\right)_{\substack{\theta \to \delta_e \\ h \to \delta_e,\delta_T}} = \frac{Y_{\delta_e u}\left(N_{u_{\delta_e}} + Y_{\delta_T h}N^{h\ u}_{\delta_T\delta_e}\right) + Y_{\delta_T u}\left(N_{u_{\delta_T}} + Y_{\delta_e\theta}sN^{u\ \theta}_{\delta_T\delta_e} + Y_{\delta_e h}N^{u\ h}_{\delta_T\delta_e}\right)}{\Delta + Y_{\delta_e\theta}N_{\theta_{\delta_e}} + Y_{\delta_e h}N_{h_{\delta_e}} + Y_{\delta_T h}N_{h_{\delta_T}} + Y_{\delta_e\theta}Y_{\delta_T h}N^{\theta\ h}_{\delta_e\delta_T}} \qquad \text{(A-29)}$$

$$\left(\frac{h}{h_\epsilon}\right)_{\substack{\theta \to \delta_e \\ u \to \delta_e,\delta_T}} = \frac{Y_{\delta_e h}\left(N_{h_{\delta_e}} + Y_{\delta_T u}N^{u\ h}_{\delta_T\delta_e}\right) + Y_{\delta_T h}\left(N_{h_{\delta_T}} + Y_{\delta_e\theta}N^{\theta\ h}_{\delta_e\delta_T} + Y_{\delta_e u}N^{h\ u}_{\delta_T\delta_e}\right)}{\Delta + Y_{\delta_e\theta}N_{\theta_{\delta_e}} + Y_{\delta_e u}N_{u_{\delta_e}} + Y_{\delta_T u}N_{u_{\delta_T}} + Y_{\delta_e\theta}Y_{\delta_T u}N^{\theta\ u}_{\delta_e\delta_T}} \qquad \text{(A-30)}$$

If angle of attack is being used instead of airspeed, the angle of attack multiple-loop transfer functions can be obtained by substituting α for u in the equations and multiplying U_o times all terms not containing an α. If any loops are not being used (e.g., no h $\rightarrow \delta_T$ loop), the transfer functions of Eq A-28 to A-30 can be corrected by setting the corresponding $Y_{\delta_i q}$ equal to zero for the loops not being used.

APPENDIX B

GENERIC PROPERTIES OF SINGLE- AND MULTIPLE-LOOP FEEDBACK CONTROLS

A. INTRODUCTION

Examination of the transfer functions of a large number (ten) of aircraft in power-approach configuration has revealed that they all have roughly the same stability characteristics. This held true not only for a variety of single- and multi-engine swept wing types but also for two tailless delta configurations (the F7U-3 and F4D-1). The conclusion may be drawn that conventional aircraft (i.e., not rotary wing, dynasoar, etc.) have the following general stability properties in landing approach:

1. Phugoid frequency given approximately by the classical formula $\omega_p = \sqrt{2}g/U_o$, which works out to a frequency of about 0.20 rad/sec for jet carrier approach speeds

2. Phugoid damping ratio is low, $\zeta_p = 0.10 \pm 0.05$. The difference between a damping ratio of 0.15 and 0.05 is insignificant from the standpoint of stabilization and control requirements, so $\zeta_p = 0.1$ is representative of phugoid damping ratios

3. Short period frequency varies between 1.0 and 3.0 rad/sec

4. Short period damping ratio is between 0.30 and 0.50 with 0.35 an average value

The primary differences between configurations that affect the transfer functions are thrust line angle of attack and thrust line offset from the c.g. These affect the throttle control stability derivatives Z_{δ_T} and M_{δ_T} respectively, and also the airframe derivative M_u (see Ref. 10) and result in wide variations of throttle control numerators between aircraft. Effects of these variations will be considered where appropriate. The net conclusion reached, however, is that even these possible variations do not change the generalities listed above.

The discussion of single and multiple loop control systems is made with the assumption that the reader has at least a working familiarity with servo analysis echniques. Most of the cases are illustrated by root locus diagrams although

an occasional Bode diagram is included. The purpose of this Appendix is a technical justification of the rather sweeping allegations put forth in Section III of the report, and therefore no attempt has been made to present the explanations in terms other than those involving feedback control concepts.

B. AIRCRAFT SINGLE-LOOP CONTROL CHARACTERISTICS

The following discussion of single-loop control is intended to familiarize the reader both with the general properties of airframe pole-zero locations in landing approach configuration and with the effects of pilot loop-closure. It is really preliminary to the more realistic multiple-loop systems examined in the following subsection.

1. Pitch Attitude Control, $\theta \rightarrow \delta_e$

The $\theta \rightarrow \delta_e$ single loop is fundamental to longitudinal control. The pilot's primary reference to the horizon in VFR flight or to the vertical gyro in IFR conditions attests to the importance and universal use by pilots of the pitch attitude control loop. Being employed as an inner loop, the $\theta \rightarrow \delta_e$ closure figures prominently in the minimum approach-speed criterion developed in Section IV. The handling qualities of this control loop when evaluated for the single-loop situation only (e.g., pitch attitude tracking) are dictated by the short-period characteristics. Conversely, when employed in a multiple-loop situation (e.g., where control of flight path is most important), then the phugoid or long-term characteristics become dominant. It is therefore convenient to separate the high frequency and low frequency characteristics in analyzing the $\theta \rightarrow \delta_e$ properties as related to the carrier-approach problem:

Short-Period Characteristics (ω'_{sp}, ζ'_{sp}). The unequalized closure indicated at the left in Fig. B-1 shows a tendency for decreased closed-loop damping, ζ'_{sp}, a condition readily alleviated by the pilot's generation of a small amount of lead equalization, T_L; the right-hand part of Fig. B-1 illustrates the effect of a small T_L. Therefore, if the open-loop (airframe alone) ω_{sp} and ζ_{sp} values are such that closed-loop damping in the order of $\zeta'_p \geq 0.35$ is achievable, the short-period characteristics are adequate for control during carrier approach and do not require further consideration. (Such has been assumed throughout this report.) It should be noted that the value of K_θ is selected by the pilot on the basis of attitude tracking requirements and the

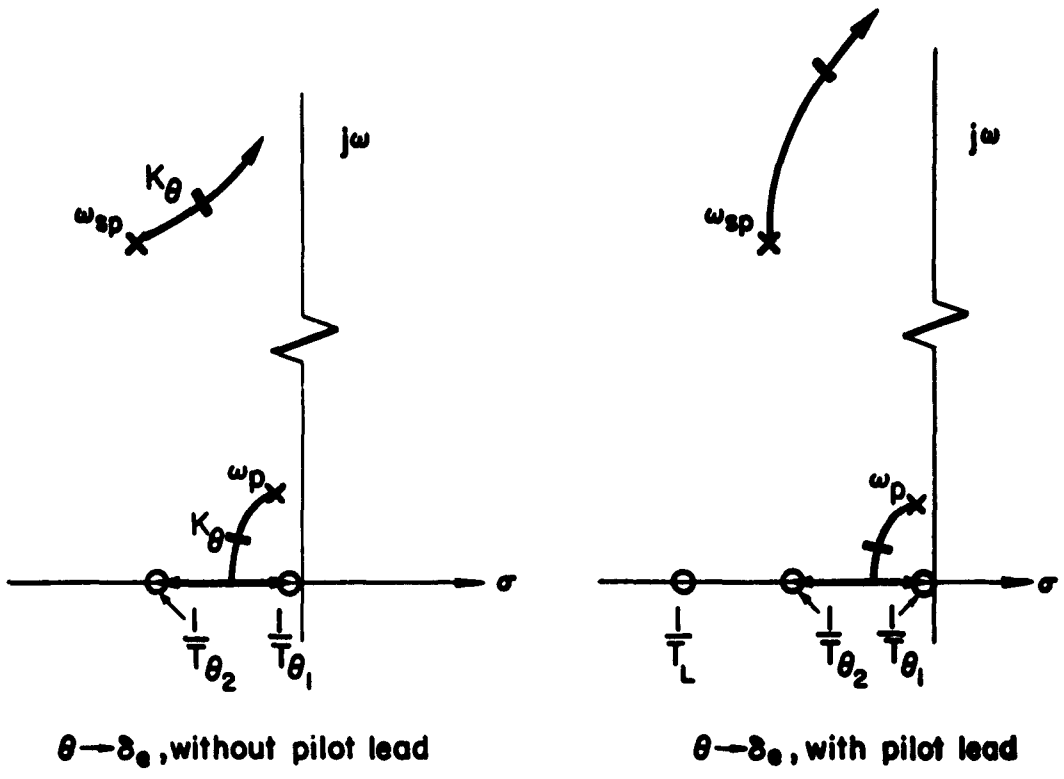

Figure B-1. Attitude Control by Pilot

aircraft's short period characteristics (even during the carrier approach condition) and not from phugoid considerations. Detailed investigations of the adequacy of short-period characteristics may be found in Ref. 5 and 6.

Phugoid Characteristics ($1/T_{\theta_1}'$, $1/T_{\theta_2}'$). The importance of the closed-loop phugoid frequency ω_p' on the minimum approach-speed criterion developed in Section IV can be readily appreciated by reference to Eq 21 (by definition $(\omega_p')^2 = 1/T_{\theta_1}' T_{\theta_2}'$). With an assumed zero thrust-offset and a large value for $1/T_{h_T}$, it is seen that the criterion can be grossly interpreted as:

$$\frac{\partial(\omega_p'')^2_{\zeta_p''=0}}{\partial K_\theta} \doteq \frac{\partial(\omega_p')^2}{\partial K_\theta} \qquad \text{(B-1)}$$

The closed-loop frequency, ω_p', is (from Eq 16)

$$(\omega_p')^2 = \frac{\omega_p^2 + K_\theta \frac{1}{T_{\theta_1} T_{\theta_2}}}{1 + K_\theta}$$

and partial differentiation yields:

$$\frac{\partial(\omega_p')^2}{\partial K_\theta} = 0 = \frac{1}{T_{\theta_1} T_{\theta_2}} - \omega_p^2 \qquad \text{(B-2)}$$

Therefore it is seen that for:

$$\frac{1}{\omega_p^2 T_{\theta_1} T_{\theta_2}} > 1, \text{ increasing } K_\theta \text{ results in increased } \omega_p'$$

$$\frac{1}{\omega_p^2 T_{\theta_1} T_{\theta_2}} < 1, \text{ increasing } K_\theta \text{ results in decreased } \omega_p'$$

(The parameter $1/\omega_p^2 T_{\theta_1} T_{\theta_2}$ is the static gain relative to the gain at the short period, and was advanced in Ref. 5 as a possible source of control difficulty. Also, the condition indicated by Eq B-2 corresponds to the speed for minimum drag for the zero thrust-offset case—see Ref. 5, Section V-c.)

The servoanalytic situation corresponding to Eq B-2 can be conveniently illustrated by use of the Sigma-Bode plot (i.e., $s = -\sigma$ rather than the usual $s = j\omega$), thoroughly explained in Ref. 17. For reasons which will become clear later, assume that the only variable parameter in Eq B-2 is the time constant $1/T_{\theta_1}$. For three selected value of $1/T_{\theta_1}$ the corresponding Sigma plots are shown in Fig. B-2. Note that the closed-loop roots, $1/T_{\theta_1'}$, $1/T_{\theta_2'}$, whose product is the closed-loop frequency, $(\omega_p')^2$, are uniquely defined by the intersection of the gain line and the curve $|G(-\sigma)|$ (see Ref. 4, 17). The condition of symmetry about ω_p in Fig. B-2b renders the value of ω_p' insensitive to gain changes. That is, increasing K_θ increases $1/T_{\theta_2'}$ and decreases $1/T_{\theta_1'}$ by the same factor so that their product is unchanged.

In actual carrier approach-speed flight conditions, it was found that for zero thrust offset $1/T_{\theta_1}$ was the only parameter that varied appreciably for

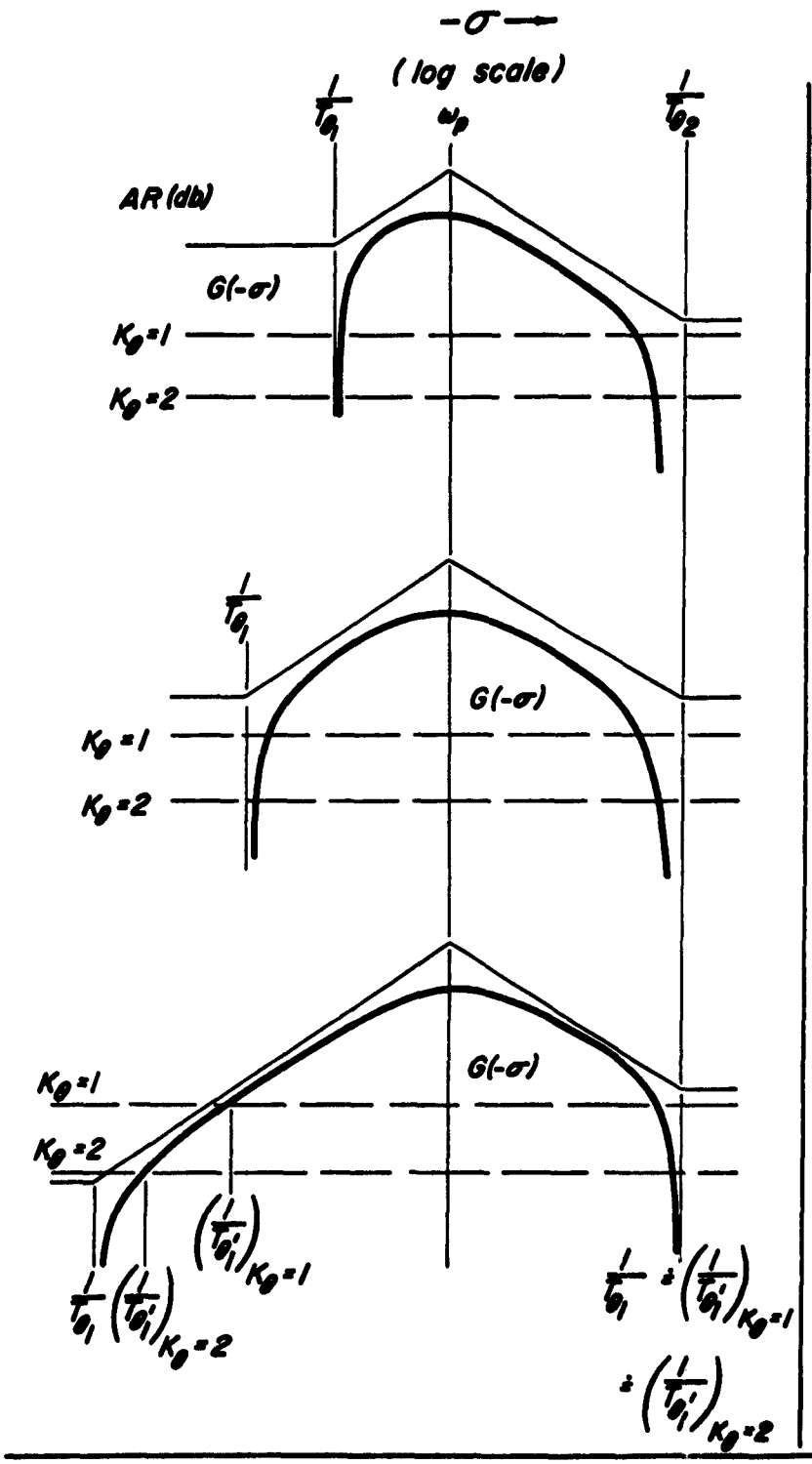

case a Speed greater than criterion speed

$$\left[\frac{1}{T_{\theta_1} T_{\theta_2}} > \omega_p^2\right]$$

Effect of increasing K_θ:

$1/T'_{\theta_1}$ decreases slowly

$1/T'_{\theta_2}$ increases moderately

$\therefore (\omega'_p)^2 = \frac{1}{T'_{\theta_1} T'_{\theta_2}}$ increases (slowly) as gain is increased

---

case b Speed equal to criterion speed

$$\frac{1}{T_{\theta_1} T_{\theta_2}} = \omega_p^2$$

Effect of increasing K_θ:

$1/T'_{\theta_1}$ decreases at same rate as $1/T'_{\theta_2}$ increases

$\therefore (\omega'_p)^2 = \frac{1}{T'_{\theta_1} T'_{\theta_2}}$ remains constant as gain is varied

---

case c Speed less than criterion speed

$$\frac{1}{T'_{\theta_1} T'_{\theta_2}} \quad \omega_p^2$$

Effect of increasing K_θ:

$1/T'_{\theta_1}$ decreases rapidly

$1/T'_{\theta_2}$ increases slowly

$\therefore (\omega'_p)^2 = \frac{1}{T'_{\theta_1} T'_{\theta_1}}$ decreases (rapidly) as gain is increased

Figure B-2. Sigma Bode Plot ($s = -\sigma$) of the Phugoid Mode for Various Values of $1/T_{\theta_1}$

different approach speeds. Thus, for conditions of zero thrust-offset and a relatively large $1/T_{h_T}$ (corresponding to a low thrust inclination), the value of $1/T_{\theta_1}$ is dominant in specifying the "reversal" speed. For example, under these circumstances, Fig. B-2 can be interpreted as a function of approach speed as follows: Fig. B-2a is representative of an approach speed exceeding the criterion minimum; Fig. B-2b represents the minimum approach speed condition in accordance with the criterion developed in Section IV; Fig. B-2c is representative of an approach speed below the criterion minimum.

In the general case, with thrust offset, the above basic considerations apply but the speed at which $1/T_{\theta_1}T_{\theta_2} = \omega_p^2$ is no longer that for minimum drag. Also, for appreciable thrust offsets and/or large inclinations, the effects of $1/T'_{h_T}$ must be considered, as in the complete criterion developed in the text.

2. Altitude Control, $h \rightarrow \delta_e$ or $h \rightarrow \delta_T$

Consider first the $h \rightarrow \delta_e$ closure. Altitude control with elevator is shown in the root locus plots of Fig. B-3. The only significant difference between these two loci is the movement of the zero $1/T_{h_1}$ from the stable to

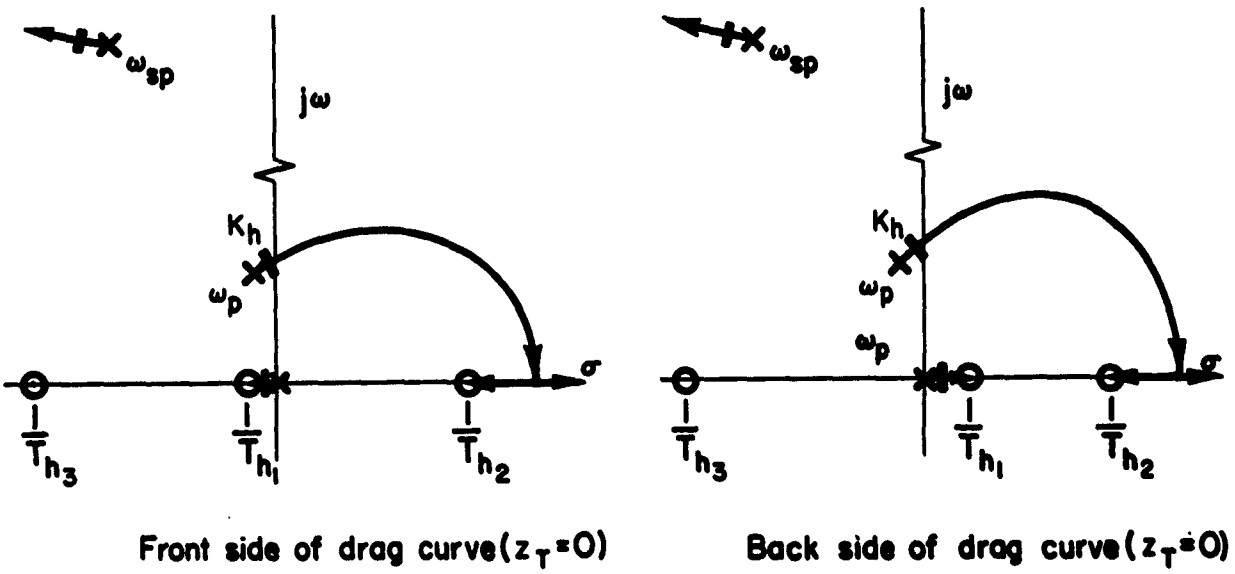

Front side of drag curve ($z_T = 0$) Back side of drag curve ($z_T = 0$)

Figure B-3. $h \rightarrow \delta_e$ Control by Pilot

the unstable half-plane below minimum drag speed. This changes the system from a stable one (at least at low gains) to one unstable for all gains. Such destabilizing motion of the time constant $1/T_{h_1}$ as a function of approach speed can be easily understood by referring to Ref. 2, Eq 6-28, which shows that for zero thrust offset ($z_T = 0$),

$$\frac{1}{T_{h_1}} \doteq \frac{1}{m}\frac{dD}{du} \qquad \text{(B-3)}$$

Thus the sign of $1/T_{h_1}$ changes at the speed corresponding to $dD/du = 0$, or the speed for minimum drag.

The effect of a thrust offset on the $h \rightarrow \delta_e$ closure can be inferred from examination of a more complete expression for $1/T_{h_1}$ (for example, see Ref. 1, Table III-1 and Eq 6-25), and noting that (Ref. 10) the increment in M_u due to eccentric thrust is

$$\Delta M_u = -\frac{2}{U_o}\frac{Tz_T}{I_y} \qquad \text{(B-4)}$$

The $h \rightarrow \delta_T$ Closure. Altitude control with throttle is depicted in Fig. B-4, again for the case of zero thrust line offset from the c.g. The zeros near the short-period poles essentially cancel the short-period mode, leaving the phugoid mode dominant. The locus shows that the phugoid frequency

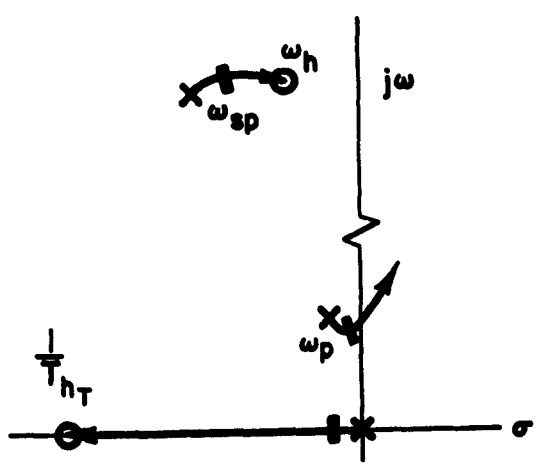

Figure B-4. $h \rightarrow \delta_T$; Front and Back Side of the Drag Curve

decreases sharply for low values of gain, regardless of speed relative to minimum drag speed (i.e., the dominant ω_p roots are relatively invariant as a function of speed). The reason for the difference relative to elevator control is the replacement of the low frequency zero, $1/T_{h_1}$, with the high frequency zero, $1/T_{h_T}$. The latter (for $z_T = 0$) is approximately equal to

$$\frac{1}{T_{h_T}} \doteq \frac{Z_u}{\alpha_{T.L.}} \doteq \frac{2g}{U_o \alpha_{T.L.}} \doteq \frac{\sqrt{2}}{\alpha_{T.L.}} \omega_p \qquad \text{(B-5)}$$

where $\alpha_{T.L.}$ is the angle of attack of the thrust line

For $\alpha_{T.L.}$ of the order of 0.1 rad, $1/T_{h_T}$ is about 10 ω_p and its influence on the phugoid mode is therefore normally minor. On the other hand, the $h \rightarrow \delta_e$ zero, $1/T_{h_1}$, is in the region of zero frequency and consequently a dominant influence on the phugoid.

The magnitude of $1/T_{h_T}$ can change drastically, however, if there exists an appreciable thrust offset. Such effect on (all) the zeros of the $h \rightarrow \delta_T$ can be investigated using the root locus technique on the N_h transfer function given in Table A-I on page 43 in the following manner:

a. Separate the thrust-offset dependent terms in the expression, viz:

$$\begin{aligned} sN_h &= As^3 + Bs^2 + Cs + D \\ &= As^3 + Bs^2 + (c - M_{\delta_T} Z_\alpha)s \\ &\quad + \left\{ d + M_u Z_{\delta_T} [X_\alpha - g)] + M_{\delta_T} [Z_\alpha X_u - Z_u (X_\alpha - g)] \right\} \end{aligned} \qquad \text{(B-6)}$$

b. Set $N_h = 0$ and manipulate equation into the form $1 \pm KG(s) = 0$:

$$1 - \frac{M_\delta Z_\alpha}{A} \left[\frac{s - X_u + \dfrac{(X_\alpha - g)(M_{\delta_T} Z_u - M_u Z_{\delta_T})}{M_{\delta_T} Z_\alpha}}{s^3 + \dfrac{B}{A} s^2 + \dfrac{C}{A} s + \dfrac{d}{A}} \right] = 0 \qquad \text{(B-7)}$$

c. The ratio $M_{\dot{\alpha}}/M_{\delta}$ is independent of thrust-offset magnitude, therefore the numerator zero as well as the denominator coefficients in Eq B-7 are constants. The locus of zeros versus the gain parameter $M_{\delta}Z_{\alpha}/A$ can then be constructed, and in turn the gain parameter may be expressed in terms of thrust-offset magnitude, i.e.

$$\text{Root locus gain} = \frac{M_{\delta}Z_{\alpha}}{A} = z_T\left(\frac{I_y}{m}\frac{Z_{\alpha}}{\alpha}\right) \qquad \text{(B-8)}$$

An illustration of the thrust line offset effect on the location of the throttle control zeros is shown in Fig. B-5. A specific airplane, the F4D-1, which normally has zero offset was used for this example. The gains

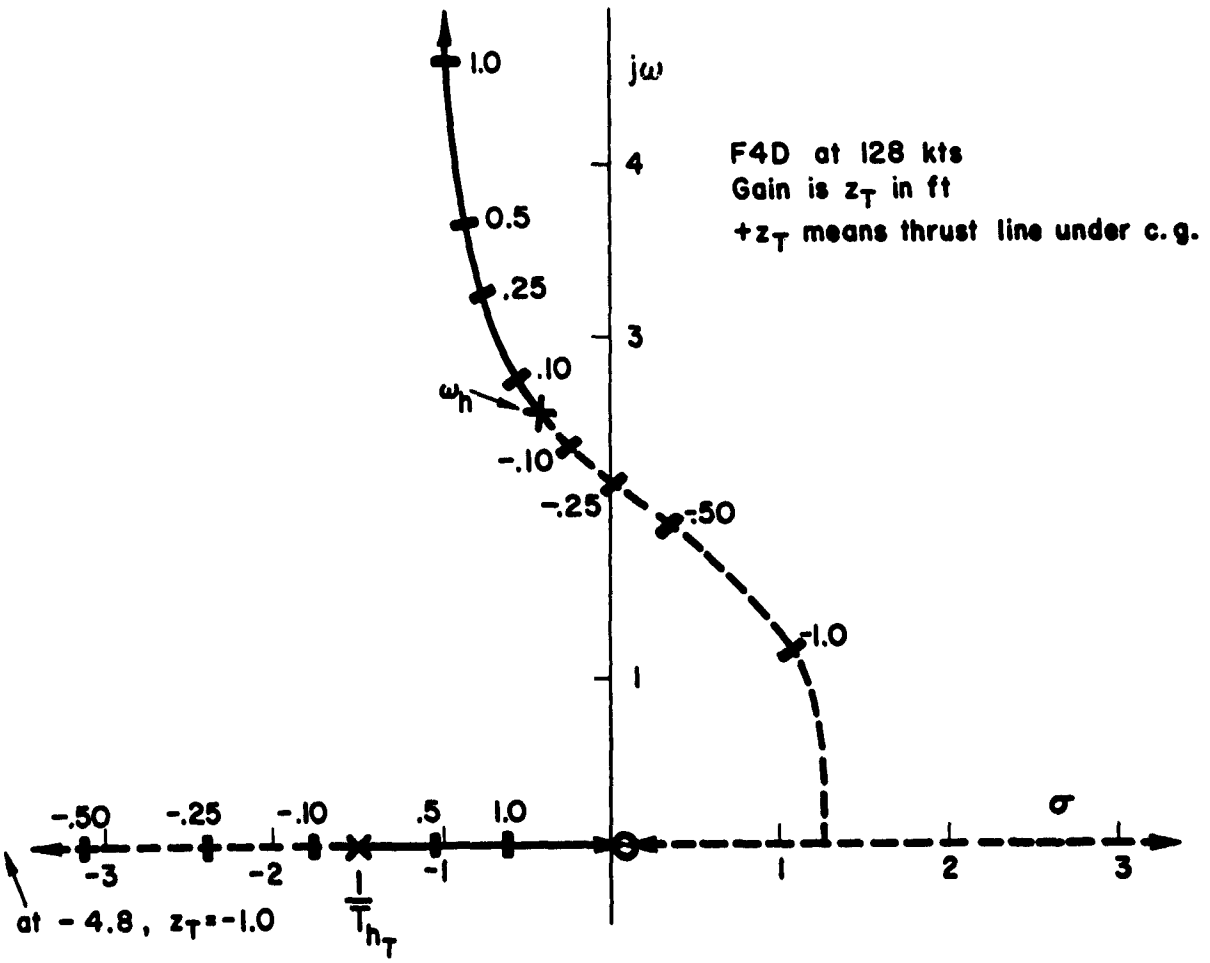

Figure B-5. Effect of Thrust Line Offset on h → δ_T Zeros

are given in feet of offset, positive meaning thrust line below the c.g. and vice versa. Typical values of offset for actual aircraft are between 0 and 0.5 ft, which gives an idea of practical limits in Fig. B-5. Conceivably, with sufficient thrust offset below the c.g. the root $1/T_{h_T}$ can exert some influence on the phugoid mode. Such an influence can be significant on the minimum approach speed criterion developed in Section IV, i.e., its effect on $\partial(\omega_p'')^2/\partial K_\theta$. The other interesting point is that with sufficiently large values of $-z_T$, a closed-loop problem could exist at short-period frequencies, especially for configurations with $\zeta_{sp} < 0.35$, because of the negatively damped ω_h.

3. Airspeed Control, $u \rightarrow \delta_e$, or $u \rightarrow \delta_T$

Root loci for airspeed control are shown in Fig. B-6. The $u \rightarrow \delta_T$ example is again for zero thrust offset. These are usually low gain loops, so their single-loop characteristics are not very significant when multiple-loop control is considered. The primary influence of these loops in the multiple-feedback control case is on the zeros of the system as will be discussed later. Both loop closures add phugoid damping (short period is almost unchanged), but $u \rightarrow \delta_e$ will increase phugoid frequency while $u \rightarrow \delta_T$ will decrease it. It should be noted that both forms of speed control are trim functions in the normal or usual piloting technique. Therefore the long-term characteristics (phugoid) are most important to the pilot.

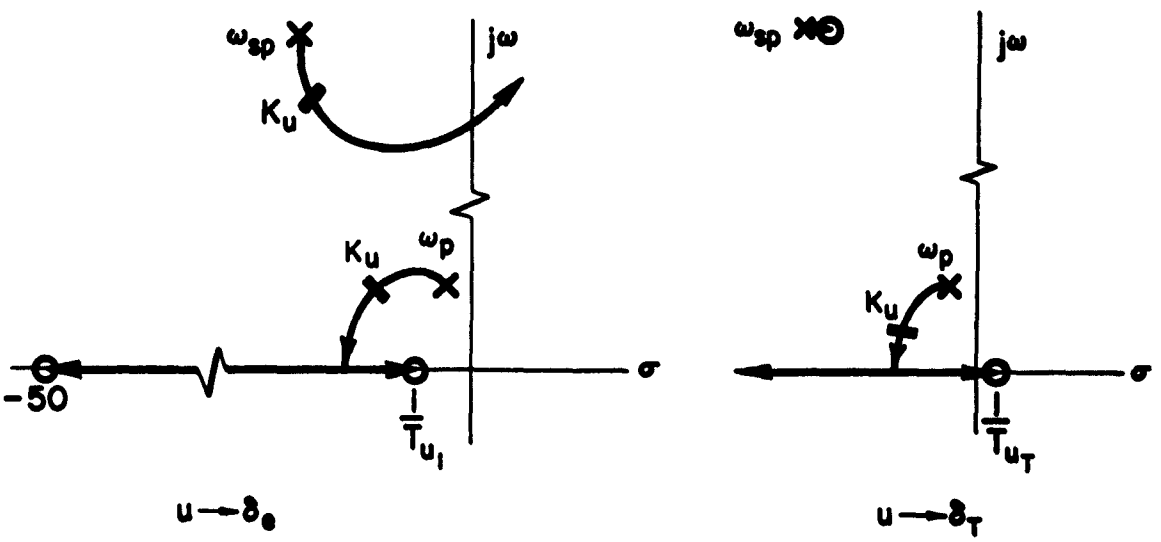

Figure B-6. Speed Control Loops

The effect of thrust line offset on the throttle control zeros is shown in Fig. B-7. This effect was similarly computed as in the h → δ_T loop previously described (Paragraph 2), employing also the F4D at 128 knots. As opposed to the altitude feedback case, it is evident that the speed control zeros are hardly affected.

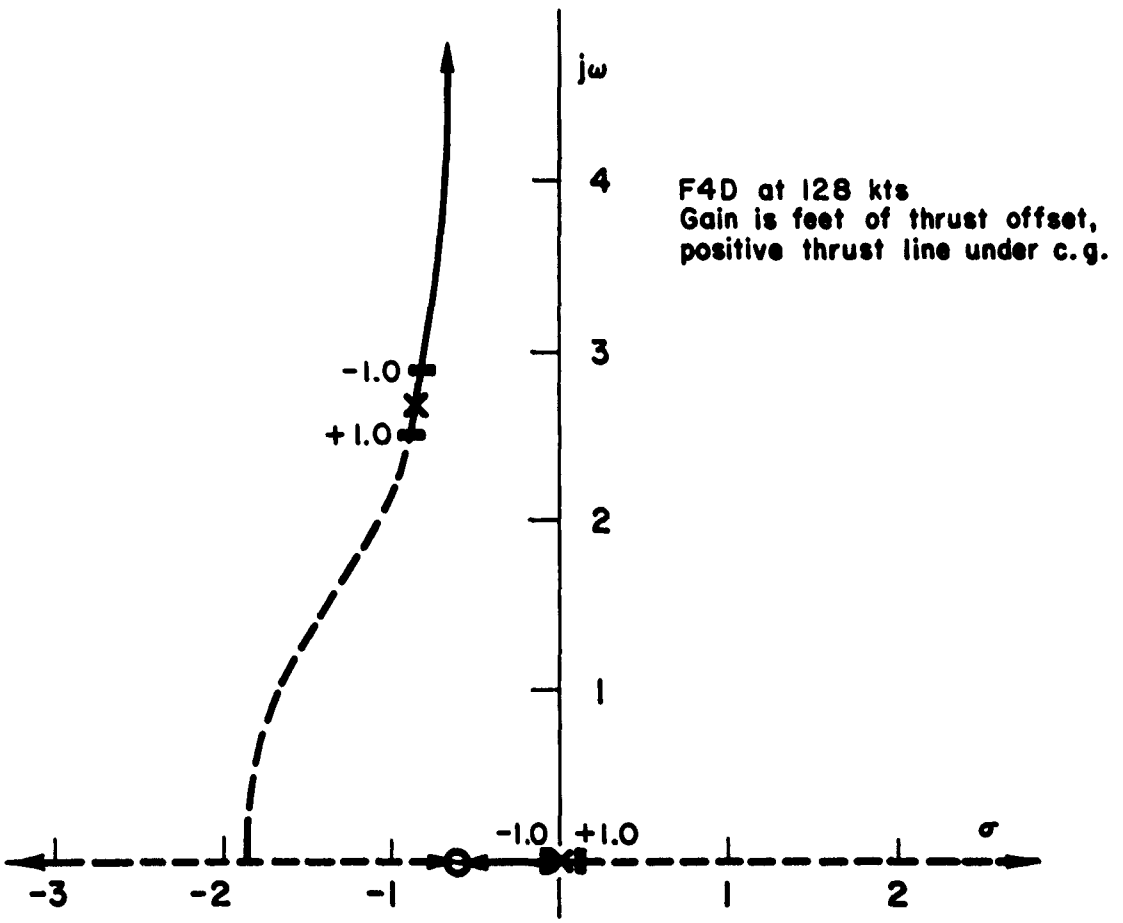

Figure B-7. Effect of Thrust Offset on u → δ_T Zeros

4. Angle of Attack Control, $\alpha \rightarrow \delta_e$, or $\alpha \rightarrow \delta_T$

Angle of attack control is again a low gain loop (when closed by a pilot). The root loci are shown in Fig. B-8. Two points should be made about this feedback loop. The first is that it is primarily a short-period phenomenon, since the open-loop phugoid mode takes place at constant angle of attack.

The second point is that the angle of attack displayed to the pilot is always heavily damped, or lagged, to remove the short-period oscillations. This is primarily significant to the multiple-loop cases examined later.

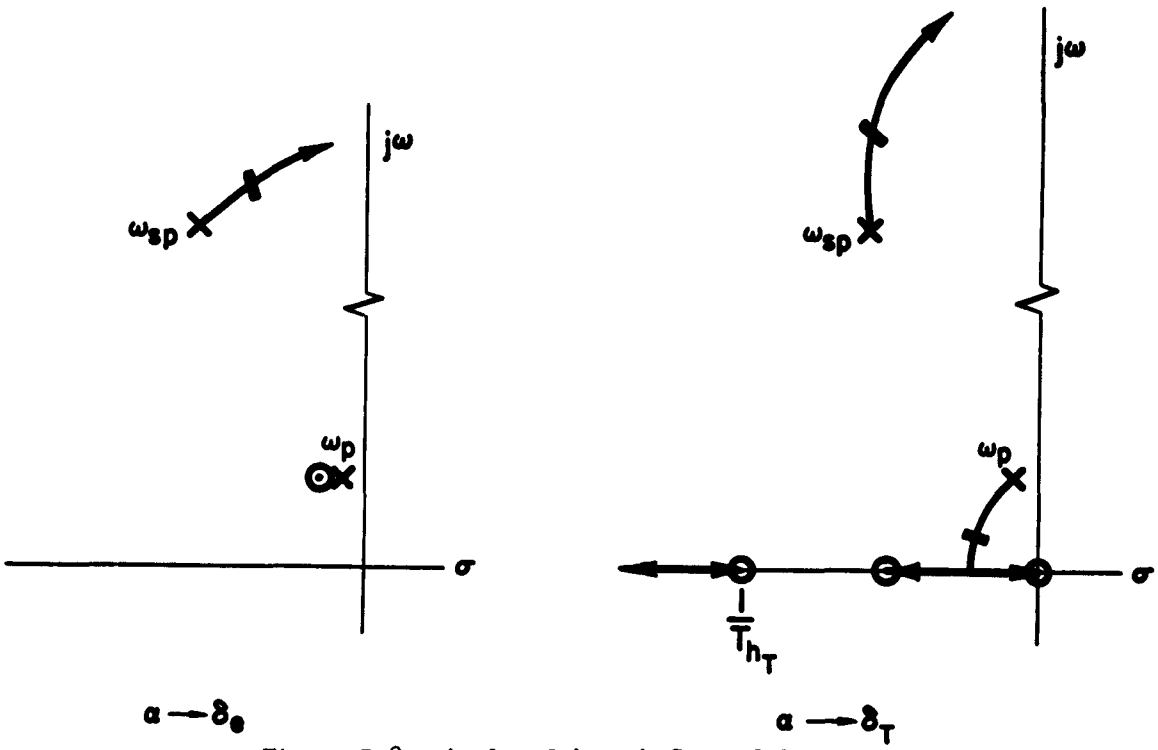

Figure B-8. Angle of Attack Control Loops

The general effect of $\alpha \rightarrow \delta_T$ is to increase phugoid damping. On the other hand, $\alpha \rightarrow \delta_e$ has almost no effect on the phugoid, as the zeros are in close proximity to the poles. Since the classical phugoid occurs at constant angle of attack, this conclusion is not surprising.

In summary, the most important properties of these single-loop closures in connection with the carrier approach problem are their general effects on phugoid damping and frequency. These carry over to multiloop systems, but some loops are typically higher gain than others and therefore their closures by the pilot have more important consequences. The $\theta \rightarrow \delta_e$ and $h \rightarrow \delta_e$ or δ_T loops are the most important of the single loops since these appear to be most universally used by pilots for carrier approach (see discussion in Section III).

C. MULTIPLE-LOOP CONTROL CHARACTERISTICS

The intent of this subsection is to show generically how the results described in Section III were obtained. The successive loop closures are illustrated by root loci for the three control techniques examined. No specific numbers are used, the results being a generalization of specific studies such as the one given in Appendix C. The three pilot control techniques discussed in Section III are the ones examined here.

1. $h \rightarrow \delta_e$, $\theta \rightarrow \delta_e$, u or $\alpha \rightarrow \delta_T$

Altitude Response. Using the results from Appendix A, the open-loop transfer function of elevator control of altitude, with $\theta \rightarrow \delta_e$ and $u \rightarrow \delta_T$ inner loops, is

$$Y_{\delta_e h}\left(\frac{h}{\delta_e}\right)_{\substack{\theta \rightarrow \delta_e \\ u \rightarrow \delta_T}} = \frac{Y_{\delta_e h}\left(N_{h\delta_e} + Y_{\delta_T u} N^{h\ u}_{\delta_e \delta_T}\right)}{s\left(\Delta + Y_{\delta_e \theta} N_{\theta \delta_e} + Y_{\delta_T u} N_{u \delta_T} + Y_{\delta_e \theta} Y_{\delta_T u} N^{\theta\ u}_{\delta_e \delta_T}\right)} \tag{B-9}$$

The outer loop characteristic equation is found by summing the inner loop transfer functions, which is the mathematical process for closing the inner loops. The summation process is as follows:

$$\Delta + Y_{\delta_e \theta} N_{\theta \delta_e} = \Delta\left(1 + \frac{Y_{\delta_e \theta} N_{\theta \delta_e}}{\Delta}\right) \tag{B-10}$$

$$= \Delta' \tag{B-11}$$

where Δ' is the closed-loop transfer function which results from closing the $\theta \rightarrow \delta_e$ loop. (Note that $Y_{\delta_e \theta} N_{\theta \delta_e} / \Delta$ in Eq B-10 is the $\theta \rightarrow \delta_e$ open-loop transfer function and $(\Delta + Y_{\delta_e \theta} N_{\theta \delta_e})$ is the closed-loop equation.) This $\theta \rightarrow \delta_e$ loop has already been discussed under single-loop control, in which it was shown that the closure resulted in a well-damped phugoid and a high frequency short period. Therefore the root locus of this loop closure is the same as that in Fig. B-1.

Going now to the speed control loop, and for the time being neglecting coupling between the θ and u loops,

$$\Delta' + Y_{\delta_T u} N_{u_{\delta_T}} = \Delta' \left(\frac{1 + Y_{\delta_T u} N_{u_{\delta_T}}}{\Delta'} \right) \tag{B-12}$$

The root locus for this loop is shown in Fig. B-9. The important point to note is that this is a very low gain loop for reasonable values of pilot throttle gain (see Appendix C). Therefore the aircraft's phugoid and short-period characteristics are not appreciably changed by the pilot's throttle movements to control airspeed. But as is shown later, this closure does have a very important (stabilizing) effect through the numerator coupling with the $h \rightarrow \delta_e$ zeros (i.e., allowing stable flight on the back side of the drag curve with $h \rightarrow \delta_e$ control).

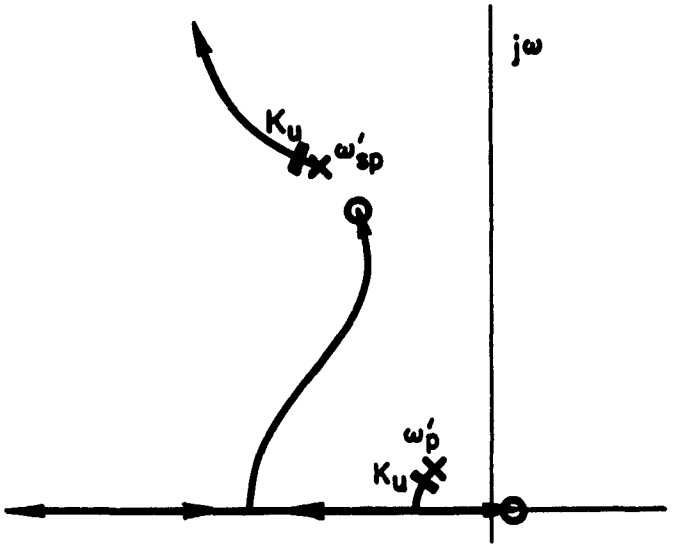

Figure B-9. Pilot Closure of the $u \rightarrow \delta_T$ Loop

The final denominator loop is the coupling between θ and u control.

$$\Delta' \left(1 + \frac{Y_{\delta_T u} N_{u_{\delta_T}}}{\Delta'} \right) + Y_{\delta_e \theta} Y_{\delta_T u} N^{\theta\ u}_{\delta_e \delta_T} = \Delta'' \tag{B-13}$$

The method of closure is the same as before, and specific cases have shown that this too is a low gain effect, so the final inner loop denominator characteristics are very close to those given by the $\theta \rightarrow \delta_e$ single-loop closure. This illustrates the great importance of pilot closure of the θ loop.

The altitude control zeros are changed only by the coupling with the $u \rightarrow \delta_T$ loop. From the numerator of Eq B-9,

$$N_{h\delta_e} + Y_{\delta_T u} N_{u\delta_T} = N_{h\delta_e}\left(1 + \frac{Y_{\delta_T u} N_{u\delta_T}}{N_{h\delta_e}}\right) \qquad \text{(B-14)}$$

$$= N'_{h\delta_e} \qquad \text{(B-15)}$$

Closure of the loop denoted by the terms in the bracket is depicted in Fig. B-10. It is seen that the primary effect is to stabilize the altitude control zero, $1/T_{h_1}$, which is in the unstable half plane when the aircraft is on the back side of the drag curve. For speeds above minimum drag, this effect is unnecessary, therefore the $u \rightarrow \delta_T$ closure is redundant and not required for altitude control.

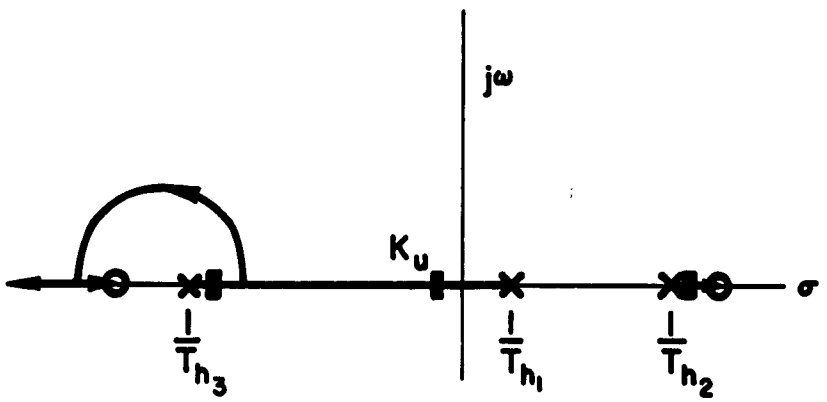

Figure B-10. Effect of $u \rightarrow \delta_T$ on $h \rightarrow \delta_e$ Zeros

The underlying reason for this stabilizing effect is that the pilot gain in the $u \rightarrow \delta_T$ loop modifies the X_u equivalent stability derivative. From Ref. 2, the approximate value for $1/T_{h_1}$ in terms of stability derivatives is

$$\frac{1}{T_{h_1}} \doteq -X_u + (X_\alpha - g)\frac{M_u Z_{\delta_e} - Z_u M_{\delta_e}}{M_\alpha Z_{\delta_e} - Z_\alpha M_{\delta_e}} \tag{B-16}$$

and augmenting <u>either</u> X_u <u>or</u> X_α makes $1/T_{h_1}$ more positive. Closing this coupling loop indicates the gain required of the pilot in order to stabilize $1/T_{h_1}$ or, alternatively, to return the aircraft to the "effective" front side of the drag curve.

The final outer loop characteristic equation is now

$$Y_{\delta_e h}\left(\frac{h}{\delta_e}\right)_{\substack{\theta \rightarrow \delta_e \\ u \rightarrow \delta_T}} = \frac{Y_{\delta_e h} N'_{h\delta_e}}{s\Delta''} \tag{B-17}$$

where Δ'' is the result of the loop closure of Eq B-13, and $N'_{h\delta_e}$ is the closure from Eq B-15. The effect of various pilot transfer functions on altitude control can now be examined. But first it should be noted that this outer loop was arrived at with only two assumptions regarding pilot control in inner loops:

a. A "good" closure of the $\theta \rightarrow \delta_e$ loop from the standpoint of adequate short-period damping

b. Enough gain in the $u \rightarrow \delta_T$ loop to stabilize the back side of the drag curve condition

These seem like reasonable demands on the pilot provided he has a suitable display of airspeed error. Note also that if the aircraft had initially been on the front side of the drag curve, the altitude control transfer function would have looked approximately like this even if the pilot did not touch the throttle. Therefore this altitude control method produces results similar to being on the front side of the drag curve or, alternatively, similar to automatic throttle control for flight on the back side of the drag curve.

Altitude control for a nonequalized pilot is compared to control with lead equalization in Fig. B-11. The phugoid frequency is greatly increased before the phugoid branch goes unstable for the pure-gain pilot. The addition of lead equalization (on the order of $1/T_L = 1.0 \rightarrow 1.5$ rad/sec) will greatly increase the bandpass of this phugoid branch.

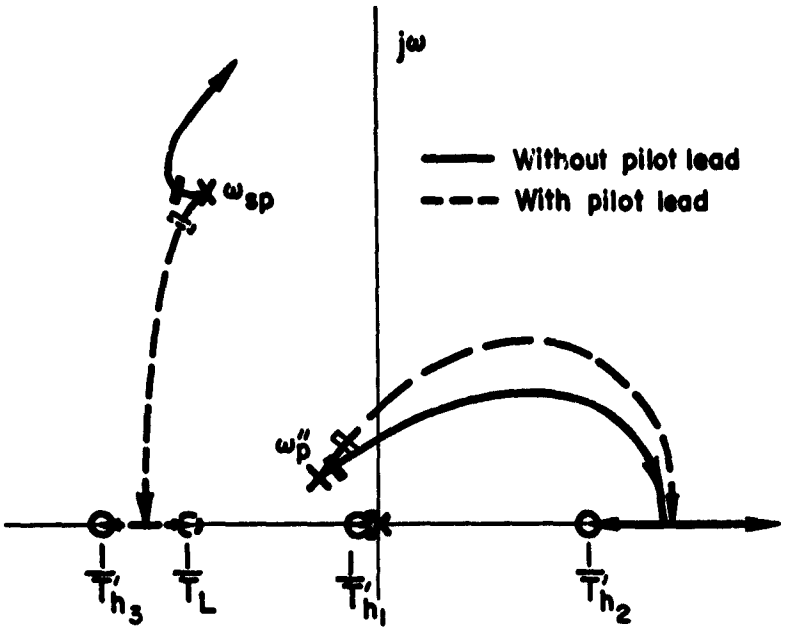

Figure B-11. Altitude Control with Elevator

Airspeed Response. Both forms of pilot characteristics result in reasonable control system characteristics, the lead-equalized one being the better of the two. Having established that the altitude control is adequate, airspeed control can be checked. The airspeed control open-loop transfer function is

$$Y_{\delta_T u}\left(\frac{u}{\delta_T}\right)_{\substack{h \to \delta_e \\ \theta \to \delta_e}} = \frac{Y_{\delta_T u}\left(sN_{u_{\delta_T}} + Y_{\delta_e h}N^{h\ u}_{\delta_e \delta_T} + Y_{\delta_e \theta}sN^{\theta\ u}_{\delta_e \delta_T}\right)}{s\Delta + Y_{\delta_e \theta}sN_{\theta_{\delta_e}} + Y_{\delta_e h}N_{h_{\delta_e}}} \qquad \text{(B-18)}$$

so the airspeed control zeros can be calculated from the numerator, using the same pilot gains for θ and h control as were used in the previous case.

$$N''_{u_{\delta_T}} = sN_{u_{\delta_T}} + Y_{\delta_e h}N^{h\ u}_{\delta_e \delta_T} + Y_{\delta_e \theta}sN^{\theta\ u}_{\delta_e \delta_T} \qquad \text{(B-19)}$$

A typical airspeed closed loop is shown in Fig. B-12. The proximity of the phugoid and short-period poles and zeros indicates that airspeed control with throttle is primarily a slow first-order convergence (i.e., a trim function). The higher the throttle gain, the faster will be this convergence. This is

probably acceptable to the pilot if the airspeed disturbances are not too severe.

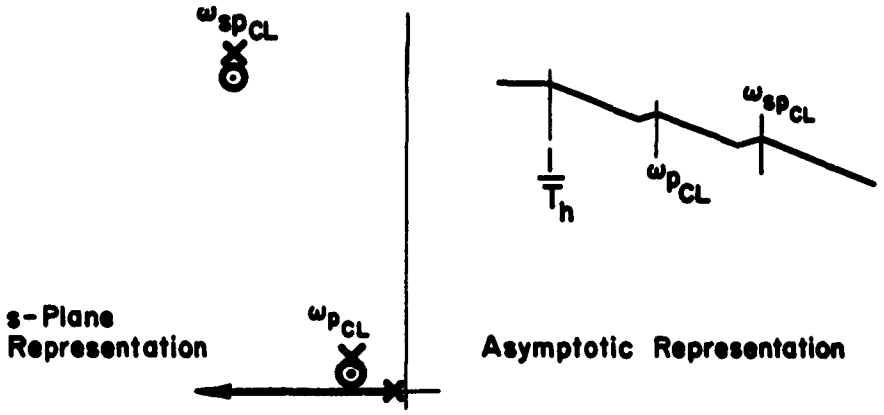

Figure B-12. $u \rightarrow \delta_T$ Closed Outer Loop

Angle of Attack Response. The altitude response with an $\alpha \rightarrow \delta_T$ inner loop is the same as with a $u \rightarrow \delta_T$ inner loop if the gain is high enough to stabilize the $1/T_{h_1}$ divergent zero. Equation B-17 indicates that changing either X_u or X_α will stabilize $1/T_{h_1}$.

The $\alpha \rightarrow \delta_T$ closed-loop zeros are positioned somewhat differently than the airspeed zeros, however, as shown for a typical case in Fig. B-13. The presence of a large residue (or distance) between the phugoid poles and zeros indicates that a moderate phugoid oscillation will be present in the angle of attack response. But the basic response is essentially similar to the $u \rightarrow \delta_T$ discussed previously.

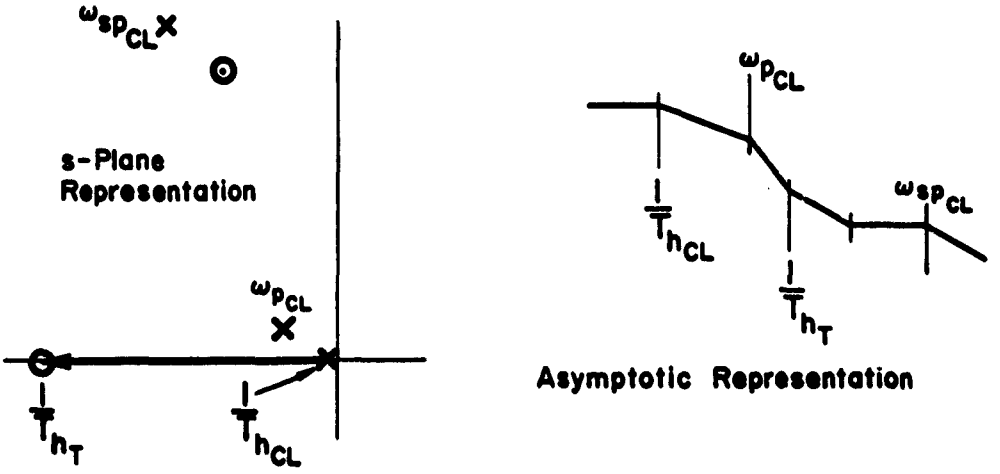

Figure B-13. $\alpha \rightarrow \delta_T$ Closed Outer Loop

2. $h \rightarrow \delta_T$, u or $\alpha \rightarrow \delta_e$, $\theta \rightarrow \delta_e$

Altitude Response. The predominant inner loop effect is from the $\theta \rightarrow \delta_e$ loop. The $u \rightarrow \delta_e$ or $\alpha \rightarrow \delta_e$ loop does not have a very large effect on the altitude response although it adds a little phugoid damping. The outer-loop locus is shown in Fig. B-14. The basic similarity to the single-loop $h \rightarrow \delta_T$ is noteworthy (see Fig. B-4), the significant change being the added phugoid damping from the $\theta \rightarrow \delta_e$ loop closure. The general effects of throttle loop closure are the same, however, being characterized by an initial decrease in phugoid damping and frequency for moderate values of pilot gain, on the order of 0.10 in. δ_T deflection per 20 ft of altitude error. It is important to note that pilot lead cannot help this situation because the phugoid frequencies (which dominate the response) are lower than his lead capabilities. The advantage of this system is that it does not change its characteristics in transition from flight on the front to the back side of the drag curve. So the pilot always has a basically stable system to control although one with a low bandpass.

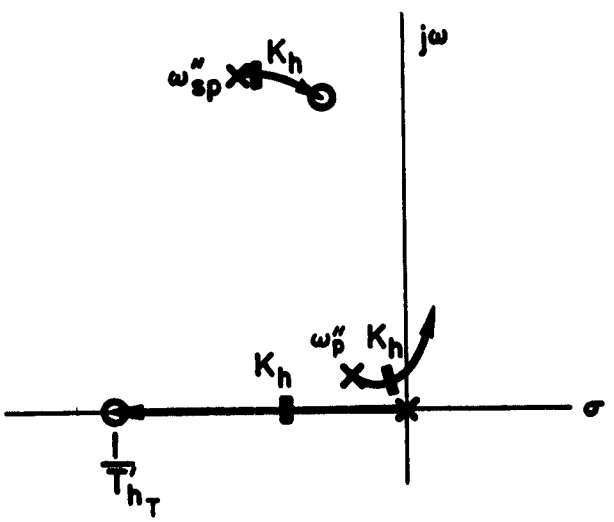

Figure B-14. $h \rightarrow \delta_T$, Final Closure

Airspeed or Angle of Attack Response. The coupling between the $h \rightarrow \delta_T$ inner loop and the $u \rightarrow \delta_e$ outer loop moves the outer-loop zeros to a position as shown in Fig. B-15. This indicates that airspeed response is stable but slow. Gust disturbances at frequencies higher than the already low closed-loop phugoid cannot be followed quickly. Therefore speed control will not be precise in turbulent air, but there will be no stability problem. The pilot will probably accept this as inevitable rather than attempt better control, since speed control is not as critical as altitude control for a carrier landing and there is no way of improving the system using this control technique.

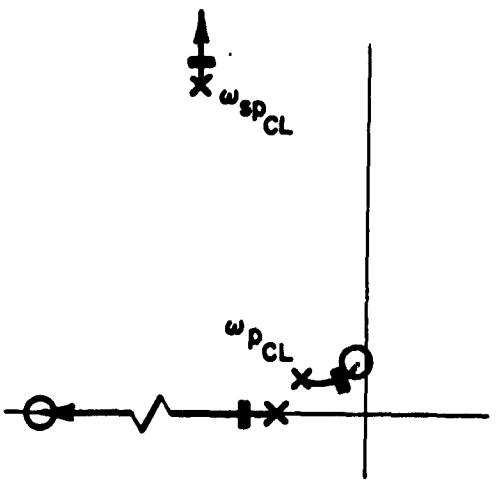

Figure B-15. s-Plane Representation of Closed $u \rightarrow \delta_e$ Outer Loop

Angle of attack response is quite similar in nature when the angle of attack indicator is well damped to eliminate the short-period oscillations. The dominant characteristic again will be the phugoid oscillation which is low in frequency due to the $h \rightarrow \delta_T$ loop.

APPENDIX C

A DETAILED EXAMPLE OF THE ANALYSIS TECHNIQUE

The F4D-1 in power-approach configuration at an airspeed of 120 knots is used for this example. The dimensional stability derivatives and aircraft transfer functions are listed in Table C-1. The purpose of this appendix is to illustrate how a series of loops are closed, how the gains for loop closure are chosen, and finally how the resulting closed-loop system is adjudged.

A. PILOT CONTROL WITH $\theta \rightarrow \delta_e$, $u \rightarrow \delta_T$, $h \rightarrow \delta_e$

1. Altitude Control

The altitude control outer-loop transfer function, using Eq A-31 derived in Appendix A and setting the terms $Y_{\delta_e u}$ and $Y_{\delta_T h}$ to zero, is

$$\left[\frac{h}{h_c}\right]_{\substack{\theta \rightarrow \delta_e \\ u \rightarrow \delta_T \\ h \rightarrow \delta_e}} = \frac{\overbrace{Y_{\delta_e h}\left(N_{h_{\delta_e}} + Y_{\delta_T u} N^{h\ u}_{\delta_e \delta_T}\right)}^{2}}{s\Big[\underbrace{\Delta + Y_{\delta_e \theta} N_{\theta_{\delta_e}}}_{1\text{-}a} + Y_{\delta_T u}\Big(\underbrace{N_{u_{\delta_T}} + Y_{\delta_e \theta} N^{\theta\ u}_{\delta_e \delta_T}}_{1\text{-}b}\Big)\Big]} \qquad \text{(C-1)}$$

$\overbrace{\qquad\qquad\qquad\qquad\qquad\qquad\qquad\qquad}^{3}$

A convenient method for the solution of Eq C-1 to render a factored polynomial is to perform the additions, or loop closures, in the order indicated by the brackets. The designated order is the proper sequence to give most insight into the synthesis of the pilot's control functions and to minimize the number of iterations in this process. Unfortunately there is no unique set or sequence of operations which will accomplish this for general multiple-loop control, but there are guidelines to govern this "art." The more pertinent of such guidelines, fairly extensively treated in Ref. 11, are:

TABLE C-1

CHARACTERISTICS OF THE F4D-1 AT 120 KNOTS, WITH $X^*_{\delta_e} = 0$

A. DIMENSIONAL STABILITY DERIVATIVES

$X_u = -0.055$	$Z_u = -0.31$	$M_u = 0.000$ (assumed)
$X_w = -0.103$	$Z_w = -0.89$	$M_w = -0.030$
$X_\alpha = -20.9$	$Z_\alpha = -180$	$M_\alpha = -6.07$
$X^*_{\delta_e} = 0.000$ (assumed)	$Z_{\delta_e} = -31.3$	$M_{\dot{\alpha}} = 0.000$ (assumed)
$X_{\delta_T} = 1.0T_{\delta_T}/m$	$Z_{\delta_T} = -0.23T_{\delta_T}/m$	$M_{\delta_e} = -3.74$
	$\alpha_0 = 13.1$ deg	$M_{\delta_T} = 0.000$ (assumed)

$U_o = 202$ ft/sec ; $T_{\delta_T} = 4000$ lb/in. ; $m = 468$ slugs

B. AIRCRAFT TRANSFER FUNCTIONS

(See Tables A-1 and A-2 for literal factored forms)

$$\Delta = \left[s^2 + 2(0.10)(0.21)s + 0.21^2\right]\left[s^2 + 2(0.31)(2.6)s + 2.6^2\right]$$

$$N_{\theta\delta_e} = M_{\delta_e}(s + 0.0041)(s + 0.69)$$

$$N_{u\delta_e} = Z_{\delta_e}X_w(s + 0.39)(s + 62.3)$$

$$sN_{h\delta_e} = -Z_{\delta_e}(s - 0.073)(s - 3.52)(s + 4.36)$$

$$N_{u\delta_T} = X_{\delta_T}(s - 0.033)\left[s^2 + 2(0.31)(2.6)s + 2.6^2\right]$$

$$U_oN_{\alpha\delta_T} = Z_{\delta_T}\left[s(s + 0.71)(s + 1.4)\right]$$

$$sN_{h\delta_T} = -Z_{\delta_T}(s + 1.40)\left[s^2 + 2(0.14)(2.5)s + 2.5^2\right]$$

$$N^{\theta\ u}_{\delta_e\delta_T} = M_{\delta_e}X_{\delta_T}(s + 0.66)$$

$$sN^{h\ u}_{\delta_e\delta_T} = -Z_{\delta_e}X_{\delta_T}(s - 3.8)(s + 4.5)$$

$$U_oN^{\theta\ \alpha}_{\delta_e\delta_T} = (M_{\delta_e}Z_{\delta_T} - M_{\delta_T}Z_{\delta_e})(s + 1.4)$$

$$sN^{h\ \alpha}_{\delta_e\delta_T} = (M_{\delta_e}Z_{\delta_T} - M_{\delta_T}Z_{\delta_e})(s + 1.4)$$

*This case study was made before the importance of the X_{δ_e} term for the F4D-1 was discovered.

a. Relative bandwidths of the several possible loop closure sequences—The bandwidth of a given loop closure is measured roughly by the crossover frequency, ω_c. (If more than one crossover frequency exists, the largest is taken as ω_c.) The general sequence of loop closures in a multiloop system should then be in order of decreasing ω_c, e.g., $\omega_{c_{\text{inner loop}}} > \omega_{c_{\text{outer loop}}}$.

b. "Command" loop—Ordinarily made the last, or outer, loop.

In the present case the θ loop which must provide adequate control of short-period frequencies has the highest crossover frequency (i.e., is "tightest") and is the obvious choice for the first closure. The h loop represents the command function and is therefore last to be closed, leaving the u loop as the intermediate closure.

Implementing this philosophy, we commence with closure of the high frequency $\theta \rightarrow \delta_e$ loop or solution of the bracketed term, 1-a, which may be rewritten in the more conventional form

$$\Delta + Y_{\delta_e}\theta^N\theta_{\delta_e} = \Delta\left(1 + \frac{Y_{\delta_e}\theta^N\theta_{\delta_e}}{\Delta}\right) = \Delta' \qquad \text{(C-2)}$$

The factors of Δ' are plotted in Fig. C-1 as a function of pilot gain, $K_{\delta_e\theta}$, and various values of pilot lead equalizations, T_L. A pilot reaction time delay of $\tau = 0.2$ sec is assumed throughout as represented by its magnitude and phase characteristics in the s-plane through the relationships

$$\text{magnitude} = e^{-\tau\sigma}$$
$$\text{phase angle} = -\tau\omega$$

Vertical lines in the s-plane correspond to loci of constant $e^{-\tau s}$ magnitudes; similarly, horizontal lines are loci of constant $e^{-\tau s}$ phase (e.g., for $\tau = 0.2$ sec, a horizontal line of constant $j\omega = 5$ has a phase contribution due to $e^{-0.2s}$ of -57.3 deg for any value of s along that line). A phase-amplitude grid so constructed enables simple inclusion of the $e^{-\tau s}$ contributions to the total system phase amplitude as a function of the complex variable, s. Since a constant value of τ is assumed, the phase-amplitude grid is the same on every plot which contains a Y transfer function.

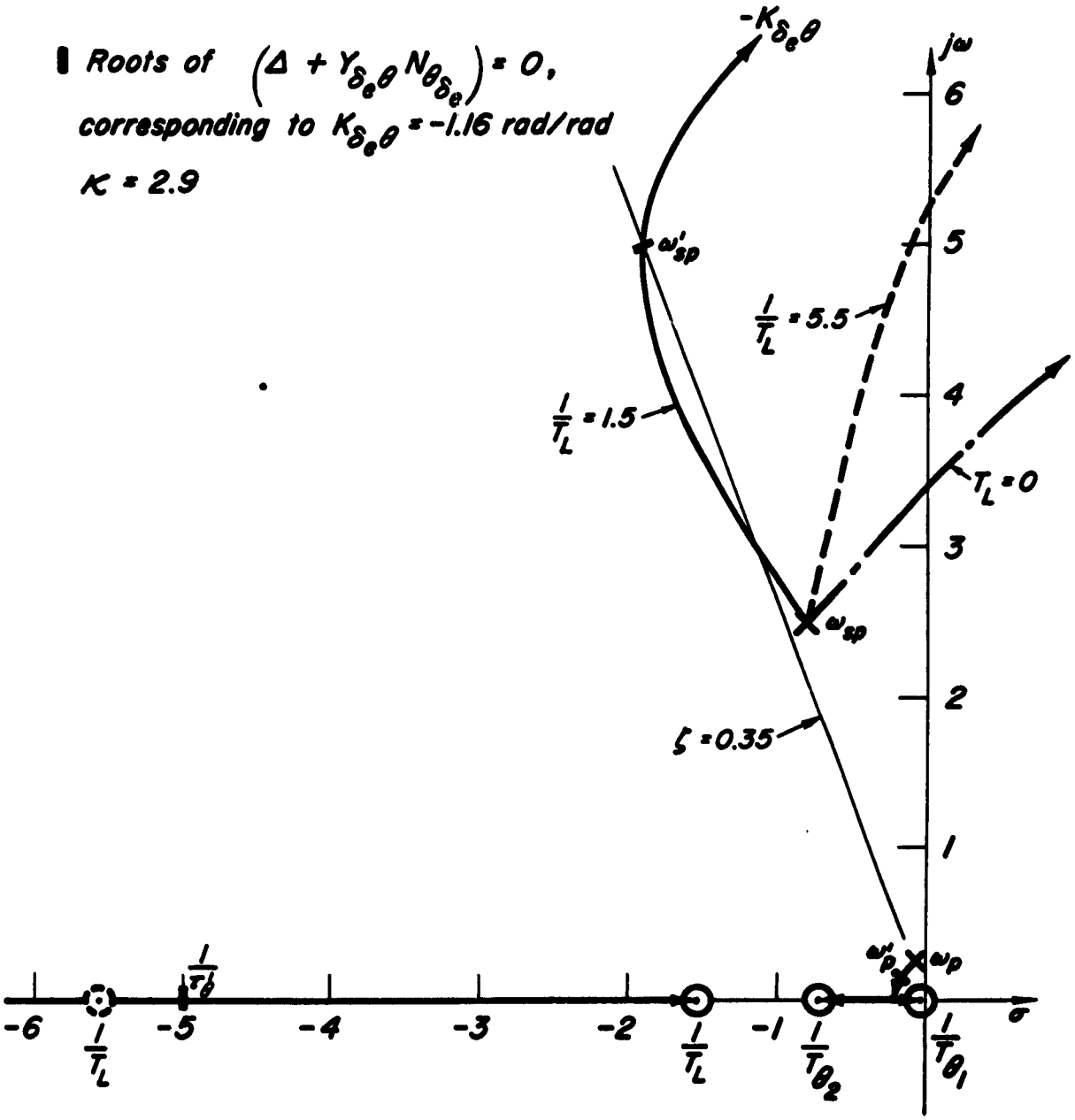

Figure C-1. Closure of the Piloted $\theta \rightarrow \delta_e$ Loop

Assuming that desirable short-period control corresponds to a closed-loop damping, $\zeta'_{sp} \geq 0.35$ (Ref. 5, 6), the required pilot lead equalization, $1/T_L$, is approximately 1.5 as shown. Loop closure gain is then determined by intersection of the $\zeta = 0.35$ radial with this selected short-period locus at the highest frequency permitted (i.e., tightest control). Phugoid and reaction delay closed-loop roots, ω'_p and $1/\tau'_\theta$, are then specified by this gain value. Notice that the order of Δ' as given by the closed-loop roots (symbol ■) shown in Fig. C-1 is higher than that of Δ because of the additional $1/\tau'_\theta$ first order. The corresponding factor, $s + 1/\tau'_\theta$, is only a first approximation to the closed-loop factors emanating from the open-loop $e^{-\tau s}$ because the latter is transcendental in nature. If $e^{-\tau s}$, itself, is also approximated by a single first-order factor, the $1/\tau'_\theta$ factor is essentially cancelled. To show this, rewrite Eq C-2 with $Y_{\delta_e\theta}$ given simply by $e^{-\tau s}$, i.e.,

$$\Delta' = \Delta + e^{-\tau s} N_{\theta\delta_e} = \frac{e^{\tau s}\Delta + N_{\theta\delta_e}}{e^{\tau s}} \qquad \text{(C-3)}$$

The numerator of the last expression to a first approximation contains the factor $s + 1/\tau'_\theta$, as in Fig. C-2. The denominator, to the same degree of approximation, becomes

$$e^{\tau s} \doteq 1 + \tau s \doteq \tau\left(s + \frac{1}{\tau}\right) \qquad \text{(C-4)}$$

For the value of $\tau = 0.2$ actually used, the cancellation is almost "exact" in the case at hand.

The next closure (1-b) simply involves factoring since all the terms are now specified. That is, substituting the numerators of Table C-1 and the $Y_{\delta_e\theta}$ equation determined from the previous closure into the 1-b bracket of Eq C-1 yields

$$N_{u_{\delta_T}} \left\{ 1 + \frac{(-3.74)(-1.16)e^{-0.2s}(0.667s + 1)(s + 0.66)}{(s - 0.033)\left[s^2 + 2(0.31)(2.6)s + (2.6)^2\right]} \right\} \qquad \text{(C-5)}$$

The factors of Eq C-5 are computed by the conventional root locus technique as is shown in Fig. C-2; the closed-loop poles, as denoted by ■, are the factors of Eq C-5. Here, again, the near-cancellation of the added $s + 1/\tau'_\theta$ factor as in the closure above will occur. Notice also that the root locus

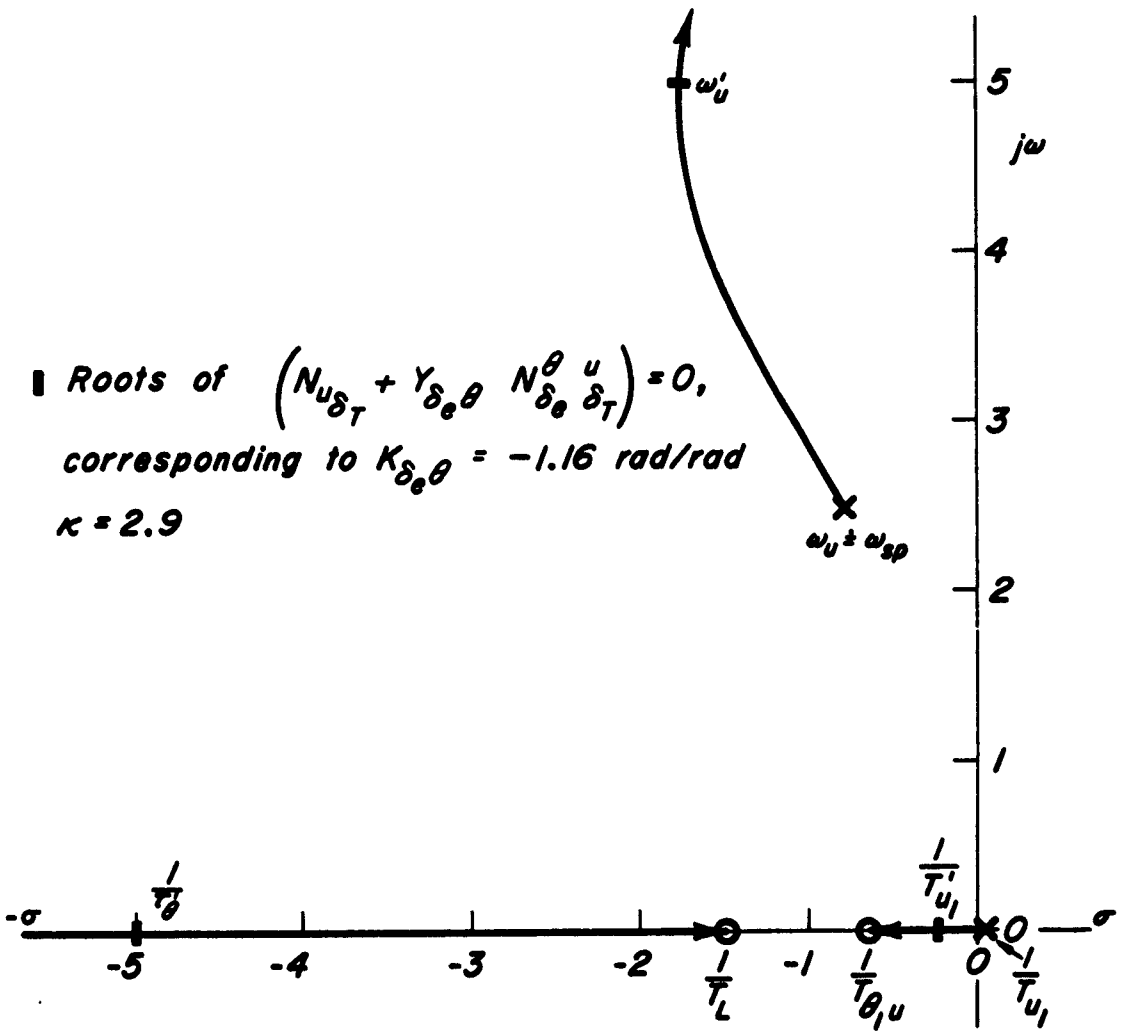

Figure C-2. Factorization of $N_{u\delta_e} + Y_{\delta_e\theta} N^{\theta\ u}_{\delta_e\ \delta_T}$

gain, κ, for this closure corresponds exactly to that of the previous closure (Fig. C-1). Such correspondence holds approximately for all simultaneous closures of multiple loops (Ref. 11) and exactly in the present cases, and is an invaluable aid in conducting the loop closure sequence. It can easily be checked by comparing the high frequency (i.e., $s \to \infty$) behavior of the open loops. Thus, for example, for the closures indicated as 1-a and 1-b in Eq C-1 (values from Table C-1),

$$\text{Closure 1-a:} \quad \left.\frac{Y_{\delta_e\theta} N_{\theta_{\delta_e}}}{\Delta}\right]_{s \to \infty} = \frac{Y_{\delta_e\theta} M_{\delta_e} s^2}{s^4} = \frac{Y_{\delta_e\theta} M_{\delta_e}}{s^2}$$

$$\text{Closure 1-b:} \quad \left.\frac{Y_{\delta_e\theta} N^{\theta\ u}_{\delta_e\delta_T}}{N_{u_{\delta_T}}}\right]_{s \to \infty} = \frac{Y_{\delta_e\theta} M_{\delta_e} X_{\delta_T} s}{X_{\delta_T} s^3} = \frac{Y_{\delta_e\theta} M_{\delta_e}}{s^2}$$

Similarly, for closures 2 and 3,

$$\text{Closure 2:} \quad \left.\frac{Y_{\delta_{Tu}} N^{h\ u}_{\delta_e\delta_T}}{N_{h_{\delta_e}}}\right]_{s \to \infty} = \frac{Y_{\delta_{Tu}} (-Z_{\delta_e} X_{\delta_T}) s^2}{-Z_{\delta_e} s^3} = \frac{Y_{\delta_{Tu}} X_{\delta_T}}{s}$$

$$\text{Closure 3:} \quad \left.\frac{Y_{\delta_{Tu}} \left(N_{u_{\delta_T}} + Y_{\delta_e\theta} N^{\theta\ u}_{\delta_e\delta_T} \right)}{\Delta + Y_{\delta_e\theta} N_{\theta_{\delta_e}}}\right]_{s \to \infty} = \frac{Y_{\delta_{Tu}} X_{\delta_T} s^4}{s^5} = \frac{Y_{\delta_{Tu}} X_{\delta_T}}{s}$$

Closure 2 is based on the stability problem associated with $\theta \to \delta_e$, $h \to \delta_e$ control and the remedying effects of the $u \to \delta_T$ loop which are qualitatively described in Appendix B, Paragraphs A-2 and C-1, respectively. Rewriting the bracketed numerator terms of Eq C-1 in a factored form and substituting values from Table C-1, we obtain the expression

$$N_{h_{\delta_e}} + Y_{\delta_{Tu}} N^{h\ u}_{\delta_e\delta_T} = N_{h_{\delta_e}} \left\{ 1 + \frac{Y_{\delta_{Tu}} (X_{\delta_T}) (s - 3.8)(s + 4.5)}{(s - 0.073)(s - 3.52)(s + 4.36)} \right\} \qquad \text{(C-6)}$$

▌ *Roots of* $\left(N_{h_{\delta_e}} + Y_{\delta_T u} N^{h\ u}_{\delta_e\ \delta_T}\right) = 0$, *corresponding to 6 db gain margin for stabilizing* $1/T_{h_1}$. *Pilot's gain corresponding to this closure is* $K_{\delta_T u} = .0176$ *in/ft/sec.*

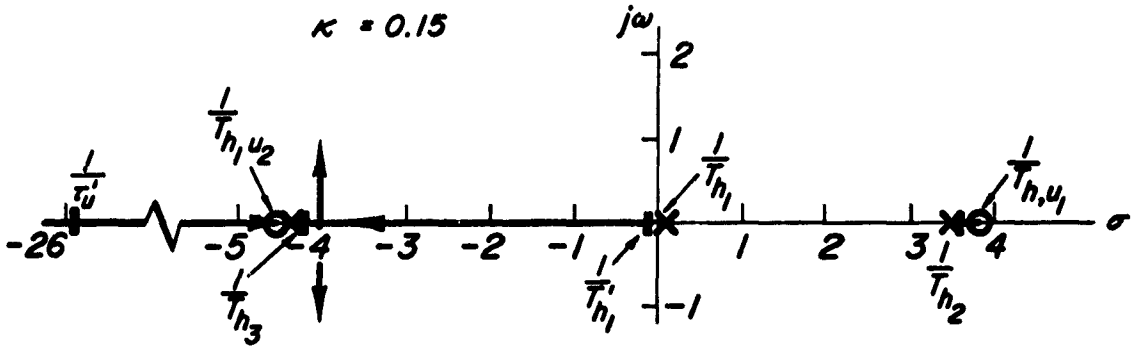

Figure C-3. Closure to Effect Stabilization of the Altitude Control Zero

Assuming a pure gain pilot model (i.e., $Y_{\delta_T u} = K_{\delta_T u} e^{-0.2s}$), the locus of roots of Eq C-6 is shown in Fig. C-3. Clearly, the simple gain closure is sufficient to move the root $1/T'_{h_1}$ into the left-half plane; employing a factor of two in gain over that just required to move the root $1/T_{h_1}$ into the stable region, the factors of Eq C-4 are as noted by the symbol ▌. Pilot gain, $K_{\delta_T u}$, corresponding to this value of closure gain is determined from the root locus gain, κ, through the relationship

$$K_{\delta_T u} = \frac{\kappa}{X_{\delta_T}} = 0.0176 \text{ in./ft/sec}$$

This value should be considered a <u>conservative</u> <u>minimum</u> for altitude control stability. Obviously the pilot will not close the $u \rightarrow \delta_T$ loop solely on this basis, since higher values of $K_{\delta_T u}$ may be dictated on the more probable basis of maintaining airspeed errors which are acceptably small. Higher $K_{\delta_T u}$ than that indicated above would not appreciably change the altitude control dynamics; however, lower values could result in altitude control instability.

Closure 3 in Eq C-1 follows in the same manner as closure 1-b since all of the quantities are now specified. By combining the factors of closure 1-a and 1-b (from Fig. C-1 and C-2) and including the pilot equation $Y_{\delta_{Tu}}$ (from Fig. C-3), the terms in brackets of Eq C-1 can be written as

$$\left[\Delta + Y_{\delta_e\theta} N_{\theta\delta_e}\right]\left\{1 + \frac{0.0176\, X_{\delta_T}(s+0.25)\cancel{(s+5)}\left[s^2 + 2(0.34)(5.34)s + (5.34)^2\right]}{\cancel{(s+5)}\left[s^2 + 2(0.78)(0.23)s + (0.23)^2\right]\left[s^2 + 2(0.35)(5.35)s + (5.35)^2\right]}\right\} \tag{C-7}$$

Here, to keep the order correct, the $s+5$ terms corresponding to the $-1/\tau_{\theta_1}$ factors are cancelled. Strictly speaking, this manipulation is <u>not</u> mathematically valid, but it is a reasonable approximation in this case. Probably a better procedure in general would be to use the Padé approximation,

$$e^{-\tau s} \doteq \frac{s - (2/\tau)}{s + (2/\tau)}$$

throughout the entire analysis. This apparently crude representation is a good approximation to both amplitude and phase for frequencies less than about 4 rad/sec. Furthermore, it allows all cancellation effects to be accurately made within the limits of the approximation form. The use of "exact" $e^{-\tau s}$ appears, on the other hand, to be quite inexact as regards cancellations. Nevertheless, the present example will continue with the "exact" representation to avoid confusion.

The factors of Eq C-7 are determined from the loci of closed-loop roots versus $K_{\delta_{Tu}}$ as shown in Fig. C-4. Since the pilot's gain in the speed loop is very small (i.e., $K_{\delta_{Tu}} = 0.0176$), this closure has essentially no effect on the denominator of Eq C-1. Therefore the factors of Eq C-7 could have been validly assumed identical to those of Eq C-2; and Eq C-1 could have been factored with two closures instead of four. The important point to note from Fig. C-4 is that for higher values of $K_{\delta_{Tu}}$

a. The short-period roots are largely unaffected
b. There can be a large increase in phugoid damping

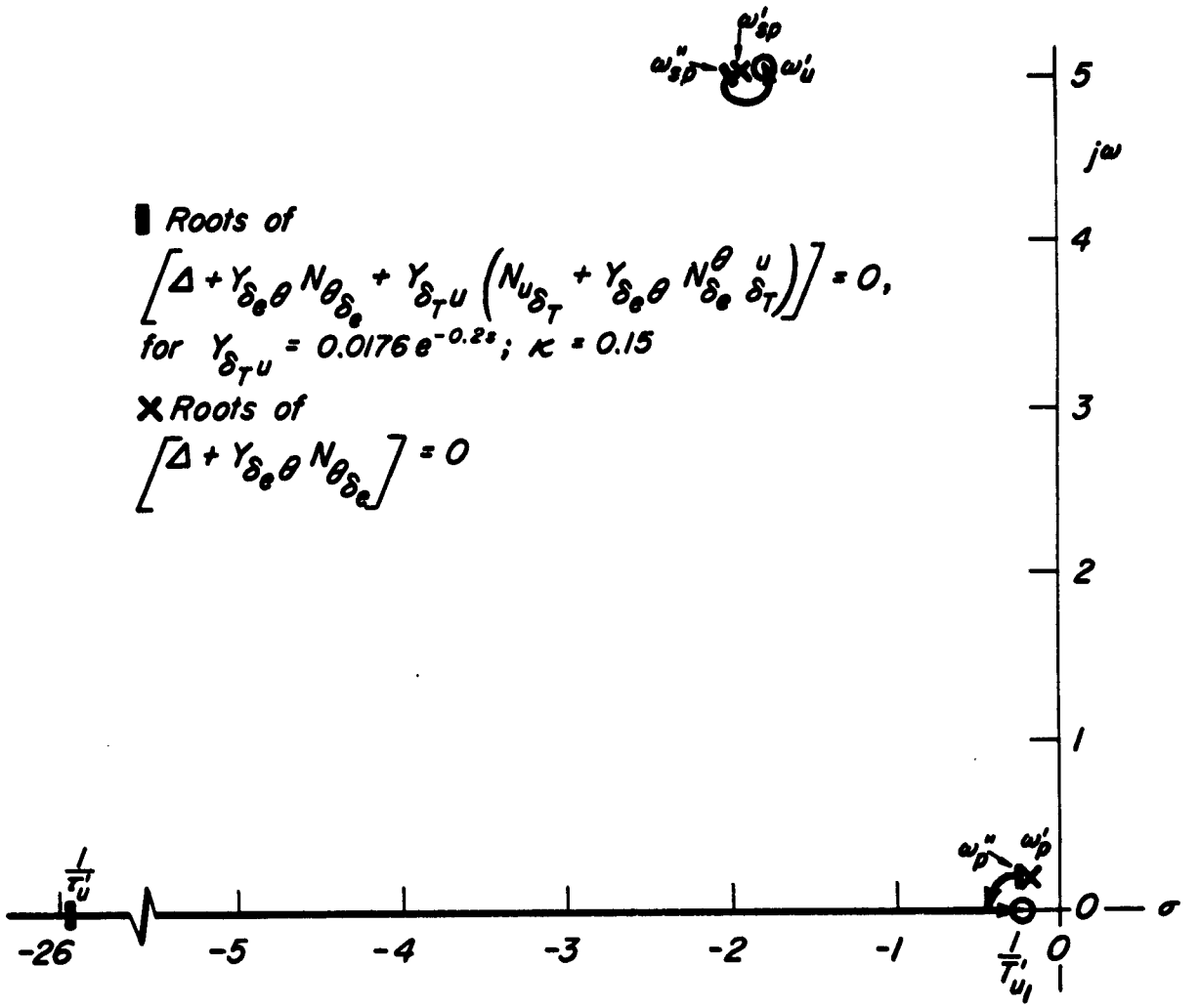

Figure C-4. Effect of the Speed Control Loop Closure on the Altitude Control Denominator

Equation C-1 can now be written in factored form from the root locations found in Fig. C-3 and C-4.

(C-8)

$$\left[\frac{h}{h_c}\right]_{\substack{\theta \to \delta_e \\ u \to \delta_T \\ h \to \delta_e}} = \frac{Y_{\delta_e h}}{s}\left\{\frac{-Z_{\delta_e}(s+0.075)(s-3.6)(s+4.4)\cancel{(s+26)}}{\cancel{(s+26)}\left[s^2+2(0.82)(0.31)s+(0.31)^2\right]\left[s^2+2(0.37)(5.38)s+(5.38)^2\right]}\right\}$$

Equation C-8 is the total open-loop $h \to \delta_e$ control transfer function with both $\theta \to \delta_e$ and $u \to \delta_T$ loops closed. Altitude tracking performance is

obtained by closing this last loop as in Fig. C-5, which is shown for a pure gain pilot characteristic (i.e., $Y_{\delta_e h} = K_{\delta_e h} e^{-0.2s}$). The closed-loop $h \rightarrow \delta_e$ roots as a function of $K_{\delta_e h}$ are shown, as are the amplitude-phase characteristics of the open-loop $h \rightarrow \delta_e$ function. The region of probable pilot gain adjustment shown in that figure is such that phugoid damping rapidly deteriorates with increasing gain while frequency rapidly increases. Whether this region represents adequate performance for the approach will depend on the nature of the system disturbances, i.e., atmospheric turbulence (including carrier-induced effects) and ship's motion. For disturbances of frequency content well below that of the probable closure region, altitude tracking performance will be adequate.

In conclusion, the $\theta \rightarrow \delta_e$, $u \rightarrow \delta_T$, $h \rightarrow \delta_e$ control technique appears adequate for control of altitude during carrier-approach conditions and it circumvents the stability problem normally associated with $h \rightarrow \delta_e$ control for flight on the backside of the drag curve.

2. Airspeed Control

While the pilot's primary task is to control altitude, an important secondary task is to control airspeed. For this secondary task, $u \rightarrow \delta_T$ is now the outermost loop with both $\theta \rightarrow \delta_e$ and $h \rightarrow \delta_e$ as inner loops. The u control problem as seen by the pilot, when at the same time controlling θ and h with δ_e, corresponds then to ($Y_{\delta_e u} = 0$ in Eq A-30).

$$\left[\frac{u}{u_c}\right]_{\substack{\theta \rightarrow \delta_e \\ h \rightarrow \delta_e \\ u \rightarrow \delta_T}} = \frac{Y_{\delta_T u} \left\{ s\left[N_{u_{\delta_T}} + Y_{\delta_e \theta} N^{\theta\, u}_{\delta_e \delta_T} \right] + Y_{\delta_e h} N^{h\, u}_{\delta_e \delta_T} \right\}}{s\left[\Delta + Y_{\delta_e \theta} N_{\theta_{\delta_e}} \right] + Y_{\delta_e h} N_{h_{\delta_e}}} \qquad \text{(C-9)}$$

Evaluation of the factors of Eq C-7 is facilitated by recognizing that the indicated additions enclosed in squared brackets have already been computed. Taking first the numerator, factors of the square-bracketed term were

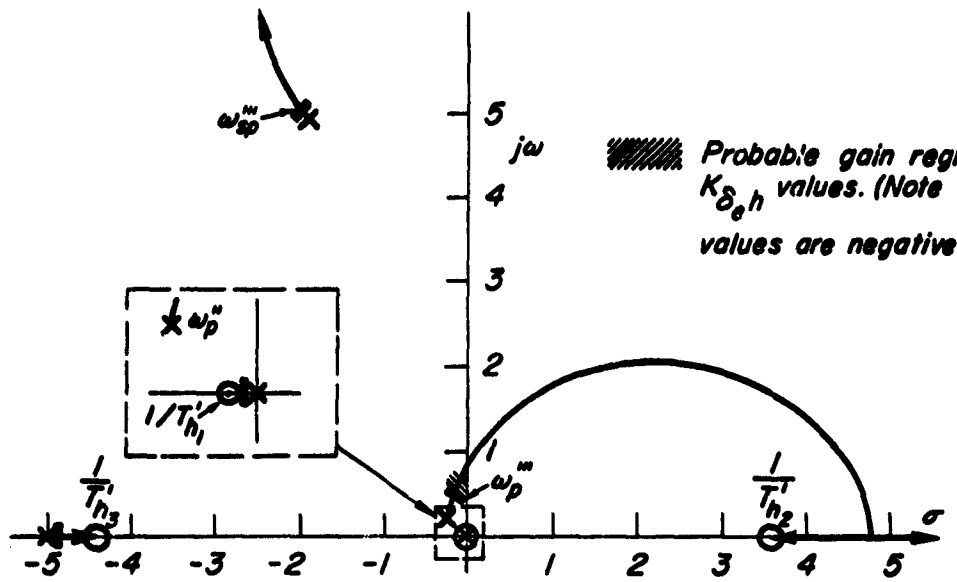

$$Y_{OL} = \frac{31.3\, K_{\delta_e h}\, e^{-\tau s}(s+0.075)(s-3.6)(s+4.4)}{s\left[s^2+2(.82)(.31)s+(.31)^2\right]\left[s^2+2(.37)(5.38)s+(5.38)^2\right]}$$

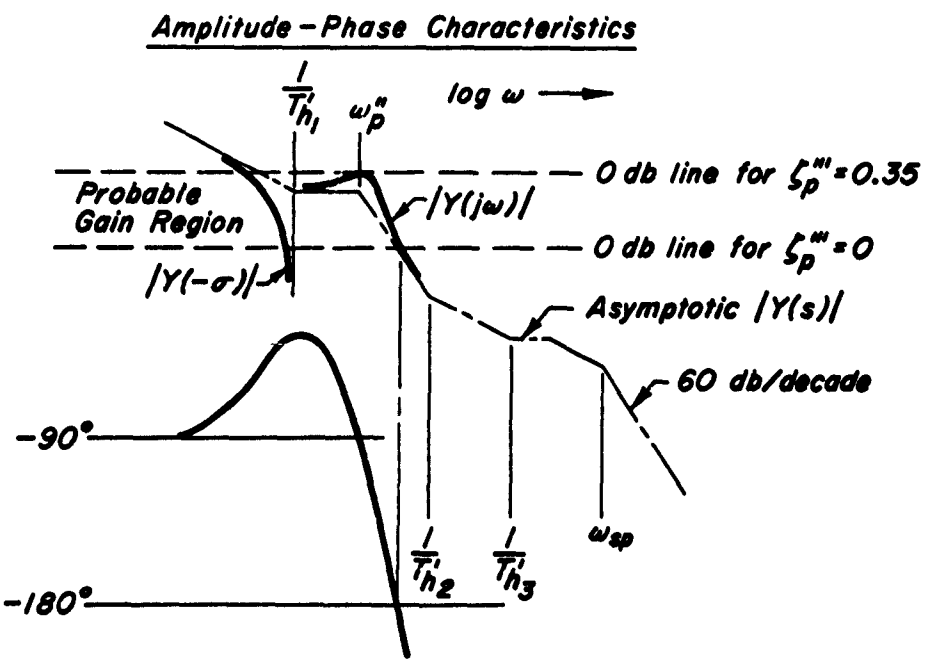

Figure C-5. Altitude Control with $\theta \rightarrow \delta_e$, $u \rightarrow \delta_T$ Inner Loops Closed

determined previously in Fig. C-2; these factors are combined with the remaining term through the root locus technique in Fig. C-6, yielding the complete numerator factors as shown. Note that the gain variable of the locus is $K_{\delta_{eh}}$ and the value selected for closure is that consistent with Fig. C-5 for a $\zeta_p''' = 0.35$.

The denominator factors of Eq C-9 are similarly determined. The factors of the square-bracketed term were determined in Fig. C-1 and when combined with the remaining term, as is done in Fig. C-7, yield the denominator factors shown. Note that the gain variable in Fig. C-7 is also $K_{\delta_{eh}}$, and that the root locus gain for the selected closure must be identical to that used in Fig. C-5 and C-6.

Collecting the factors from Fig. C-6 and C-7 yields the factored open-loop $u \rightarrow \delta_T$ transfer function

$$\left[\frac{u}{u_\epsilon}\right]_{\substack{\theta \rightarrow \delta_e \\ h \rightarrow \delta_e \\ u \rightarrow \delta_T}} = Y_{\delta_T u} X_{\delta_T} \left\{ \frac{\cancel{(s+5)}\left[s^2 + 2(0.44)(0.275)s + (0.275)^2\right]\left[s^2 + 2(0.35)(5.34)s + (5.35)^2\right]}{(s-0.025)\cancel{(s+5)}\left[s^2 + 2(0.3)(0.47)s + (0.47)^2\right]\left[s^2 + 2(0.36)(5.4)s + (5.4)^2\right]} \right\} \qquad \text{(C-10)}$$

The significant dynamic characteristics shown in Eq C-10 very nearly reduce to the easily controlled element K/s. The pilot accordingly should find closure of the speed loop a very simple task.

For that value of $K_{\delta_T u}$ assumed to stabilize altitude control, the <u>closed-loop</u> characteristic factors of the speed loop must be identical to those of the altitude loop computed previously in Fig. C-5. (Note that the closed-loop $u \rightarrow \delta_T$ denominator, given by the summation of open-loop numerator and denominator terms in Eq C-9, is identical to the similarly computed closed-loop $h \rightarrow \delta_e$ denominator from Eq C-1.) The closed-loop speed control equation can therefore be written directly by collecting the numerator and denominator factors from Fig. C-6 and C-5, respectively, which gives the following polynomial:

$$\left[\frac{u}{u_c}\right]_{\substack{\theta \rightarrow \delta_e \\ h \rightarrow \delta_e \\ u \rightarrow \delta_T}} = K_{\delta_T u} X_{\delta_T} \left\{ \frac{\left[s^2 + 2(0.44)(0.275)s + (0.275)^2\right]\left[s^2 + 2(0.35)(5.34)s + (5.35)^2\right]}{(s+0.025)\left[s^2 + 2(0.36)(0.5)s + (0.5)^2\right]\left[s^2 + 2(0.375)(5.5)s + (5.5)^2\right]} \right\} \qquad \text{(C-11)}$$

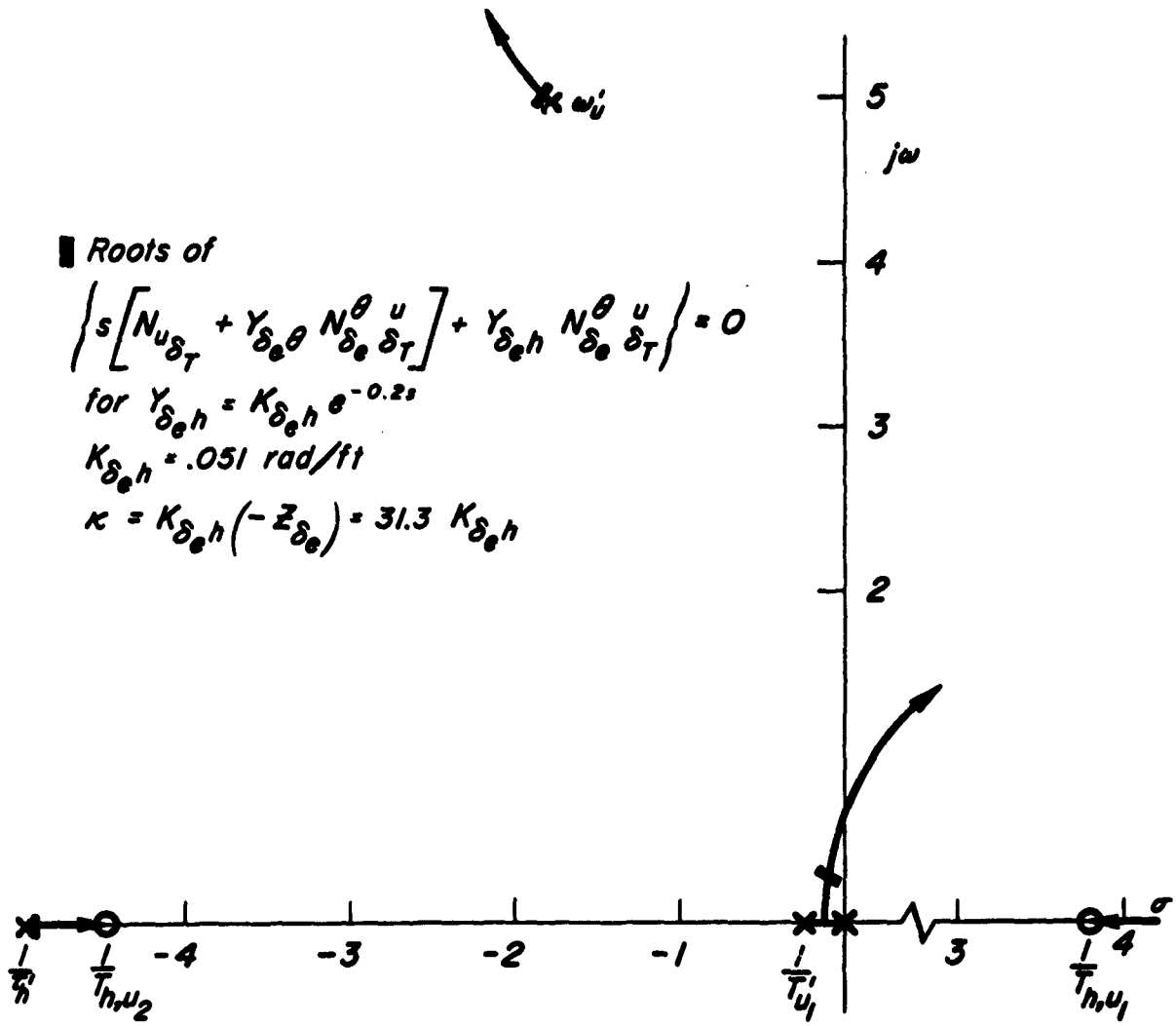

Figure C-6. Effect of the Altitude Control Loop Closure on the Airspeed Control Numerator

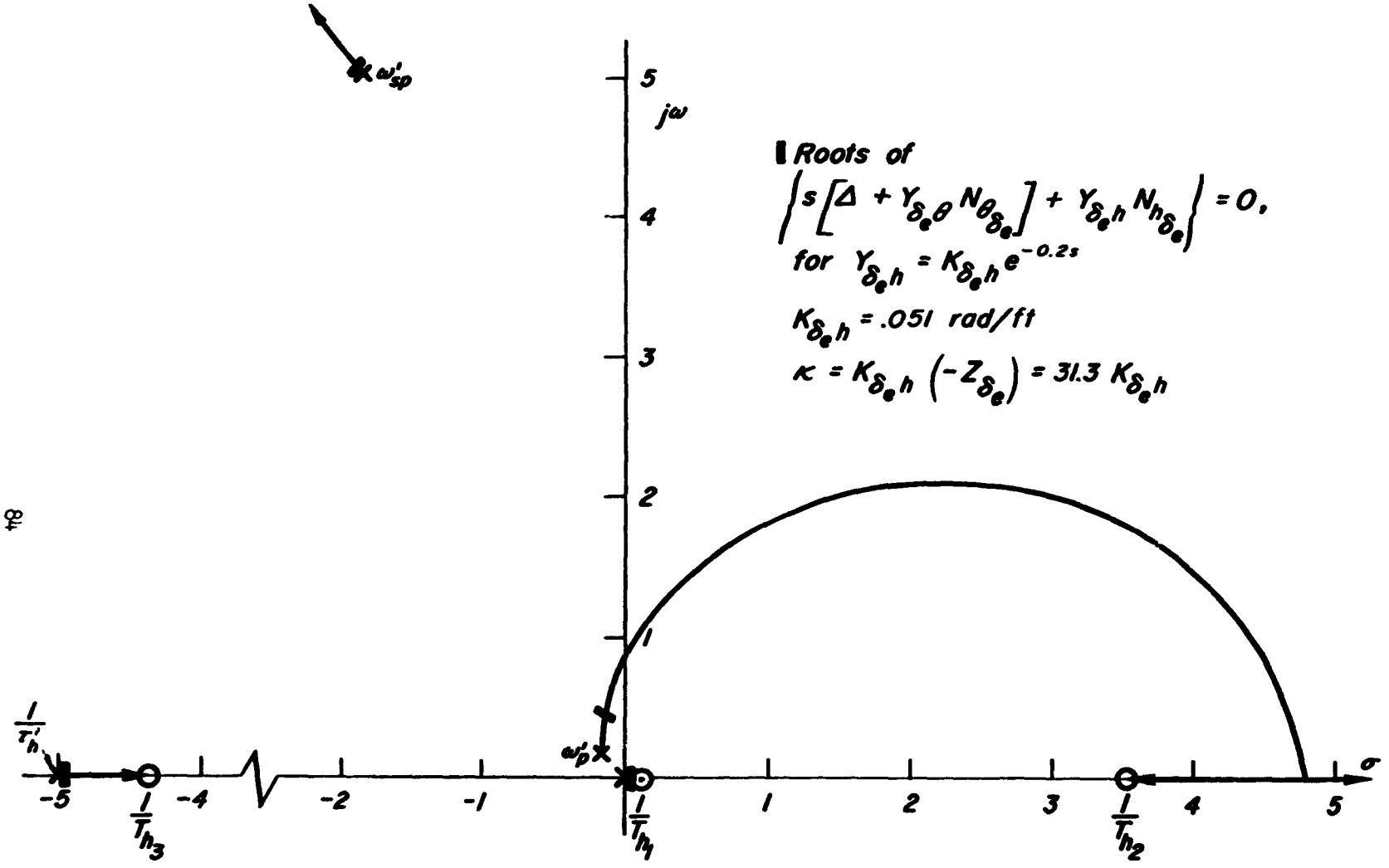

Figure C-7. $\theta \rightarrow \delta_e$, $h \rightarrow \delta_e$ Inner Loop Effects on Airspeed Open-Loop Denominator (Eq C-9)

Closed-loop speed control is characterized by a slow first-order convergence, indicating that the selected value of $K_{\delta_T u}$ could have been made larger. Since a higher speed loop gain improves both altitude and airspeed tracking, the next logical step is to recompute the altitude and airspeed closed-loop dynamics with a higher $K_{\delta_T u}$. Such a reiteration process, while worthwhile from the standpoint of optimized design, is not necessary to reach the over-all conclusions:

a. For the minimum airspeed loop gain assumed to stabilize altitude tracking, adequate altitude control results, and the speed loop is stable—but very sluggish.

b. For higher airspeed loop gains better altitude bandwidths result and afford a much faster responding airspeed control.

c. The assumed piloting technique provides adequate control for carrier approach of the F4D airplane regardless of flight speeds above or below that of minimum drag, although the speed loop closure is not required for speeds above that of minimum drag.

B. PILOT CONTROL WITH $\theta \rightarrow \delta_e$, $h \rightarrow \delta_e$, $\alpha \rightarrow \delta_T$

The previous example shows that good system characteristics are achievable with throttle control of airspeed. But current Naval practice is to use angle of attack rather than airspeed as a measure of the approach situation which is less subject to variations due to weight and external configuration. It is therefore pertinent to examine the use of $\alpha \rightarrow \delta_T$ (rather than $u \rightarrow \delta_T$) as an alternative technique. As will be shown below, $\alpha \rightarrow \delta_T$ for proper instrument dynamics is essentially equivalent to $u \rightarrow \delta_T$ and there is no essential difference between these feedbacks, assuming both are equally accessible to the pilot.

Because control of the phugoid appears to be the central problem in properly executing the approach, angle of attack fluctuations at short-period frequency must be damped or lagged out of the α display. In effect the α_{δ_T} dynamics as displayed must be similar to those of u_{δ_T}. This requirement is also consistent with the use of the α reading as an indication of trim speed, i.e., steady state, not fluctuating, angle of attack information is desired.

Normally, then, filtering of the short-period α response is provided in the indicator itself. The effect of this filtering is to make the α indicator an equivalent airspeed indicator calibrated in degrees instead of knots. The only difference, then, between the $\alpha \rightarrow \delta_T$ and $u \rightarrow \delta_T$ as an inner stabilizing loop is the required minimum gain for stabilizing the $h \rightarrow \delta_e$ closure. Paralleling the procedure adopted previously, the $\alpha \rightarrow \delta_T$ closure gain requirement is computed below.

The altitude control numerator with $\theta \rightarrow \delta_e$ and $\alpha \rightarrow \delta_T$ as inner loops can be derived from Appendix A and is stated as Eq C-11.

$$\left[N_{h\delta_e}\right]_{\substack{\theta \rightarrow \delta_e \\ \alpha \rightarrow \delta_T}} = Y_{\delta_e h}\left(U_o N_{h\delta_e} + Y_{\delta_T \alpha} N^{h\ \alpha}_{\delta_e \delta_T}\right) \qquad \text{(C-11)}$$

Recalling from the previous example that for stable altitude control non-negative low frequency numerator zeros are not permissible, sets the gain term of $Y_{\delta_T \alpha}$. The roots of Eq C-11 versus the pilot's gain $K_{\delta_T \alpha}$ (assuming that $Y_{\delta_T \alpha} = K_{\delta_T \alpha} e^{-0.2s}$) are shown in Fig. C-8. Again using a gain twice that

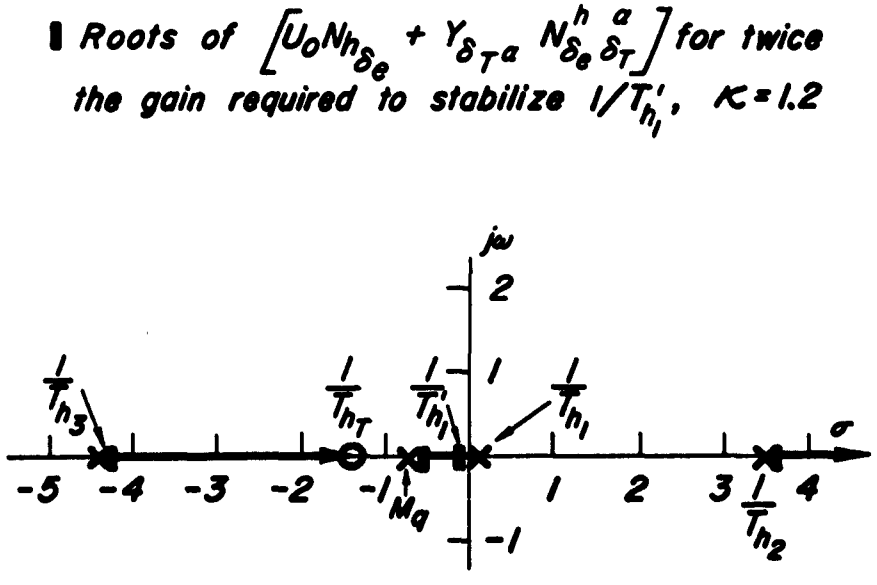

Figure C-8. Effect of $\alpha \rightarrow \delta_T$ on Altitude Control Zeros

required to move the root $1/T'_{h_1}$ into the left-half plane, the resulting closure corresponds to a root locus gain of $\kappa = -1.2$. The required minimum pilot gain can then be computed from the relationship:

$$\kappa = K_{\delta_T \alpha} \frac{(M_{\delta_e} Z_{\delta_T} - M_{\delta_T} Z_{\delta_e})}{-Z_{\delta_e}} \qquad \text{(C-12)}$$

Substituting values from Table C-I and the specified root locus gain, we obtain

$$K_{\delta_T \alpha} = \frac{(-1.2)(31.3)}{(7.36)(57.3 \text{ deg/rad})}$$

$$= -0.089 \text{ in./deg}$$

Since a one-degree change in angle of attack correspondingly changes the trim speed of the F4D-1 approximately four knots, the required throttle motion in tracking angle of attack is approximately equal to that in tracking airspeed for equal errors in airspeed.

In conclusion, the angle of attack indicator may be substituted for the airspeed indicator to produce results comparable to the $\theta \rightarrow \delta_e$, $u \rightarrow \delta_T$, $h \rightarrow \delta_e$ control technique described previously.